Evaluation of the Egmond shoreface nourishment

Part II: Validation of the morphological UNIBEST-TC model

N.R. Wiersma

Supervisors:
prof. dr. ir. M.J.F. Stive
prof. dr. ir. L.C. van Rijn
prof. dr. ir. G.S. Stelling
dr. ir. J. van de Graaff
ir. D.J.R. Walstra

June 2002

Preface

The present M.Sc. thesis forms the completion of my education at the Delft University of Technology, Faculty of Civil Engineering and Geosciences, Department of Civil Engineering, Division of Hydraulic and Offshore Engineering.

The study concerns the evaluation of the shoreface nourishment at Egmond aan Zee and in particular the hydrodynamic and morphodynamic influence of this shoreface nourishment. The study is divided in three parts, consisting of a data analysis, a hindcast study using the modelling program Unibest-TC and a hindcast study using the modelling program Delft3D-MOR. Here the hindcast study with the UNIBEST-TC model is described. The morphodynamic model is designed, calibrated, validated, and evaluated. After which the performance of the shoreface nourishment is evaluated on the basis of the measured and modelled results. The study has been carried out at WL | Delft Hydraulics and was funded by the Delft Cluster Project Coasts (03.01.03) and the RIKZ (Rijks Instituut voor Kust en Zee).

I would like to thank my supervisors, prof. dr. ir. M.J.F. Stive (Delft University of Technology), prof. dr. ir. L.C. Van Rijn (University of Utrecht), prof. dr. ir. G.S. Stelling (Delft University of Technology), dr. ir. J. van de Graaff (Delft University of Technology) and ir. D.J.R. Walstra (WL | Delft Hydraulics) for sharing their knowledge and support during this study. Furthermore, I am very grateful for the opportunity WL | Delft Hydraulics has offered me to complete my study at their institute and I would like to thank my temporary colleagues and fellow graduate students at WL | Delft Hydraulics for showing their interest and making my stay a very pleasant one. Finally I would like to thank my family and friends for their support during the years I spent in Delft.

Summary

In Holland a large part of the Dutch mainland is protected from the sea by dunes. The dunes (and therefore the coastline) used to be a moving defence system in a dynamic equilibrium. At present the Dutch coast is fixed in its landward movement because of man-built structures (e.g. houses), which makes it necessary to prevent the current coastline from erosion. An often-used soft method to maintain the coastline is sand nourishment at the beach or shoreface. Advantages of this method are the relatively small (negative) effects on adjacent coastlines and the relatively low impact on the ecosystem.

There are however some locations along the Dutch coast, where the sand nourishment on the beach is less effective. The beach nourishment has to be applied every (other) year, which makes this protection method relatively expensive. One of these locations is Egmond aan Zee.

In the summer of 1999 a beach nourishment combined with a shoreface nourishment took place in Egmond aan Zee. The shoreface nourishment was carried out to see if this method is a more effective way of nullification of coastline erosion. In order to watch the development of the coast as a result of the shoreface nourishment, the bathymetry has been regularly measured.

This report is the second part of a study to understand the behaviour and effects of shoreface nourishments. The first part of the study exists of an extensive data analysis in order to reach a good understanding of the data, the dominant processes and their corresponding changes. This second part of the study consists of a hindcast study using the UNIBEST-TC model, to see if this model is able to calculate with profiles including a shoreface nourishment and to reach an even better understanding of the dominant processes.

The main objective of this study is to calibrate, validate and evaluate the morphodynamic UNIBEST-TC model with the observations made by RIKZ (bathymetry data) and to evaluate the effect of the shoreface nourishment on the morphodynamics.
The conclusions will be used as reference for calibration and validation of the UNIBEST-TC model. If the UNIBEST-TC model gives results similar to the measured results, it might be possible to use this model for further study on the shoreface nourishment at Egmond and perhaps also at other locations.

The model is calibrated on the averaged cross-shore profile of the section south of the shoreface nourishment. This cross-shore profile is most representative for the undisturbed situation since the net longshore transport at Egmond aan Zee is in northern direction.
The calibration leads to the conclusion that the model performance on the undisturbed situation is satisfying. Variations in friction factors have large influence on the model results. Small variations in the grain size parameter however, do not lead to significant changes in the model performance.

After the calibration the model is validated on a longshore averaged cross-shore profile of a section, that includes the middle part of the shoreface nourishment. The validation study

showed that the model is able to compute profile changes for a cross-section including a shoreface nourishment. The detachment of the outer breaker bar from the shoreface nourishment as well as the generation of a trough between them is predicted to some extent by the UNIBEST-TC model, although both processes are underestimated. For cross-shore profiles including a shoreface nourishment as well as for profiles in an undisturbed situation, the model predicts a too high bed level in the nearshore area.
Remarkable is the fact that the UNIBEST-TC model appears to be able to calculate satisfying bottom profile predictions for longshore averaged cross-shore profiles of sections south or north of the nourishment and sections, in which the middle part of the nourishment is located. For cross-shore profiles of sections including one of the ends of the shoreface nourishment, a poor model performance is observed. This leads to the conclusion that around the ends of the nourishment 3D processes, which are not included in the UNIBEST-TC model, play an important role.

Besides evaluating the cross-shore profile changes, it is desirable to discover where, according to the UNIBEST-TC model, in the cross-shore profile sedimentation or erosion occurs and in what way the sediment in the cross-shore profile is redistributed during the investigated period.
The volume calculations with the UNIBEST-TC model appeared to be an over-estimation of the observed volumes. This is probably caused by the fact that the model imports sediment from deep water into the investigated area.

The model is not able to predict sedimentation and erosion patterns for the section south of the nourishment. For the section, including the middle part of the nourishment, on the other hand, the predicted patterns are in accordance with the observed patterns. This could indicate that in this section the cross-shore processes are dominant, in contrast to those in southern section.

The volume calculations of the model confirm the assumption, made in the data analysis, that behind the shoreface nourishment a lot of sediment is gathered as a result of the lee effect of the nourishment in cross-shore direction. Large waves break at the shoreface nourishment, which causes a reduction of the wave height behind the shoreface nourishment. This calmer wave climate results in less stirring of the sediment and a decreasing wave-induced return flow (cross-shore currents). The decreasing return flow results in less offshore transport, which corresponds to a sediment increase in the area shoreward of the shoreface nourishment.

Whether the shoreface nourishment has a positive effect on the actual beach, can not be concluded from the results of the UNIBEST-TC model. However, the assumption can be made that the shoreface nourishment has a small negative effect on the ‘visible’ beach (the part above water level), since the sediment transport diagram of the section, including the nourishment, showed export from the nearshore area to the surf zone. In the southern section the transport is just the reverse.

It is recommended to do research on this shoreface nourishment over a longer period and on shoreface nourishments at other locations. The results of this proposed research might be useful for confirmation of the assumptions made in this study.

Contents

1 Introduction

In Holland a large part of the Dutch mainland is protected from the sea by dunes. The dunes (and therefore the coastline) used to be a moving defence system. These days that system is limited in its landward movement by man-built structures (e.g. houses), which makes it necessary to prevent the current coastline from erosion. An often-used soft method to maintain the coastline is sand nourishment at the beach or shoreface. Advantages of this method are the relatively small (negative) effects on adjacent coastlines.

There are however a few locations along the Dutch coast, where the sand nourishment on the beach is less effective. The nourishment has to be renewed every (other) year, which makes this protection method quite expensive. One of these locations is Egmond aan Zee.

Egmond aan Zee is located in the central part of the Dutch North Sea coast. See Figure 1.1. Typical for this particular coastline is the presence of almost uniform sandy beaches, which are dominated by two longshore bars intersected by local rip channels. The area consists of a straight, natural, sandy beach and there are no structures in the vicinity.

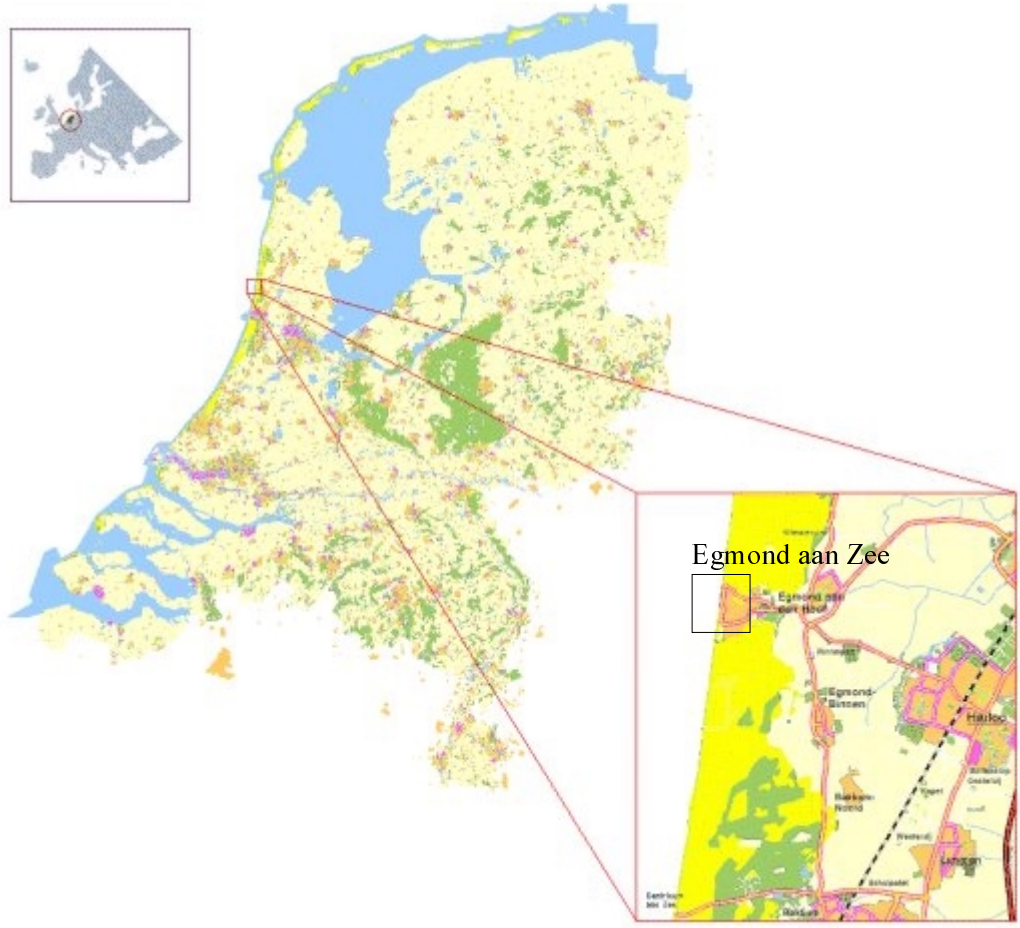

Figure 1.1: Location of Egmond aan Zee

In the summer of 1999 a beach nourishment combined with a shoreface nourishment took place in Egmond aan Zee. The shoreface nourishment was carried out to see if this method is a more effective way of nullification of coastline erosion. In order to watch the development of the coast as a result of the shoreface nourishment, the bathymetry has been regularly measured.

This report is the second part of a study to understand the behaviour and effects of shoreface nourishments. The first part of the study exists of an extensive data analysis in order to reach a good understanding of the data, the occurred processes and their corresponding changes. This second part of the study consists of a hindcast study using the modelling program UNIBEST-TC, in order to reach an even better understanding of all the processes that played a role. The data analysis is used to compare the modelled results to the measured data. The third part of the study consists of a hindcast and sensitivity study using the modelling program Delft3D-MOR, in order to reach an even better understanding of all the dominant processes [Van Duin, 2002].

The aim of this study is to calibrate, validate and evaluate the morphodynamic UNIBEST-TC model with the observations made by RIKZ (bathymetry data) and to evaluate the effect of the shoreface nourishment on the morphodynamics.

Chapter 2 of this report starts with an analysis of the bottom data. It is a short summary of the first part of the study. The morphological aspects of the Egmond site and the bathymetry per data set are discussed. The chapter concludes with the conclusions found during the data analysis [Van Duin and Wiersma, 2002].

The UNIBEST-TC model is described in Chapter 3. Besides a step by step explanation of the model and the accompanying equations, all input parameters and their default values are given.

Chapter 4 discusses the sensitivity analysis and the calibration of the UNIBEST-TC model, carried out on a section that represents the undisturbed situation. First the parameters to be varied, the statistical tools, which are used for evaluation of the model, and the results of the sensitivity analysis and the default run are presented. Subsequently the results of the calibration are discussed. The chapter ends with the conclusions found in the calibration.

In Chapter 5 the calibration results are validated on a section, in which the shoreface nourishment is located. First the default run is described, next the validation results are presented. The chapter is closed with a brief description of the model behaviour on other sections of the Egmond site and the conclusions drawn from the validation study.

Reflections on sediment transports within the cross-shore profiles and the model performance in the computation of volume changes and MCL (= Momentary Coast Line) volumes are given in Chapter 6.

In Chapter 7 conclusions are drawn towards the influence of the shoreface nourishment on the Egmond coast and the model performance for cross-shore profiles including a shoreface

nourishment. Furthermore recommendations with respect to modelling in UNIBEST-TC and study on shoreface nourishments are given.

2 Data description

2.1 Introduction

The first part of this study consisted of an extensive data analysis and can be found in "Evaluation of the Egmond shoreface nourishment, Part I: Data analysis" [Van Duin & Wiersma, 2002]. This chapter only gives a short summary of the analysed data.

Section 2.2 describes the available data, Section 2.3 the nourishments at Egmond aan Zee in the investigated period and Section 2.4 describes the basic features of the morphology. Finally the bathymetry per data set is described in Section 2.5.

2.2 Available data

The bathymetry data has been gathered both by ship and WESP (Water En Strand Profiler) soundings by the RIKZ (Rijks Instituut voor Kust en Zee). The main transect of the investigated area is in front of the lighthouse, Jan van Speijk. Jan van Speijk has the RD co-ordinates 103011, 514782. This main transect also crosses the centre of the shoreface nourishment and beach pole km 38.00. The location and orientation of the study area are shown in Figure 2.1, as well as the location of the shoreface nourishment.

The shoreface nourishment was applied in August 1999, therefore only data available after this date are of interest to this study.

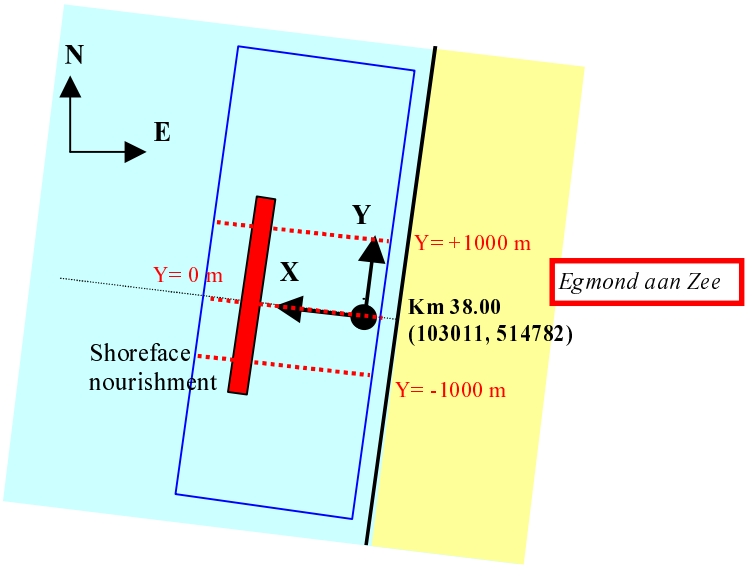

Figure 2.1: Location and orientation of study area and shoreface nourishment (x=0 represents beach pole line; measures in m)

2.3 Nourishments at Egmond aan Zee

At Egmond aan Zee a combined nourishment of the shoreface and the beach is applied in 1999. The centre of the shoreface nourishment is in front of the lighthouse, Jan van Speijk, or beach pole 38. The nourishment is approximately two kilometres long and 200 meters wide. In July 2000 another beach nourishment is applied. More details can be found in Table 2.1 below.

Table 2.1: Data on the beach and shoreface nourishments at Egmond aan Zee

	Shoreface nourishment	Beach nourishment 1999	Beach nourishment 2000
Start of construction	23 June 1999	April 1999	30 June 2000
End of construction	08 Sept 1999	May 1999	05 July 2000
Southern boundary	RSP 39.124 (y = -1125 m)	RSP 38.750 (y = -750 m)	RSP 38.800 (y = -800 m)
Northern boundary	RSP 36.875 (y = +1124 m)	RSP 37.250 (y = +750 m)	RSP 38.000 (y = 0 m)
Characteristic volume of nourishment	400 m^3/m	200 m^3/m	258 m^3/m
Total sand volume	900.000 m^3	300.000 m^3	207.000 m^3

In the data analysis all data was interpolated to a local grid. The grid orientation is as follows:

x : perpendicular to local orientation of the coastline (i.e. 278°N)

y : parallel to local orientation of the coastline (i.e. 8°N)

The grid has its origin at beach pole 38 (co-ordinates (0,0)) and the normal to the orientation of 278°N (i.e. parallel to the local shoreline). The spacing of the soundings is 50 meters.

Figure 2.2 shows three transects at Y = +1000m, Y = 0m and Y = -1000m. The locations of the transects are shown in Figure 2.1.

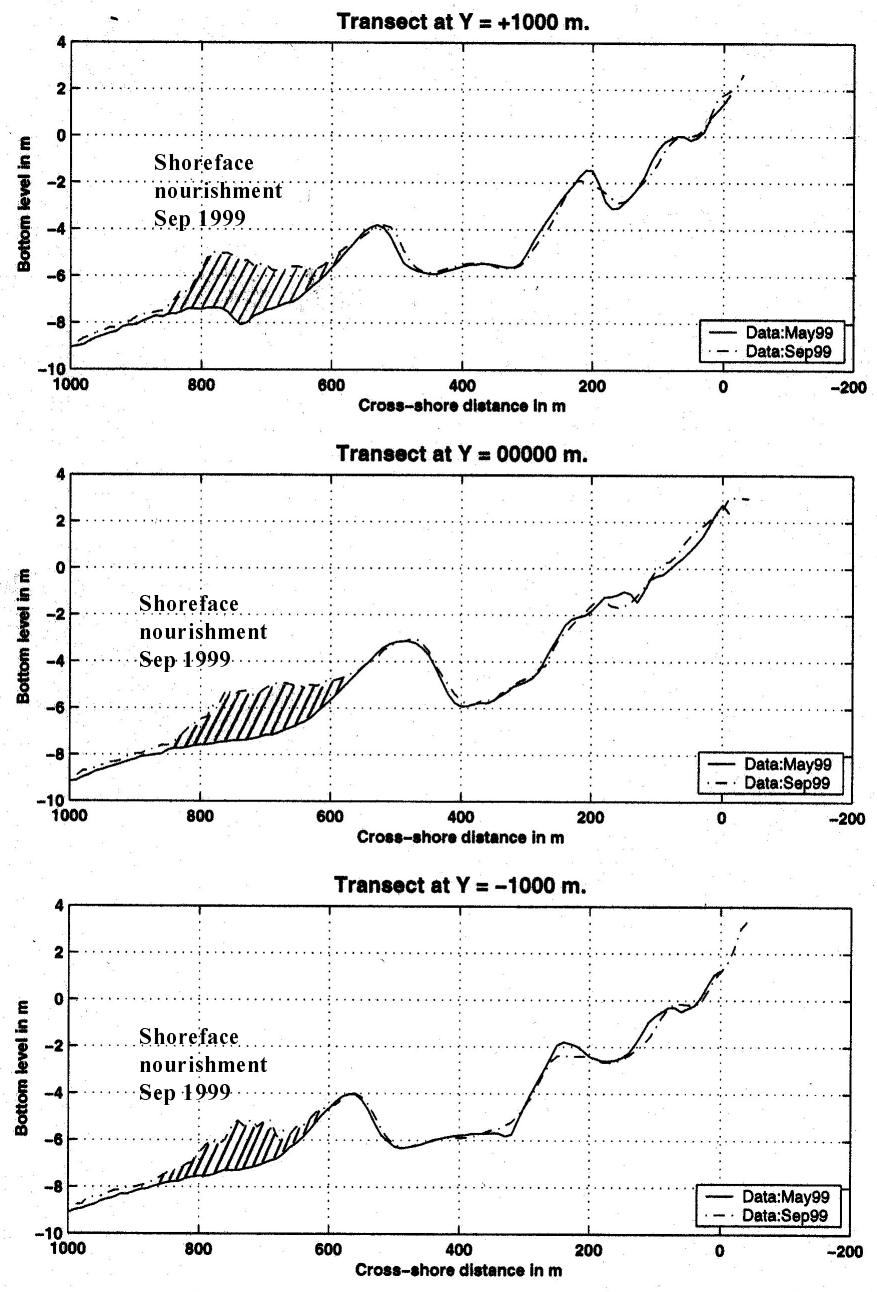

Figure 2.2: Transects showing the shoreface nourishment

2.4 Morphological aspects of the Egmond site

The Egmond site shows some key features which are described below and can also be seen in Figure 2.3:

- The coastal profile at Egmond is a three bar system: two breaker bars in the surf zone and a swash bar.
- The outer bar is most pronounced, the crest is located at depths below NAP -3 m.
- The trough between the outer and inner bar is about 100 m wide and reaches depths of NAP -5 m.
- The inner bar crest is located 300 m landward from the outer bar crest.

- Between inner bar and swash bar is a trough that is less pronounced as the offshore trough and reaches depths of NAP -2 m.
- The bars show longshore non-uniformities, rhythmic patterns are present. With a longshore interval of approximately 2000 m “rip cells” can be distinguished (see also Figure 2.4).

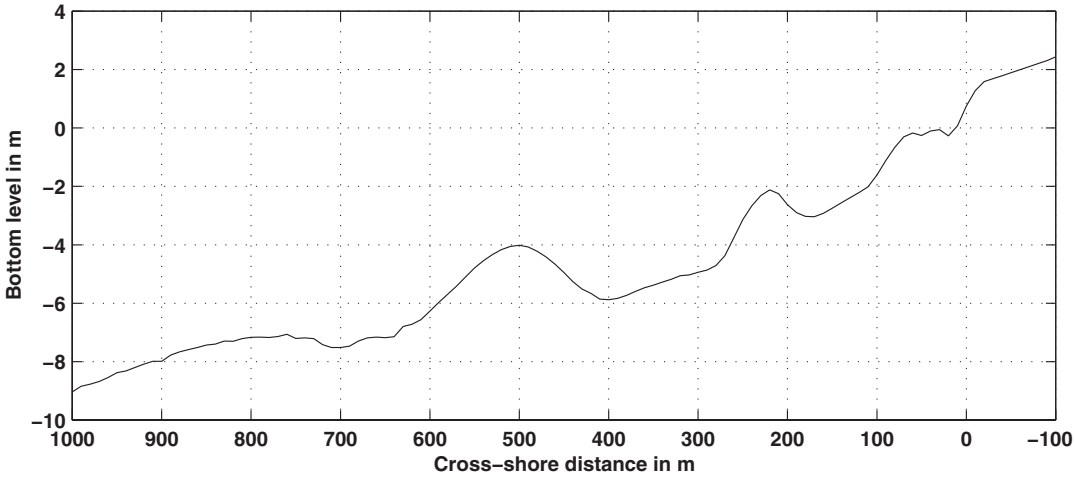

Figure 2.3: Typical cross-shore profile at Egmond

2.5 Description of the bathymetry

Figure 2.4, 2.5 and 2.6 show the 2D-plots of the surveyed data. As can be seen from the figures, the system is a three bar system as described above.

In May 1999 (left plot, Figure 2.4) the direction of the original outer bar is not parallel to the longshore axis. If the location of the crest of the original outer bar at y = 0 m is taken as the pivot point, a clockwise rotation of the crest of the original outer bar can be noticed in the study area. The height of the original outer bar slightly decreases to the south.

September 1999 (right plot, Figure 2.4) clearly shows the shoreface nourishment seaward of the original outer bar. The nourishment is located between 600 and 800 m cross-shore distance and between -1150 and +1200 m longshore distance. The bathymetry for September 1999 is a composite of the WESP survey of September 1999, in which data of Jarkus June 1999 are added since a few WESP data are missing. The added area is shown in Figure 2.6.

In the winter period from September 1999 to May 2000 (upper left plot, Figure 2.5) the shoreface nourishment smoothens and forms a clear bar at 700 m cross-shore. The original outer bar migrates shoreward and a trough is formed between the original outer bar and the shoreface nourishment. The width of the trough between the inner and original outer bar shows a general decrease, especially behind the shoreface nourishment a drastic onshore migration of the original outer bar took place. South of the shoreface nourishment the original outer bar remains in place and becomes detached from the adjacent original outer bar, a rip channel arises. The shape of the inner bar is changing behind the shoreface nourishment. At the centre line of the shoreface nourishment the inner bar is at x = 300 m

whereas at the ends of the shoreface nourishment (y = -1150 and y = +1200 m) the inner bar has moved shoreward, it has transformed into a boomerang shape.

From May 2000 to September 2000 (upper right plot, Figure 2.5) no large morphological changes took place. The centre section of the beach has risen as a result of a beach nourishment, placed in the first week of July 2000. In longshore direction the beach nourishment reaches from y = -800 m to y = 0 m.

During the winter period 2000-2001 considerable morphological changes took place again. Behind the shoreface nourishment the original outer bar develops into the same boomerang shape as the inner bar. The shoreface nourishment also seems to develop into a boomerang shape, but to a lesser extent. The centre of the shoreface nourishment has stayed in place whereas the ends have moved shoreward. The original outer bar starts to replace the inner bar and the shoreface nourishment seems to become the new outer bar.

At June 2001 (lower right plot, Figure 2.5) the original outer bar has straightened somewhat behind the shoreface nourishment. The trough between inner and original outer bar became wider in the centre. In general the profile has smoothened. The shoreface nourishment has not changed much.

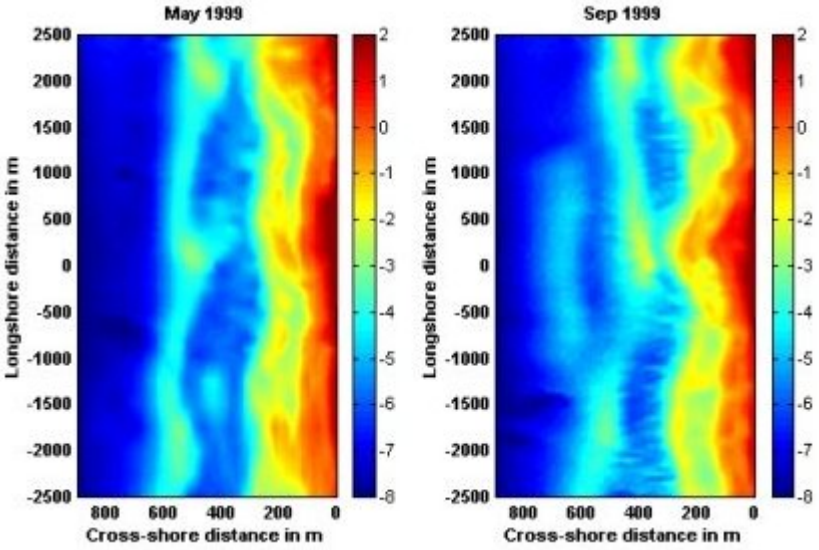

Figure 2.4: 2D-plots of measured bathymetries at Egmond (colour-scale in m w.r.t. NAP)

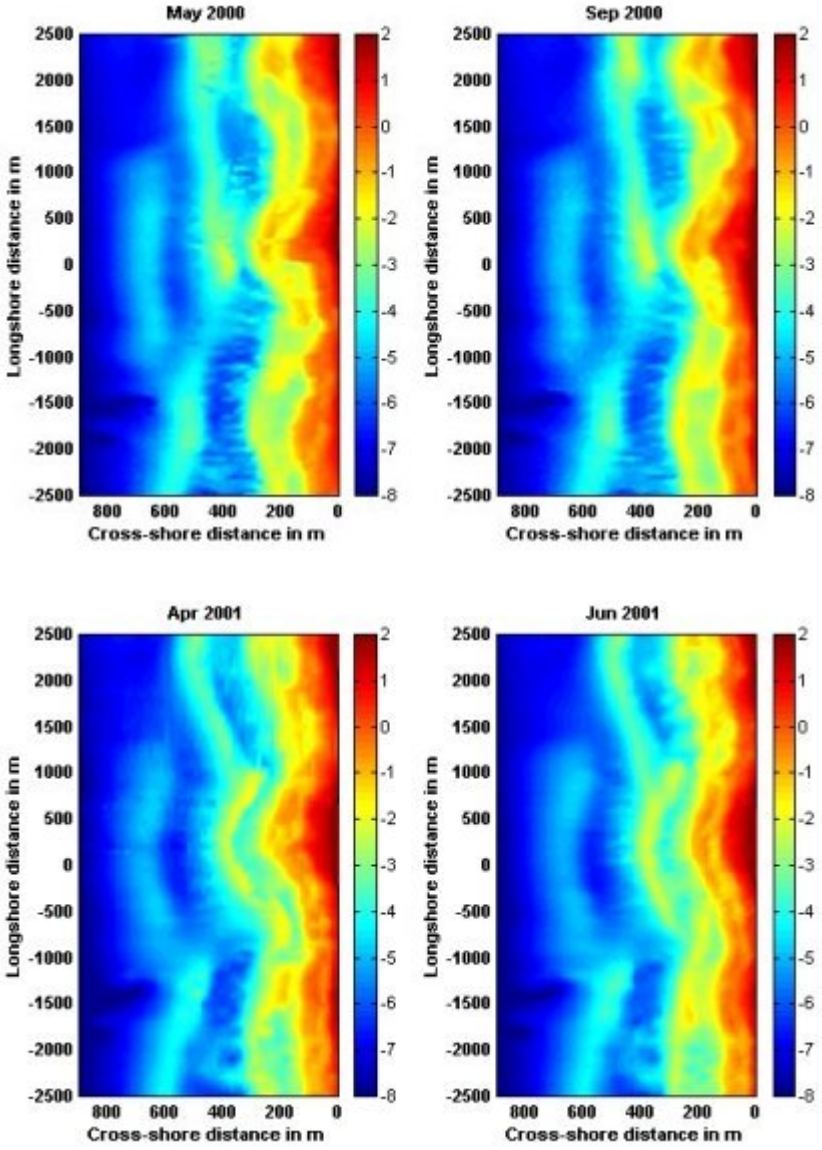

Figure 2.5: 2D-plots of measured bathymetries at Egmond (colour-scale in m w.r.t. NAP)

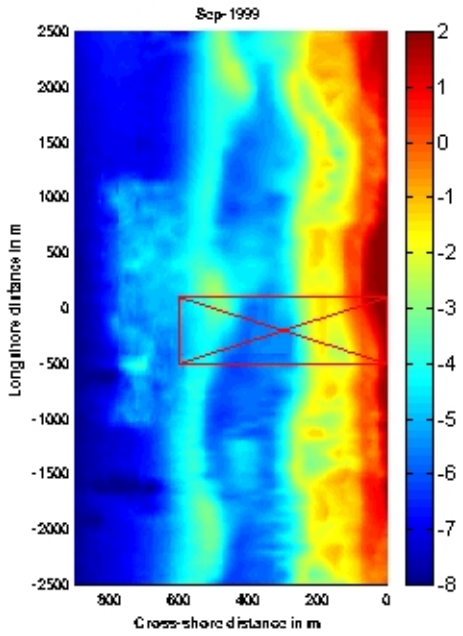

Figure 2.6: 2D-plot of Egmond bathymetry September 1999, with data gap (colour-scale in m w.r.t. NAP)

As can be seen from the 2D-plots (Figure 2.4 and Figure 2.5) the shoreface nourishment acts as outer bar, taking over the function of the original outer bar. It hardly changes in height and place. In the lee of the shoreface nourishment the most radical changes take place. The original outer bar migrates shoreward, but the latest survey seems to indicate that the shoreward migration has stopped, but it is too early to make any definite conclusions.

An explanation for the stability of the nourishment can be the location. The nourishment was done in an area where morphological changes occur at a large time scale. The time scale in which morphological changes occur is years for the location of the shoreface nourishment. The beach zone however has a time scale of days in which large morphological changes can occur.
The data, used in this evaluation, are only of a relatively short period of time (two years after the nourishment).

2.6 Conclusions

The first part of this study, the data analysis, is only shortly described in this chapter. The conclusions that resulted from the first part of this study are shown below:

- The shoreface nourishment at Egmond aan Zee has not changed in height or location. Therefore it has not increased the beach sand volume directly, i.e. by redistribution of the nourished sand. The northern and southern ends of the nourishment have moved shoreward.
- Although no significant decrease of the sand volume of the shoreface nourishment occurred, the investigated area showed a net gain of sand in the surveyed period. Therefore this sand has to come from longshore or cross-shore transport.

- The shoreface nourishment seems to function as a reef. The reef effect causes a lee shoreward of the shoreface nourishment and has effect on both the cross-shore and longshore transport.
- The large bar movements indicated a change in the original inner and outer bars. Because of the large shoreward movement of the original outer bar, the shoreface nourishment seems to become the new outer bar. The original outer bar becomes the new inner bar.
- The level of the bar crest has effect on the beach volumes. Caljouw and Kleinhout [2000] suggested stable beach volumes for inner bar crest levels higher than -1.5 m. This corresponds to the observed beach volumes and inner bar crest levels of this study.
- The first beach nourishment applied in April 1999 showed a strong decrease in sand volume after the following winter (May 1999 to May 2000), whereas the second beach nourishment applied in June/July 2000 showed a relatively small decrease in sand volume after the following winter (September 2000 to June 2001). This second beach nourishment is better protected by the inner bar, which has moved shoreward because of the influence of the shoreface nourishment. Therefore it may be concluded that the combination of a shoreface nourishment with a beach nourishment seems to have functioned as planned.

These conclusions will be used as reference for calibration and validation of the UNIBEST-TC model. If the UNIBEST-TC model gives results similar to the measured results, it might be possible to use this model for further study on the shoreface nourishment at Egmond and perhaps also at other locations.

3 The UNIBEST-TC model

3.1 Introduction

This chapter describes the UNIBEST-TC model, based on Bosboom et al. [1997]. The model derives its name from **Uni**form **Be**ach **S**ediment **T**ransport - **T**ime Dependent **C**ross-shore. UNIBEST-TC is a process-based model that incorporates models for hydrodynamic processes, which in turn provides input to the sediment transport and bed level models.

3.2 Schematisation of the UNIBEST-TC model

3.2.1 General

The basic assumption in the model is that the coast is uniform in longshore direction. A wave energy balance based on Battjes and Janssen (1978) can be used to provide the cross-shore distribution of wave height, dissipation and set-up. These parameters in turn drive local models for the longshore and cross-shore velocity profiles, in which also wind and tidal influences are included. Combined with a model for the near-bed orbital velocity this information is used in the prediction of longshore and cross-shore sediment transport rates.

The cross-shore distribution of the transport determines the changes in the profile depth. These changes are fed back into the profile and the process is repeated over a number of morphological time steps, using a robust, fully implicit numerical scheme.

The model requires an initial profile, grain sizes and offshore boundary conditions for waves, water level, tidal velocity and wind velocity. These boundary conditions usually vary in time. The morphological time step must be small enough to represent the natural fluctuations.

The UNIBEST-TC model consists of the following five sub-models.

- Wave propagation model
- Mean current profile model
- Wave orbital velocity model
- Bed load and suspended load transport model
- Bed level model

A schematic representation of the UNIBEST-TC model is given in Figure 3.1.

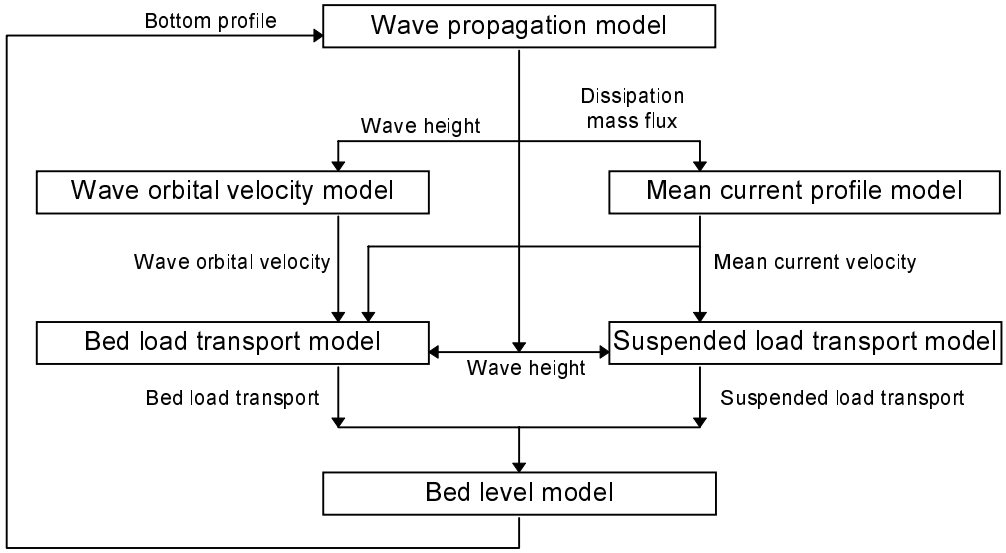

Figure 3.1: Schematic representation of the UNIBEST-TC model

3.2.2 Wave propagation model

The wave propagation model computes the wave energy decay along a cross-shore ray including the effects of shoaling, refraction and energy dissipation. The UNIBEST-TC wave propagation model consists of three first-order differential equations, viz. the wave energy balance [Battjes & Janssen, 1978], the wave set-up equation and the balance equation for the energy contained in surface rollers in breaking waves [Nairn et al., 1990]. The three coupled equations are solved by numerical integration over the cross-shore profile. These equations generate the input required by the local models for the vertical velocity profile, the concentration vertical and the bed-load transport.

The first differential equation, the wave energy balance for waves perpendicular to the coast reads:

$$\frac{\partial Ec_g}{\partial x} + D_b + D_f = 0 \qquad (3.1)$$

in which:

Ec_g	energy flux	[W/m]
c_g	wave group velocity	[m/s]
E	wave energy	[J/m^2]
D_b	dissipation due to breaking	[J/m^2/s]
D_f	dissipation due to bottom friction	[J/m^2/s]
x	position perpendicular to the coastline	[m]

The energy flux in this equation is defined as follows:

$$Ec_g = \frac{1}{8}\rho_w g H_{rms}^2 \cdot c_g \tag{3.2}$$

with:

ρ_w	density of water	[kg/m^3]
g	gravitational acceleration	[m/s^2]
H_{rms}	root mean square wave height	[m]

The dissipation due to breaking is modelled as:

$$D_b = \frac{1}{4}\cdot\alpha\cdot Q_b \cdot f_p \cdot \rho_w \cdot g \cdot H_{\max}^2 \tag{3.3}$$

with:

α	dissipation coefficient	[-]
f_p	peak frequency	[s^{-1}]
Q_b	fraction of breaking waves	[-]
H_{max}	maximum wave height non breaking waves	[m]

The model applies a so-called clipped Rayleigh through the surf-zone, assuming that the waves smaller than H_{max} are not breaking and Rayleigh distributed, and that all waves larger than H_{max} are breaking. This maximum wave height is defined as a function of the local water depth, according to:

$$H_{\max} = \frac{0.88}{k}\tanh\left(\frac{\gamma kh}{0.88}\right) \tag{3.4}$$

in which:

k	local wave number	[rad/m]
h	local water depth	[m]
γ	wave breaking parameter	[-]

Gamma is a wave breaking parameter to determine the maximum local wave height. The default setting for gamma is the Battjes and Stive (1985) relation (GAMMA='0'). In this relation the values for γ vary with the offshore wave steepness $s_0 = H_{rms,0}/L_0$, according to

$$\gamma = 0.5 + 0.4\tanh(33 s_0) \tag{3.5}$$

Gamma can be varied with values in the range of 0.6 to 0.9. Besides these variations, a variable gamma can be applied (GAMMA='1'). This variable gamma is dependent of kh and is described as follows (see Ruessink, Walstra and Southgate, 2002):

$$\gamma_{\text{var}} = 0.76kh + 0.29 \tag{3.6}$$

The variable gamma is a new concept, on which no research is done yet.

The dissipation due to bottom friction is modelled as:

$$D_f = \rho_w \frac{f_w}{16\sqrt{\pi}} \cdot \left[\frac{\omega H_{rms}}{\sinh(kd)} \right]^3 \tag{3.7}$$

with:

f_w	friction factor	[-]
ω	angular frequency	[rad/s]

The friction factor f_w is the bottom friction factor that influences the amount of wave dissipation due to bottom friction. If wave calculations are made over a relatively long distance (3 to 10 km) this parameter can influence the wave height predictions significantly. Within the surf zone this parameter has little influence as wave breaking is dominant.

The second differential equation, the equation for wave set-up, is defined as:

$$\frac{dS_{xx}}{dx} + \rho_w g(d + \overline{\eta}) \frac{d\overline{\eta}}{dx} = 0 \tag{3.8}$$

in which:

S_{xx}	cross-shore radiation stress	[N/m]
d	water depth	[m]
$\overline{\eta}$	mean wave set-up	[m]

The cross-shore radiation stress is defined as follows:

$$S_{xx} = ((2n - 0{,}5)E + 2E_r) \tag{3.9}$$

with

$$n = \frac{1}{2} + kd / \sinh(2kd) \tag{3.10}$$

in which:

d	water depth	[m]
k	wave number	[rad/m]

The kinetic energy in a roller, E_r is defined as:

$$E_r = \frac{1}{2} \rho_w c^2 \frac{A}{L} \tag{3.11}$$

with:

A	roller area	[m^2]
L	roller length	[m]

The third equation, the roller balance equation is modelled as follows:

$$\frac{\partial(2E_r c)}{\partial x} = D_b - Diss \tag{3.12}$$

in which:

E_r	amount of kinetic energy in a roller	[J/m^2]
c	wave propagation speed	[m/s]
$Diss$	dissipation of roller energy	[J/m^2/s]

The roller energy balance is closed by modelling the dissipation *Diss* of roller energy as the power per unit length performed by the shear stress between roller and water surface:

$$Diss = \beta\rho_w gc\frac{A}{L} = 2\beta g\frac{E_r}{c} \tag{3.13}$$

where β is the slope of the face of the wave (normally in the range 0.05-0.10) and A is written in terms of E_r via Equation 3.10.

Beta (written as 'BETD' in the UNIBEST-TC model) is a roller parameter according to Nairn et al. [1990], expressing the steepness of the wave front. This parameter determines the cross-shore distribution of the surface shear stress due to wave breaking. The best value for beta can probably be found in the range of 0.05 to 1. Instead of a fixed beta, a variable beta can be applied (BVAR=1). The variable beta varies in time and place is defined as (see Walstra et al. [1996] (ICCE 1996)):

$$\beta_{\text{var}} = 0.1kH_{rms}\frac{(h - H_{rms})}{H_{rms}} \tag{3.14}$$

where k is the wave number [rad/m], h is the local water depth and H_{rms} is the root mean square wave height.

3.2.3 Mean current profile model

The mean current profile model is a local model. It computes the vertical distribution of the wave-averaged mean current in both longshore and cross-shore direction accounting for wind shear stress, wave breaking, bottom dissipation in the wave boundary layer and the slope of the free surface.
The determination of the time averaged current profile is done according to Roelvink and Reniers [1994] who use a quasi-3D model.
This quasi-3D model is a direct descendant of the model according to De Vriend and Stive [1987] who identify three layers (see Figure 3.2):

- the surface or trough-to-crest layer, which is represented by boundary conditions on the middle layer;
- the middle layer, from the top of the bottom (wave) boundary layer to the mean water level;
- the bottom boundary layer.

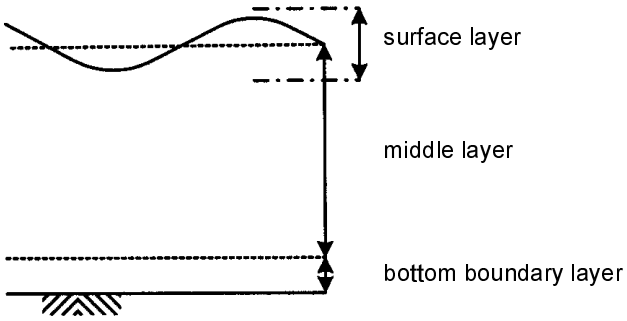

Figure 3.2: Division of current profile in three layers

The time averaged current profile is obtained by integration of the relation between shear stress and the velocity gradient:

$$\tau_i = \frac{\rho_w \nu_t}{d} \frac{\partial u_i}{\partial \sigma} \tag{3.15}$$

in which:

τ_i	shear stress	[kg/ms^2]
ρ_w	density of water	[kg/m^3]
ν_t	turbulent viscosity	[m^2/s]
d	water depth	[m]
u_i	current velocity	[m/s]
σ	relative height above seabed z/d	[-]

The current profile of the middle layer is determined as follows:
The effective shear stress is used as boundary condition for the top of the middle layer at mean water level. In addition to this the mass flux in the surface layer has to be known.
The shear stress in the direction of wave propagation is given by:

$$\tau_{s,wave} = \frac{Diss}{c} \tag{3.16}$$

in which:

$Diss$	dissipation of roller energy	[J/m^2/s]
c	wave propagation velocity	[m/s]

The mass flux in the surface layer is defined as:

$$m = \frac{E + 2E_r}{c} \tag{3.17}$$

with:

E	wave energy	[J/m^2]
E_r	kinetic roller energy	[J/m^2]

The boundary condition at the bottom of the middle layer is determined by estimation of the reference shear stress for breaking waves and the shear stress in the bottom layer for non-breaking waves.
Using the differential equation for the time averaged current profile and the boundary conditions, a value for the mean current is found.

3.2.4 Wave orbital velocity model

The wave orbital velocity model is a local model that calculates time series of the near-bed wave orbital velocity. These time series contain contributions due to wave asymmetry, wave group related amplitude modulation and bound long waves and therefore representative for irregular wave groups.
The model of the time variation of the near-bed velocity (orbital motion) due to non-linear short waves and long waves related to wave groups is based on the concept described in Roelvink and Stive [1989]. In short, this model consists of two parts:

- a contribution due to wave asymmetry that is computed using Rienecker and Fenton's [1981] method for monochromatic waves, where the mean wave energy and peak period are used as input for the case of random waves.
- a contribution due to bound long waves based on Sand [1982], and an empirical relationship for the phase of the bound long wave relative to the short wave envelope.

A time-series of the near-bed velocity in case of regular waves (including wave asymmetry) is defined as:

$$U_1(t) = \sum_{j=1}^{n} B_j \cos(j\omega t) \tag{3.18}$$

with:

U_1	near bed velocity	[m/s]
t	time	[s]
j	number	[-]
B	amplitude	[m]
ω	angular velocity	[rad/s]

By adding a second velocity time series which is slightly out of phase with the first according to Eq. (3.18), the amplitude modulation on the time scale of a wave group is introduced yielding a time series $U_2(t)$:

$$U_2(t) = \sum_{j=1}^{n} \cos(j\omega t)\varepsilon^j = \sum_{j=1}^{n} \cos(j\omega t)\left[\frac{1}{2}(1+\cos(\Delta\omega t))\right]^j \tag{3.19}$$

in which:

$\Delta\omega$	ω/m	[rad/s]
m	number of waves in one wave group (set to 7 in UNIBEST-TC)	[-]
ε	formulation for second time series	[-]

Finally, the magnitude of U_2 is corrected to U'_2:

$$U_2'(t) = \left(\frac{\frac{1}{T}\int_0^T U_1^3 dt}{\frac{1}{mT}\int_0^{mT} U_2^3 dt} \right)^{1/3} U_2(t) \tag{3.20}$$

If two wave groups with different angular velocities occur, they generate a bound long wave with a much higher angular velocity.
The long-wave amplitude resulting from two waves groups with equal amplitudes is estimated by Sand [1982] as:

$$\xi_a = -G_{nm}\frac{a_n a_m}{d} \tag{3.21}$$

In the equation above (Eq. 3.18) the short wave amplitudes are equal to:

$$a_n^2 = a_m^2 = \frac{1}{8}H_{rms}^2 - \frac{1}{2}\xi_a^2 \tag{3.22}$$

with:

ξ_a	long-wave amplitude	[m]
G_{nm}	transfer function	[-]
a_n, a_m	short wave amplitudes	[m]
d	local water depth	[m]

The orbital velocity time series $U_3(t)$ due to the long wave component is described by:

$$U_3(t) = \hat{u}_l \cos(\omega_l t + \varphi) \tag{3.23}$$

where

$$\hat{u}_l = \xi_a \frac{\sqrt{gd}}{d} \tag{3.24}$$

and

$$\omega_l = \frac{\omega}{m} \tag{3.25}$$

with:

ω_l	long-wave angular velocity	[rad/s]
φ	phase shift between long-wave and short-wave envelope	[rad]

Final step is the computation of the time series $U_4(t)$ of the total orbital velocity, by simply adding the effects due to the short-wave envelope and the bound long-wave:

$$U_4(t) = U_2^{'}(t) + U_3(t) \tag{3.26}$$

3.2.5 Bed load and suspended load transport model

In the sediment transport model one can distinguish between the bed load and suspended load module respectively. It is assumed that the suspended load transport is dominated by the transport by the mean current; the suspended sediment flux is computed as the product of the wave-averaged current and concentration profiles, which are obtained from the mean current profile model and a time-averaged advection-diffusion equation respectively. The bed-load transport is computed as a function of the instantaneous bed shear stress. The near-bed velocity signals, determining the instantaneous bed shear stresses, are composed of the generated time-series for the near-bed wave orbital velocity plus the time-averaged current velocity near the bed.
Separate transport formulations are used for bed load transport, bed load being that part of the load that is in more or less continuous contact with the bed, and suspended load transport.

Bed load transport
The non-dimensional instantaneous bed load transport vector Φ_{bd}, defined as the ratio of bed load transport rate q_b and the square-root of a parameter representing the specific underwater weight of sand grains, is given by

$$\Phi_{bd}(t) = \frac{S_b(t)}{\sqrt{\Delta g D_{50}^3}} = 9.1 \frac{\beta_s}{(1-p)} \left\{ \left| \theta^{'}(t) \right| - \theta_c \right\}^{1.8} \frac{\theta^{'}(t)}{\left| \theta^{'}(t) \right|} \tag{3.27}$$

with:

S_b	bed load transport *including pores*	[m^3/m/s]
D_{50}	median grain diameter	[m]
Δ	relative density = $(\rho_s-\rho_w)/\rho_w$	[-]
p	porosity of the sediment (= 0.4)	[-]
g	gravity acceleration	[m/s^2]
θ'	dimensionless effective shear stress	[-]
θ_{cr}	dimensionless critical shear stress	[-]
β_s	slope factor, $\beta_s = \frac{\tan\varphi}{\tan\varphi + (dz/dx)}$	[rad]
φ	natural angle of internal friction	[rad]

For the computation of $\theta'(t)$ a quadratic friction law is applied using an intra wave near-bed velocities of the combined wave-current motion and a weighed friction factor f'_{cw} (see van Rijn [1993]):

$$\theta'(t) = \frac{\frac{1}{2}\rho f'_{cw}|u_b(t)|u_b(t)}{(\rho_s - \rho_w)gD_{50}} \tag{3.28}$$

in which u_b is the time-dependent (intra-wave) near bottom horizontal velocity vector of the combined wave-current motion at the top of the wave boundary layer (z = δ). This vector is computed in UNIBEST-TC as the sum of the near bed oscillating velocity signal and the time averaged velocity at 1 cm from the bed.

Parameter θ_c is the dimensionless critical shear stress representing the threshold of motion of sand grains. This threshold parameter is calculated according to the classical Shields curve as modelled by Van Rijn [1993] as a function of the non-dimensional grain size.

Suspended load transport

The suspended sediment transport rate (q_s) can be computed from the vertical distribution of fluid velocities and sediment concentrations, as follows:

$$q_s = \int_a^{d+\eta} VC\,dz \tag{3.29}$$

with:

$$V = v + \tilde{v} \text{ and } C = c + \tilde{c} \tag{3.30}$$

in which:

V	local instantaneous fluid velocity at height z above bed	[m/s]
C	local instantaneous sediment concentration at height z above bed	[kg/m^3]
d	water depth (to mean surface level)	[m]
η	water surface elevation	[m]
a	thickness of bed load layer	[m]
v	time and space averaged fluid velocity at height z	[m/s]
c	time and space averaged concentration at height z	[kg/m^3]
$\tilde{v}$	oscillating fluid component (including turbulent component)	[m/s]
$\tilde{c}$	oscillating concentration component (including turbulent component)	[kg/m^3]

Substituting Eq. 3.27 in Eq. 3.26 and averaging over time and space results in a time averaged current-related sediment transport rate [kg/ms]of:

$$\overline{q}_{s,c} = \int_a^d vc\,dz \tag{3.31}$$

and a time averaged wave-related sediment transport rate [kg/ms] of:

$$\overline{q}_{s,w} = \int_a^d \overline{\tilde{v}\tilde{c}}\,dz \tag{3.32}$$

In UNIBEST-TC the wave-related suspended transport is assumed to be small as compared to the current-related suspended sediment transport. The suspended load transport in volume per unit time and width [m^2/s] *including pores* is therefore computed as:

$$S_{s,c} = \frac{\overline{q}_{s,c}}{(1-p)\rho_s} \tag{3.33}$$

It is assumed that the time averaged convection-diffusion equation, applied to compute the equilibrium concentration profile in steady flow, is also valid for wave-related mixing:

$$c(z) \cdot w_{s,m} + \varphi_d \varepsilon_{s,cw} \frac{dc}{dz} = 0 \tag{3.34}$$

in which:

$w_{s,m}$	fall velocity of suspended sediment in a fluid-sediment mixture	[m/s]
$\varepsilon_{s,cw}$	sediment mixing coefficient for combined current and waves	[m^2/s]
$c(z)$	time averaged concentration at height z above the bed	[kg/m^3]
φ_d	damping factor dependent on the concentration	[-]

For combined current and wave conditions the sediment mixing coefficient is modelled as:

$$\varepsilon_{s,cw} = \sqrt{\left(\varepsilon_{s,w}\right)^2 + \left(\varepsilon_{s,c}\right)^2} \tag{3.35}$$

in which:

$\varepsilon_{s,w}$	wave-related mixing coefficient	[m^2/s]
$\varepsilon_{s,c}$	current-related mixing coefficient	[m^2/s]

The characteristics of the wave-related sediment mixing coefficient are as follows:

- constant mixing coefficient in the near-bed layer ($z \le \delta_s$)
- constant mixing coefficient in the upper half ($z \ge 0.5$ d) of the water depth
- linear variation of the mixing coefficient for $\delta_s < z < 0.5$ d

For the current mixing coefficient, a constant mixing is coefficient is assumed in the upper half of the water column which decreases linearly to zero in the lower half of the column.

Both coefficients are dependent on depth, wave height and current velocity.

In high concentration mixtures, the fall velocity of a single particle is reduced due to the presence of other particles. In order to account for this hindered settling effect, the fall velocity in a fluid-sediment mixture is determined as a function of the sediment concentration c [kg/m^3] and the particle fall velocity w_s:

$$w_{s,m} = \left(1 - \frac{c}{\rho_s}\right)^5 w_s \tag{3.36}$$

The particle fall velocity w_s is, according to Van Rijn [1993], dependent on the grain size and the relative density.

Finally, the time averaged sediment concentration as a function of z is computed as follows:

$$c(z) = c_a e^{-\int \frac{w_{s,m}}{\varepsilon_{s,cw}(z)} dz} \tag{3.37}$$

in which the reference concentration c_a [kg/m^3] is given by:

$$c_a = 0.015 \rho_s \frac{D_{50}}{a} \frac{T^{1.5}}{D_*^{0.3}} \tag{3.38}$$

with:

a	thickness of bed load layer	[m]
D_*	dimensionless particle diameter	[-]

The bed shear stress parameter T [-] is defined as follows:

$$T = \frac{\tau'_{b,cw} - \tau_{b,cr}}{\tau_{b,cr}} \tag{3.39}$$

in which:

$\tau'_{b,cw}$	time averaged effective bed shear stress	[N/m^2]
$\tau_{b,cr}$	time averaged critical bed shear stress according to Shields	[N/m^2]

3.2.6 Bed level model

After the computation of the bed load transport rates and the suspended load transport rates along the profile, the bed level changes are computed from the depth-integrated mass balance:

$$\frac{\partial z}{\partial t} + \frac{\partial S_{b+s}}{\partial x} = 0 \tag{3.40}$$

For each grid point the transport rate is computed. The difference in transport rates between two grid points results in a bed level change between these grid points.

3.2.7 UNIBEST-TC behaviour near water level and at dry profile

The sediment transport computations stop when the water depth becomes too small. At that point the relative wave period reaches a, user defined, value of:

$$T^* = T_p \sqrt{g/d} \tag{3.41}$$

in which:

T_p	peak period	[s]

When this point is reached, the latest computed sediment transport rate is extrapolated over the profile above the water level. This causes changes in the bed level landward of this point. The sediment transport rate of the profile above water level is computed as follows (see also Figure 3.3):

$$S(x) = S_s - \left(\frac{z(x) - z(x_s)}{z(x_e) - z(x_s)} \right) \cdot (S_s - S_e) \tag{3.42}$$

in which:

$S(x)$	transport in dry point x	[m^3/m/s]
S_s	transport in point of latest computed transport	[m^3/m/s]
$z(x)$	bed level in point x	[m]
S_e	transport in latest extrapolation point	[m^3/m/s]
x_e	latest extrapolation point	[m]
x_s	point of latest computed transport rate	[m]

This extrapolation is based on the original formulations of the DUROSTA model and is implemented in UNIBEST-TC by Gootjes [2000].

In the latest extrapolation point (dune top) is no transport (S_e=0).

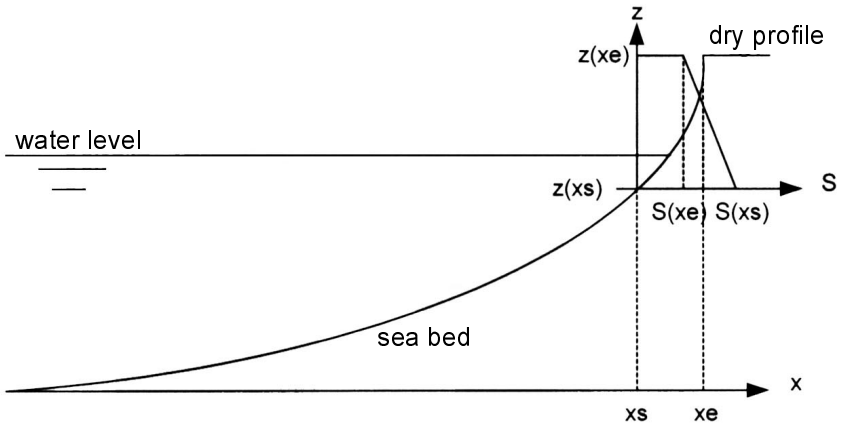

Figure 3.3: extrapolation sediment transport over dry profile

This model, with the sediment mass balance, results in the following description of the dry profile:

$$\frac{dz}{dt} + \frac{S_s - S_e}{z(x_e) - z(x_s)} \frac{dz}{dx} = 0 \tag{3.43}$$

This equation shows that UNIBEST-TC uses linear extrapolation, keeping the profile above $z(x_s)$ fixed and moving it in its entirety landward or seaward, dependent on the magnitude and direction of S_s. The slope of the dune remains the same.

3.3 Parameter settings

Subsection 3.2 showed that the UNIBEST-TC model requires a large number of input parameters. In this subsection the default parameter settings for the UNIBEST-TC model are presented. During the hindcast study, described in this report, most parameters are kept at their default settings, since previous studies on the UNIBEST-TC model [see Walstra et al., 2001; Kleinhout, 2000; Boers 1999] have shown that these settings give the most optimal model results. For a few parameters however, the default values might not be the optimal values in any case, since these parameters are empirical determined or location dependent. For these parameters the optimal values will be determined in the next chapter (Chapter 4, Calibration).
In the following table (Table 3.1) an overview is given of the default value of each parameter.

Table 3.1: default parameter settings

Run parameter	Explanation	Dimension	Default value
DT	time step	days	0.125
USTRA	sediment transport at last computational grid point	m^3/hr	0
IBOD	bottom changes	-	1
TDRY	relative wave period	-	25
K_IJL	breaker delay switch (on/off : 1/0)	-	1
F_LAM	**number wave lengths**	-	**1**
POW	power	-	1
DEEP_V	seaward boundary	m	-5000
SHALL_V	shoreward boundary	m	-5000
TANPHI1	internal friction angle	-	0.3
TANPHI2	internal friction angle	-	0.3
XF1	reference location	m	4100
XF2	reference location	m	5100
FCVISC	**viscosity coefficient**	-	**0.1**
GAMMA	**breaking parameter**	-	**Battjes&Stive**
VARGAMM	**varying gamma switch (on/off : 1/0)**	-	**0**
ALFAC	dissipation parameter	-	1
FWEE	**friction factor**	-	**0.01**
RKVAL	**friction factor**	-	**0.03**
DIEPV	reference depth tide	m	5
REMLG	fixed bed layer	-	0.5
BETD	**roller parameter**	-	**0.1**
BVAR	**varying beta switch (on/off : 1/0)**	-	**0**
D50	**D50 grain diameter**	**m**	**0.000240**
D90	**D90 grain diameter**	**m**	**0.000480**
DSS	**suspended grain diameter**	**m**	**0.000240**
DVAR	**varying grain size switch (on/off : 1/0)**	-	**0**
FDIA0	multiplication factor	-	1.1
FDIA1	multiplication factor	-	0.75
FDIA2	multiplication factor	-	1
HDIA0	reference depth	m	0
HDIA1	reference depth	m	7
HDIA2	reference depth	m	16
RC	**friction factor current**	-	**0.03**
RW	**friction factor waves**	-	**0.01**
TEMP	temperature	°C	10
SALIN	salinity	‰	28
C_R	**correlation wave groups**	-	**0.25**
FACQB	**factor of fraction of breaking waves which does not contribute to wave velocity moment**	-	**0.35**

The input parameters, which will be used to calibrate the model, are printed in bold type. A detailed description of these parameters is given below. The choice of these parameters is based on results of previous studies on the optimisation of the UNIBEST-TC model [see Walstra et al., 2001; Kleinhout, 2000; Boers 1999]. For more information about these parameters and a detailed description of all other input parameters is referred to the UNIBEST-TC User Manual [WL | Delft Hydraulics, 1999] and the Userguide for UNIBEST-TC [Walstra, 2000].

Gamma
Gamma is a wave breaking parameter to determine the maximum local wave height. The default setting for gamma is the Battjes and Stive (1985) relation (GAMMA='0') (see Subsection 3.2.2). Gamma will be varied with values in the range of 0.6 to 0.9. Besides these variations, the variable gamma (see subsection 3.3.2) will be investigated (GAMMA='1').

Betd
Beta (written as 'BETD' in the UNIBEST-TC model) is a roller parameter according to Nairn et al. [1990], expressing the steepness of the wave front. This parameter determines the cross-shore distribution of the surface shear stress due to wave breaking. Beta will be varied with values in the range of 0.05 to 1. Besides these variations the variable beta (see subsection 3.3.2) will be investigated (BVAR=1). If a variable beta is applied, the breaker delay function should be switched off, since both functions serve the same purpose, namely the delay of wave breaking effects.

Fwee
Fwee is the bottom friction factor that influences the amount of wave dissipation due to bottom friction. If wave calculations are made over a relatively long distance (3 to 10 km) this parameter can influence the wave height predictions significantly. Within the surf zone this parameter has little influence as wave breaking is dominant. Fwee will be varied with values in the range of 0.001 to 0.2.

C_R
C_R is the correlation coefficient between the wave envelope and the bound long waves. It varies from -C_R at deep water up to C_R at the shoreline. By increasing C_R the effect of the long wave will be enhanced (i.e. increased offshore transport outside the surf zone and increased onshore transport inside the surf zone). By setting C_R to zero the long wave effect is eliminated. C_R will be varied with values in the range of 0 to 1.

F_lam
F_lam is the number of wave lengths over which the weighted depth is integrated. A higher value of F_lam results in a larger weighted depth, which causes less breaking waves and thus less dissipation at the measured point and moves the location of breaking waves more shoreward. In this study F_lam will be varied in the range of 0.25 to 2.

FACQB
FACQB is a factor for the fraction of breaking waves which does not contribute to the onshore wave velocity moment. By reducing the onshore transport component via this

factor the profile development can be tuned. An increasing FACQB results in a decreased onshore transport and vice versa. The value of FACQB will be varied between 0 and 1.

FCvisc

With FCvisc, a factor in the depth averaged turbulence expression, the vertical structure of the return flow is influenced. Higher values result in increased viscosity values and hence relative straight velocity profiles, and the opposite holds for low values. FCvisc is varied in the range of 0.01 to 0.2.

RKVAL

RKVAL is the friction factor for the mean current. The friction factor is in fact a roughness height, which is related to the grain size of the bed material or to the ripple height (if present). This parameter can be used to optimise velocity results, higher values result in large bed shear stresses and vice versa. The value of RKVAL will be varied in the range of 0.001 m to 0.1 m.

RC and RW

RC and RW are the current and wave related roughness for sediment transport computation. They are used in the transport module and can have a significant effect on the resulting transports. However, the resulting transport can be somewhat unpredictable. In general, the RW value should be lower than the value for RC. The RW value will be varied between 0.001 m and 0.02 m; the RC value will be varied in the range of 0.003 m to 0.04 m.

D50, D90 and DSS

D50 is the median grain size (D_{50}) of the bed material, D90 is the 90% grain size (D_{90}) of the bed material and DSS is the median grain size (D_{50}) of the suspended sediment. The default grain sizes are based on measurements from the COAST3D Egmond field site [Kleinhout, 2000]. The D50 will be varied between 200 μm and 300 μm, the D90 will be varied in the range of 325 μm to 480 μm and the DSS will be varied between 150 μm and 300 μm. In some cases is calculated with a cross-shore varying grain size. In the UNIBEST-TC model the particle grain size can be varied cross-shore by means of specifying multiplication factors (FDIA0, FDIA1 and FDIA2) at three reference depths (HDIA0, HDIA1 and HDIA2) in the bottom profile.

4 Calibration of the UNIBEST-TC model

4.1 Introduction

Before the actual hindcast study can be carried out, the sensitivity of the model parameters needs to be analysed and the model has to be calibrated. The sensitivity analysis and the model calibration will be discussed in this chapter. Prior to this discussion the applied statistics, the input parameters, the used data, the boundary conditions and the default parameter settings will be presented.
The main purpose of this chapter is to determine the best input parameter settings for validation of the UNIBEST-TC model on the shoreface nourishment.

4.2 Input parameters

In order to find reasonable results with the UNIBEST-TC model, a lot of site specific parameters are required. Furthermore numeric and practical parameters have to be defined. An example of a practical parameter is the time step, which is desired not to be too small in order reduce the calculation time, on the other hand it should not be larger than half a tidal period (i.e. 6 hours) in order to use at least one value of each high and each low tide. All default input parameters are based on results of previous studies or at survey results of the Coast3D project [see Kleinhout, 2000]. A detailed list of all input parameters can be found in Subsection 3.3.

The available bottom profiles, resulting from WESP (Water En Strand Profiler) surveys, can be found the following table (Table 4.1). In this table is described from which date the profiles are and for what purpose they will be used.
The bottom profile of September 1999 is chosen as the input bottom profile for all model simulations, since this is the first profile measured after the placement of the shoreface nourishment. The sensitivity analysis will be carried out for the period between the first and second survey date. While this is a winter period and most morphological changes occur during the winter, the sensitivity of all parameters will be easy to detect in simulations over this period.
Since the natural dynamic sediment balance of the coastal zone is disturbed by the placement of the nourishment, it is expected that the coast needs a few years to find a new (dynamic) balance. Therefore it is decided not to use the bottom profile of September 2000, since this is the situation after only one year. The bottom profiles of April 2001 and June 2001 are very much alike, so the latest profile (i.e. June 2001) is chosen as reference profile for the calibration of the model to get the longest possible simulation period.

Table 4.1: available bottom profiles

PROFILE DATE	USED AS
September 1999	Input bottom profile
May 2000	Reference bottom profile for sensitivity analysis
September 2000	-
April 2001	-
June 2001	Reference bottom profile for calibration

For both the sensitivity analysis and the calibration the longshore averaged bottom profile of section 5 (see Figure 4.1) is used. This section is situated south of the shoreface nourishment. The main longshore currents travel from south to north, so the shoreface nourishment has hardly any influence at the currents in section 5. Since the dominant wave directions are west and south-west, the main part of the waves that enter section 5 is not influenced by the shoreface nourishment. Given the facts described above, section 5 can be considered as an undisturbed situation. This makes section 5 the best section for calibration of the model, since for the undisturbed situation most parameters are known from previous studies. It has to be noticed that in this undisturbed situation erosion is found.

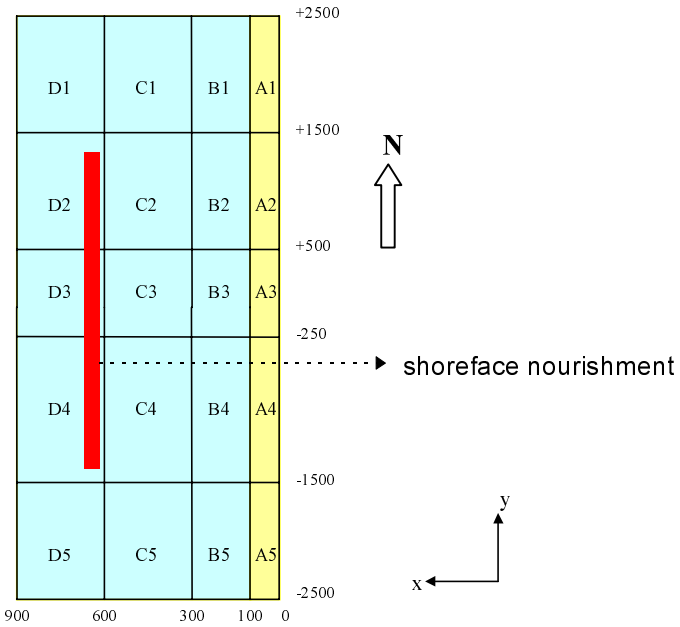

Figure 4.1: Investigated area divided in primary sections (measures in m)

The input parameters for wave height, wave period, peak wave period and tidal elevation are retrieved from Rijkswaterstaat data at the location 'IJgeul munitiestortplaats'. Gaps in these data sets are filled up with data from measuring point 'Europoort'.

Simulations in UNIBEST-TC, using all input parameters mentioned above, result in a prediction of the bottom profile at the end of the simulated period and the volume development during the simulated period.

The UNIBEST-TC model is based on the idea of no sediment import or export in the modelled profile. The survey data however (see Part I: Data analysis [van Duin and Wiersma, 2002]), show a sediment loss of 12.820 m^3 in section 5. This loss is relatively small, therefore, for all model calculations, it is assumed that the modelled area does not exchange sediment with the surroundings.

4.3 Applied statistics

The main question in evaluating the model is whether the predicted profile is more or less equal to the measured profile. Yet it is not to be expected that the predicted profile will be exactly like the measured profile. Therefore, the model will also be judged at its prediction of bar movements (landward/seaward compared to initial profile) and bar height changes (increase/decrease compared to initial profile).
Besides this 'bare eye' judgement of the profile predictions, two statistical parameters are used to evaluate the model results. These two parameters are the Root Mean Square error (RMS-error) and the Brier Skill Index (BSI). Below a summary of these parameters is given. The RMS-error is defined as:

$$RMS = \sqrt{\frac{1}{N}\sum_{i=1}^{N}(f_{comp,i} - f_{meas,i})^2} \tag{4.1}$$

The RMS-error is measured in meters and indicates the averaged error in the bottom prediction. Large values for the RMS -error indicate a poor model performance. In order to obtain better insight in the model performance in relation to the default settings, the relative RMS-error is used. This relative RMS-error is defined as:

$$RMS(rel.)_{run} = RMS_{default} - RMS_{run} \tag{4.2}$$

Positive values for the relative RMS-error indicate a better model performance than performance of the default settings, negative values indicate lesser model performance.

The second parameter is the Brier Skill Index (BSI), which is defined in terms of mean-squared differences between measured values, modelled values and a set of baseline predictions (in this case the default predictions), $f_{base,\ i}$. A value of 1 indicates a perfect score, 0 implies no better score than the baseline prediction, and a negative score is a worse prediction than the baseline prediction. In this study the baseline prediction is the prediction, using the default settings.

The BSI is defined as:

$$BSI = 1 - \frac{\frac{1}{N}\sum_{i=1}^{N}(f_{comp,i} - f_{meas,i})^2}{\frac{1}{N}\sum_{i=1}^{N}(f_{meas,i} - f_{base,i})^2} = 1 - \frac{MS_{error}}{MS_{baseerror}} \tag{4.3}$$

The statistical results of the model performance should be used with care and never without the predicted cross-shore profiles next to them. It may occur that a variation of a certain parameter results in a positive BSI score and a positive relative RMS-error, whilst the cross-shore profile, compared to the default results, shows a poor prediction.
Both statistical parameters are not applied at the total profile, but at the profile between x = 4081 m and x = 4981 m (according to the UNIBEST-TC grid), which corresponds to the profile between x = 900 m and x = 0 m in the grid used in Part I, the data analysis [van Duin and Wiersma, 2002]. This section of the total profile is the cross-shore profile of the investigated area in the data analysis. The choice for this section is based on the fact that for every point in this section survey data are available, so no extrapolation is needed, which avoids extrapolation errors.
Besides application of the statistical parameters over the total profile, they are also applied at three cross-shore sections to obtain better insight in the model performance at the different sections of the profile. The three sections are defined as follows, according to the primary cross-shore sections in Figure 4.1:

D deep water section, includes the shoreface nourishment (section D in Figure 4.1)
C middle section, includes the outer breaker bar (section C in Figure 4.1)
AB beach section, includes the inner breaker bar and the beach zone (sections A and B in Figure 4.1)

These sections can also be found in Figure 4.2 in subsection 4.5.1, which describes the default run and they should not be confused with longshore sections 1 to 5 (see Figure 4.1).

4.4 Sensitivity analysis

Before calibrating the model, it is desirable to get a general idea of the model response to specific parameter variations. To get a quick view on the model behaviour, a sensitivity analysis is carried out by varying several parameters in model runs over a short period (September 1999 to May 2000). The extensive results of this sensitivity analysis, including cross-shore profile figures and statistical results, can be found in Appendix A.

The sensitivity analysis leads to the following conclusions:

- In case of using the variable gamma, the breaker delay function has to be switched off, since both applications are used for the same purpose, namely the delay of wave breaking.
- The calibration should be done by varying one parameter at the time. Variation of two parameters together leads to poor model performances, since both variations either equal out or amplify each-other's effect.
- To all parameter variations, except variations in Fwee, the model responds more or less linear. A linear response means that increase of a certain value, compared to the default settings, generates quite the reverse reaction than that of decrease of the same value, concerning bar height and bar location.

- Variations in parameter Fwee however, lead to unpredictable model responses, especially with regard to the outer breaker bar. Therefore it is decided not to vary Fwee and set it to its default value (0.01).

Notably, nearly all parameter variations show negative BSI- and relative RMS scores in the sensitivity analysis, which means that hardly any variations show better results than the default prediction. To prevent rejecting parameter variations, that might give better results over a longer period than they do for a winter period, not all parameters with a negative score are rejected for the calibration.
The calibration will be done with the parameter variations that showed reasonable model results and had an acceptable BSI-score (-1 or higher). Parameter variations that showed very poor model results in the sensitivity analysis (i.e. unreal profile predictions or very negative BSI- and relative RMS scores) will not be used for the calibration of the model.

4.5 Calibration

This subsection discusses the actual calibration of the model. Based on the results of the sensitivity analysis several parameter variations are discarded. The table below (Table 4.2) shows an overview of the parameters, that are varied to calibrate the model. The model output is evaluated with the Brier Skill Score and the relative RMS error (see Subsection 4.3) of the cross-shore bottom profile and by comparing the cross-sections, predicted by UNIBEST-TC, to the default run with regard to the position and height of the bars.
In subsection 4.5.1 the default run will be evaluated, subsection 4.5.2 discusses the results of the parameter variations. Finally, in subsection 4.5.3 the conclusions, drawn from the calibration, will be presented.

Table 4.2: overview of varied parameters for calibration

Parameter	Dimension	Default	Values
GAMMA	[-]	Battjes&Stive	0.6, 0.7, 0.8, variable gamma [no breaker delay]
BETD	[-]	0.1	0.05, 0.15, variable beta [no breaker delay]
C_R	[-]	0.25	0, 0.5
F_LAM	[-]	1	0.25, 0.5, 2
FACQB	[-]	0.35	0.2, 0.4, 0.6
FCVISC	[-]	0.1	0.15, 0.2
(D50; D90; DSS)	[μm]	(240; 480; 240)	(240;480;240) with cross-shore varying grain size, (284; 429; 256), (250; 400; 250), (284; 429; 256) with cross-shore varying grain size
RKVAL	[-]	0.03	0.01, 0.05
(RW; RC)	[m]	(0.01; 0.03)	(0.015; 0.03); (0.02; 0.04); (0.005; 0.03)

GAMMA = Wave breaking parameter to determine maximum local wave height.
Default value is '0' according to Battjes&Stive (1985).

BETD =	Roller parameter, expressing the steepness of the wave front.
C_R =	Correlation coefficient between wave envelope and bound long waves.
F_LAM =	Number of wave lengths over which weighted depth is integrated (is part of breaker delay concept).
FACQB =	Factor for the fraction of breaking waves which does not contribute to the wave velocity moment.
FCVISC =	Viscosity coefficient for mean current computation.
D50,D90,DSS =	D_{50} grain diameter, D_{90} grain diameter, D_{50} grain diameter of suspended sediment.
RKVAL =	Friction factor for mean current computation.
RW and RC =	Wave and Current related roughness for sediment transport computation.

4.5.1 Default run

In the figure below (Figure 4.2) the result of the run with default parameter settings is shown.

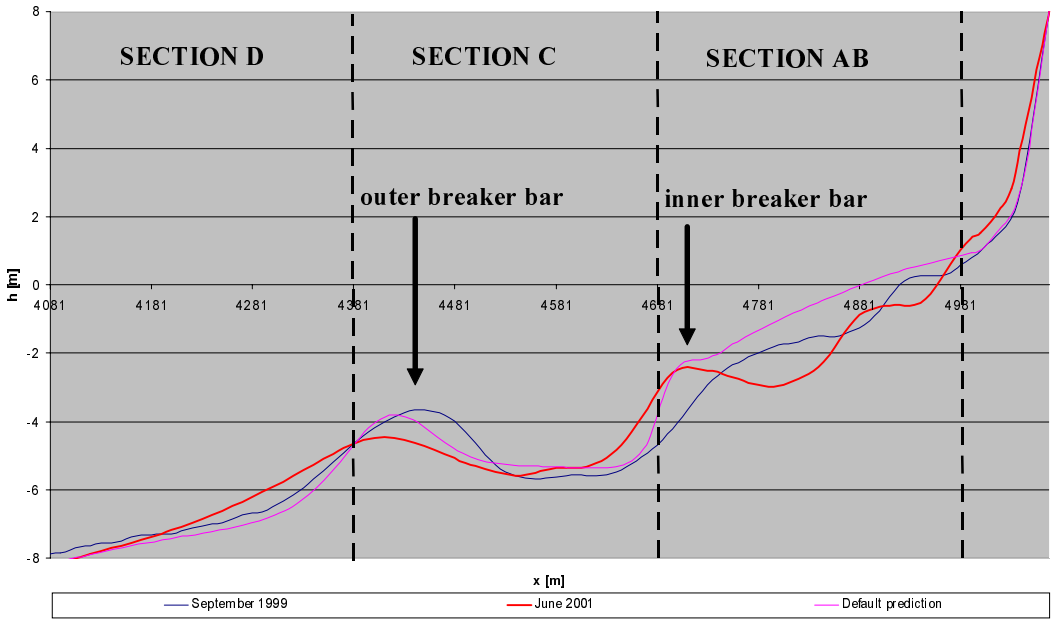

Figure 4.2: default prediction of UNIBEST-TC model for section 5 over two years

The default prediction appears to give a fairly satisfying result. Although the prediction differs from the real profile in June 2001, it shows some same tendencies of seaward movement and lowering of the outer breaker bar. In section AB the model predicts a too high bed level. This is a known over-estimation of the UNIBEST model, so the attention will be focused on the model performance in section C, in particular the behaviour of the outer breaker bar, and also section D, since this is the section in which the shoreface nourishment is located (note that it is not located in section 5, on which the calibration is done).

The RMS-error for the default run is 0.79 m for the total profile, 0.50 m for Section D, 0.46 m for Section C and 1.19 m for Section AB. These values also show that the prediction for Section AB is over-estimated.

The figure below (Figure 4.3) shows the sediment import over the seaward model boundary (d = NAP -16 m) and over the boundary of section D (d = NAP -8 m) in cross-shore section 5 over the total investigated period as computed by the UNIBEST-TC model.
In Subsection 4.2 was assumed that no sediment import or export occurred in the model, even though the survey data showed a small loss of sediment (12.820 m^3). This figure however shows a sediment import of 33.8 m^3/m over nearly two years, which comes down to a total sand volume increase of 33.800 m^3 in section 5. Over the boundary of the investigated area even more sediment is imported. The figure shows a sediment import of 158 m^3/m over nearly two years, which corresponds to a total sand volume increase of 158.000 m^3 in section 5.
This sediment import does not correspond to reality, it is a model incompleteness, which perhaps can explain the over-estimation of the bed level in section AB. In volume calculations, this 'unreal' sediment import has to be kept in mind.

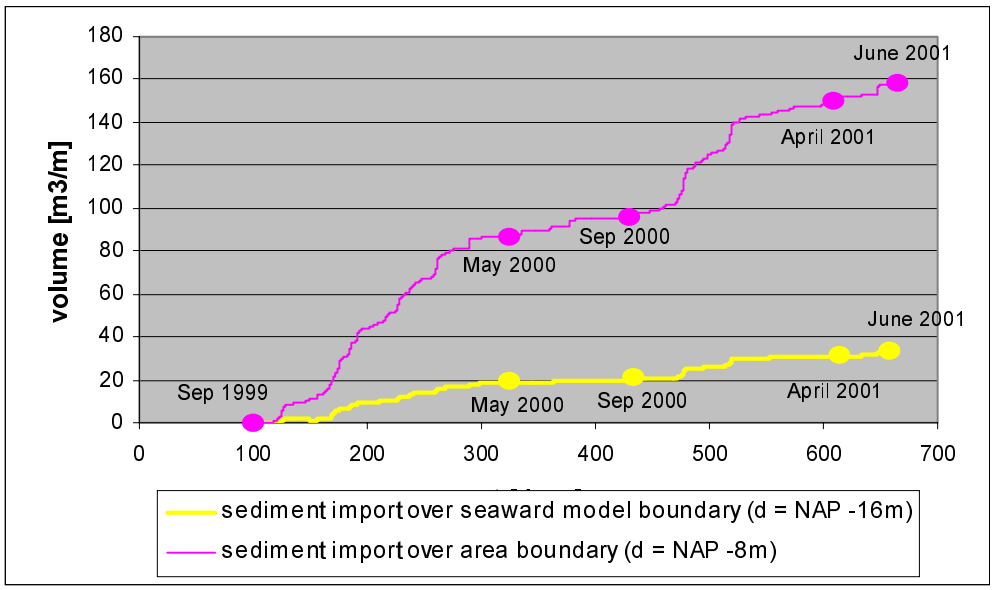

Figure 4.3: sediment import over seaward boundary in cross-section 5 from September 1999 to June 2001

In a study on the gradient in longshore transport of sediment in UNIBEST-TC [A.J. Veuger, 2001] is found that this sediment import can be cancelled out by introducing this gradient. However, this results in marginal improvements of the model performance and should only be applied after the optimal parameter setting is determined. Application of this gradient is outside the scope of this study, since the emphasis in this study is on bar behaviour in broad outlines, which is a cross-shore process.

4.5.2 Parameter variations

The main objective of the calibration study is to find model parameter settings that give the optimal model prediction. In this subsection all parameter variations (see Table 4.2) are discussed.

Wave breaking parameter: GAMMA

In the following figures (Figure 4.4 and Figure 4.5) the BSI and relative RMS-error and the cross-shore profiles are shown for variations in gamma. Apparently the best value for gamma is either the default setting or possibly gamma = 0.7. According to the statistical results the variable gamma gives a positive result, except for Section C. The cross-shore profile however, shows that the breaker bars are faded out when using the variable gamma.
A lower gamma causes more breaking waves and thus more turbulence on the outer breaker bar. This results in a more seaward outer bar, which can be seen in Figure 4.4. A higher gamma causes an opposite reaction of the outer breaker bar.

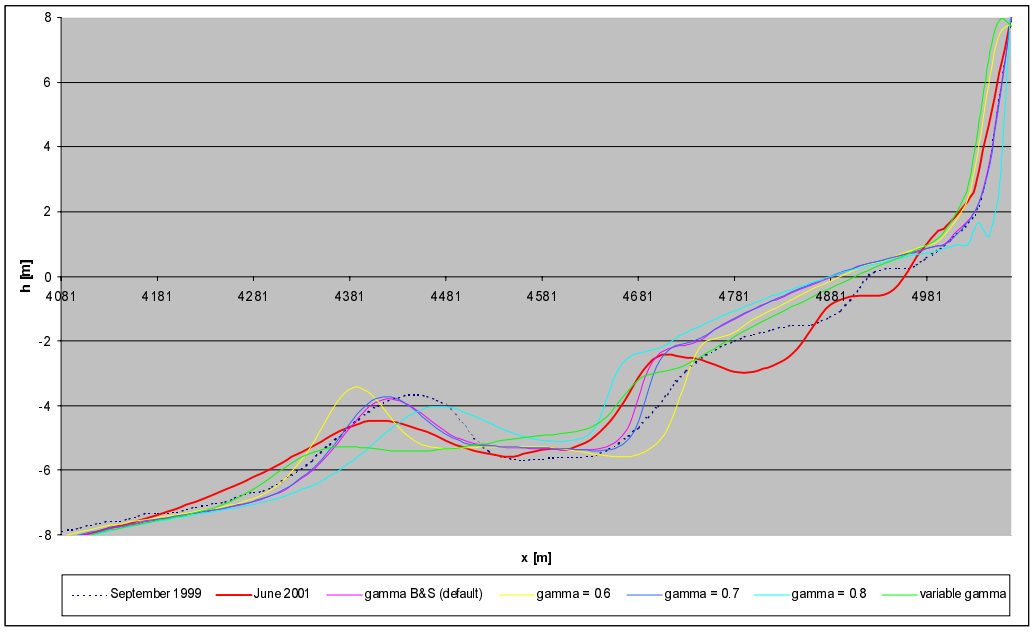

Figure 4.4: cross-shore profiles of variations in GAMMA

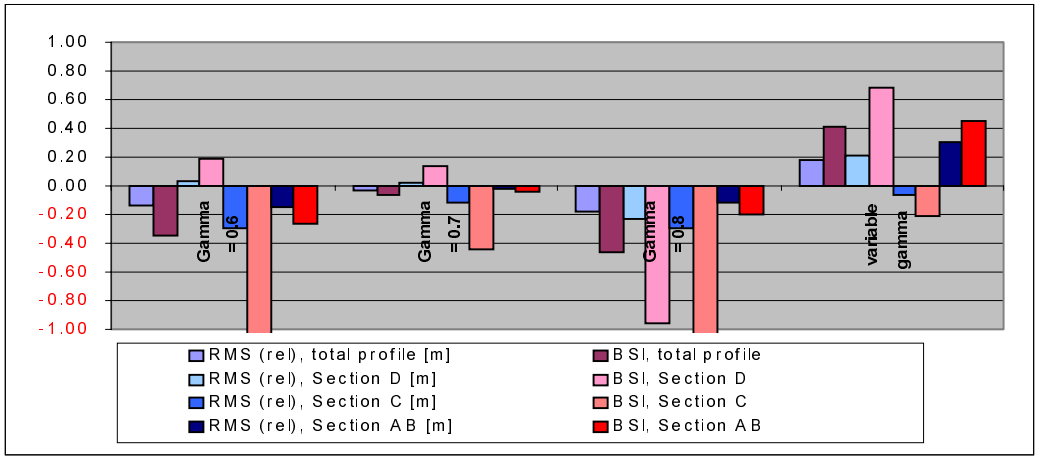

Figure 4.5: BSI-score and relative RMS-error for variations in GAMMA

Roller parameter, expressing the steepness of the wave front: BETD

Figure 4.6 shows the cross-shore profiles for various values of beta, Figure 4.7 shows the BSI and the relative RMS-error for various values of beta. Beta = 0.15 and a variable beta (without breaker delay) both give a better result than the default setting. However, shoreward of the first breaker bar these values give just the same error as the default value. Higher values of beta result in increased breaking on top of the bar. This can explain the lowering of the outer bar crest with an increasing beta. According to the statistical results beta = 0.15 improves the model results most.

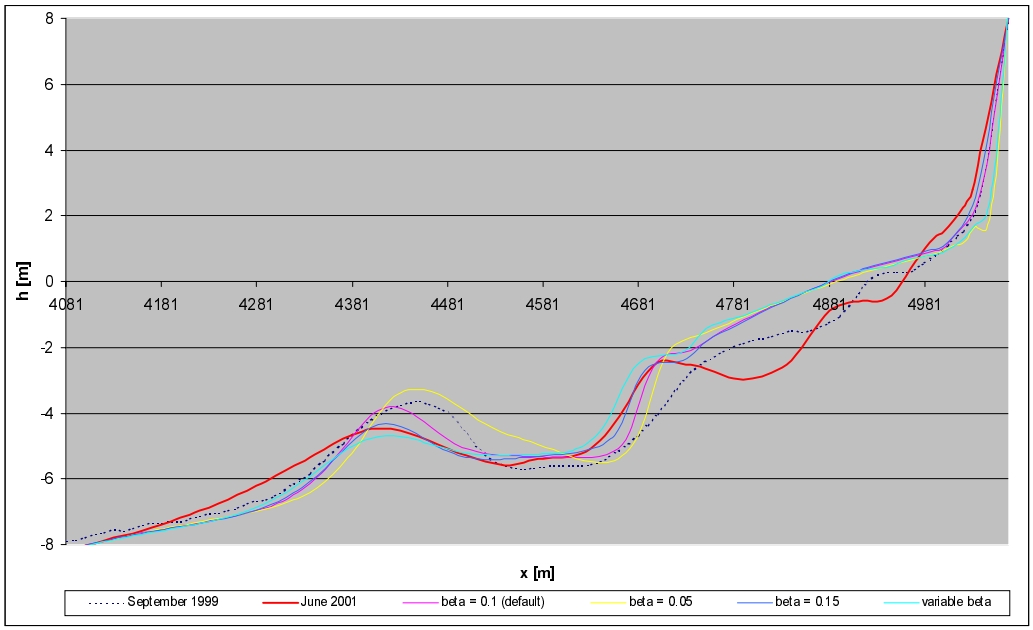

Figure 4.6: cross-shore profiles of variations in BETD

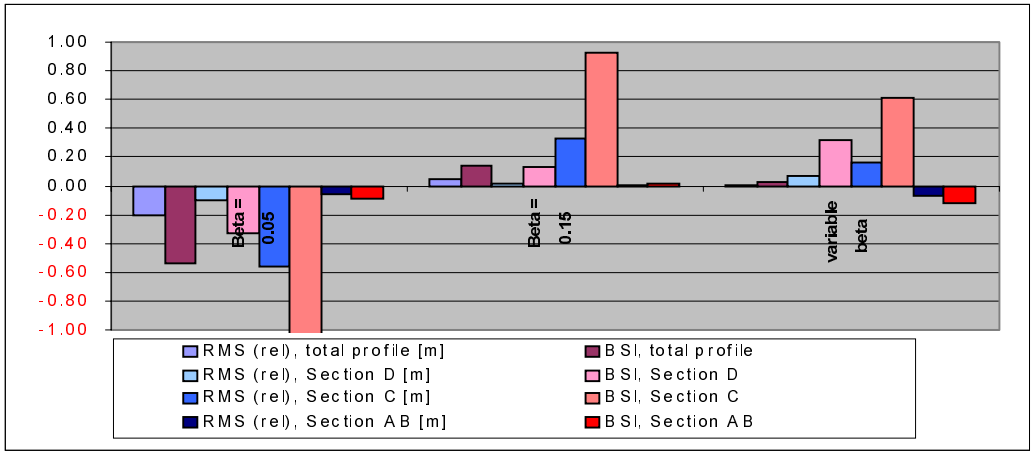

Figure 4.7: BSI-score and relative RMS-error for variations in BETD

Correlation coefficient between wave envelope and bound long waves: C_R

The figures below (Figure 4.8 and Figure 4.9) show the BSI, the relative RMS-error and the cross-shore profiles for variations in C_R. According to the statistical results both variations give a better prediction for Section C than the default value. However, the cross-shore profiles only show an improved prediction when applying C_R = 0.5. Varying C_R appears to effect Section C most, in particular the outer breaker bar, other parts of the cross-shore section are not very sensitive for these variations. An increasing C_R increase both offshore and onshore transport, which explains the flattening of the outer breaker bar for C_R is 0.5.

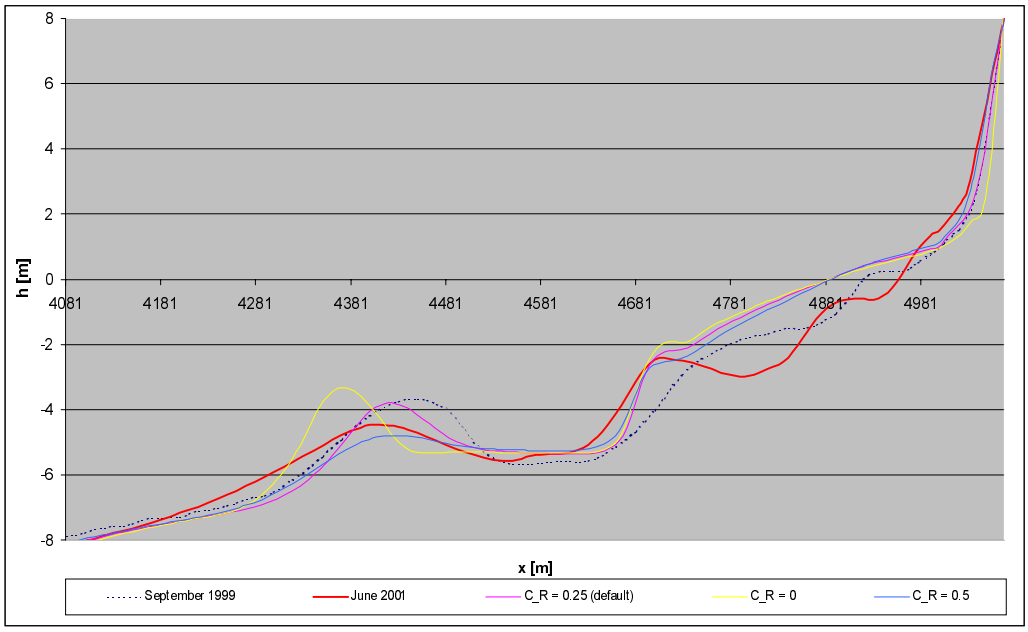

Figure 4.8: cross-shore profiles of variations in C_R

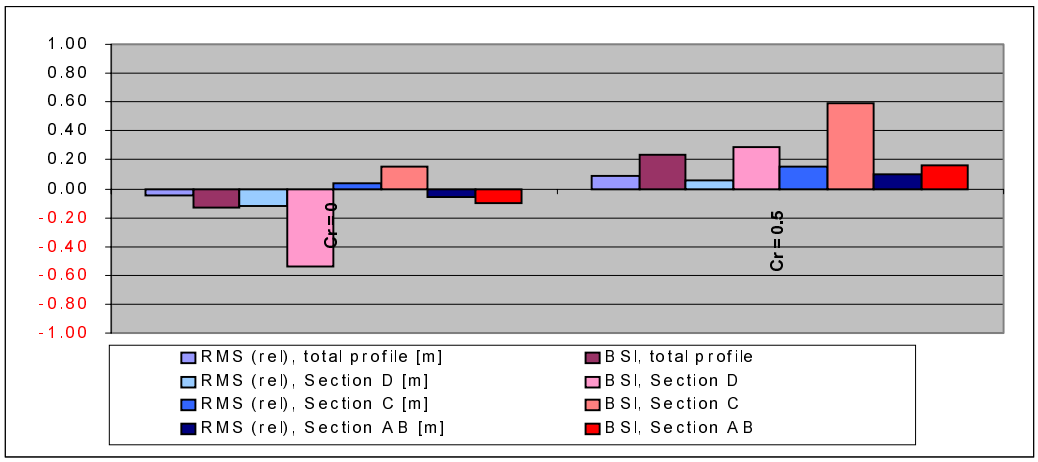

Figure 4.9: BSI-score and relative RMS-error for variations in C_R

Breaker Delay concept (number of wave lengths over which weighted depth is integrated): F_LAM

Cross-shore profiles for variations in F_LAM are shown in Figure 4.10, the BSI and the relative RMS-error for various values of F_LAM are shown in Figure 4.11. Values of F_LAM smaller than the default value of 1 seem to improve the model predictions. Most improvement is found in the height of the second breaker bar. A lower value of F_LAM results in more energy dissipation on the breaker bar, which can explain the improved prediction of the outer breaker bar height (and also the inner breaker bar height) with a lower F_LAM. Also according to the statistical results, a value of F_LAM, lower than default, leads to better model predictions. F-LAM mainly has influence on the height of the breaker bars.

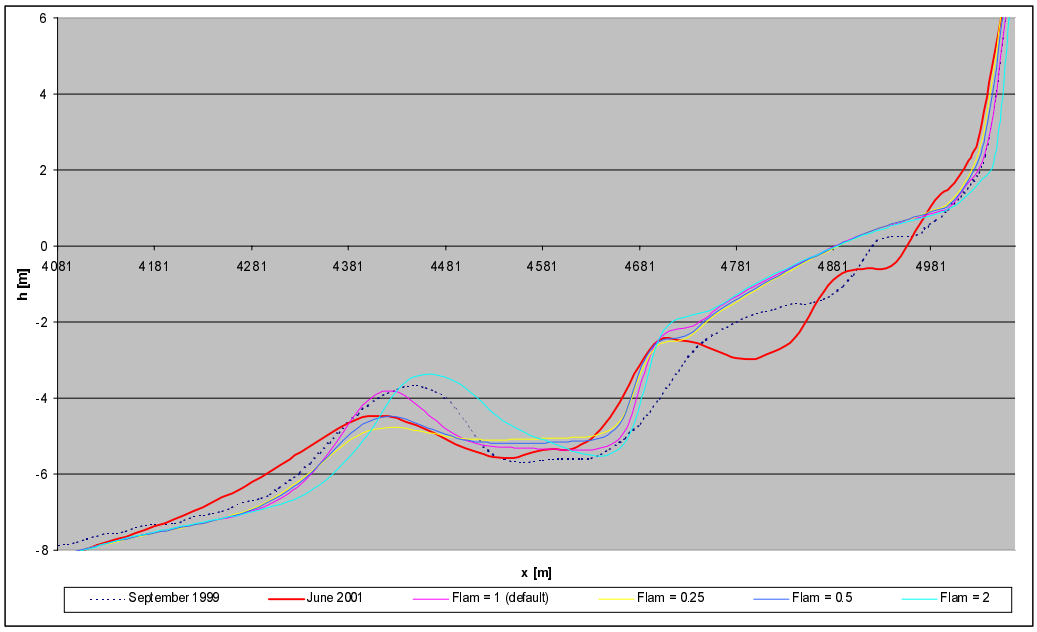

Figure 4.10: cross-shore profiles of variations in F_LAM

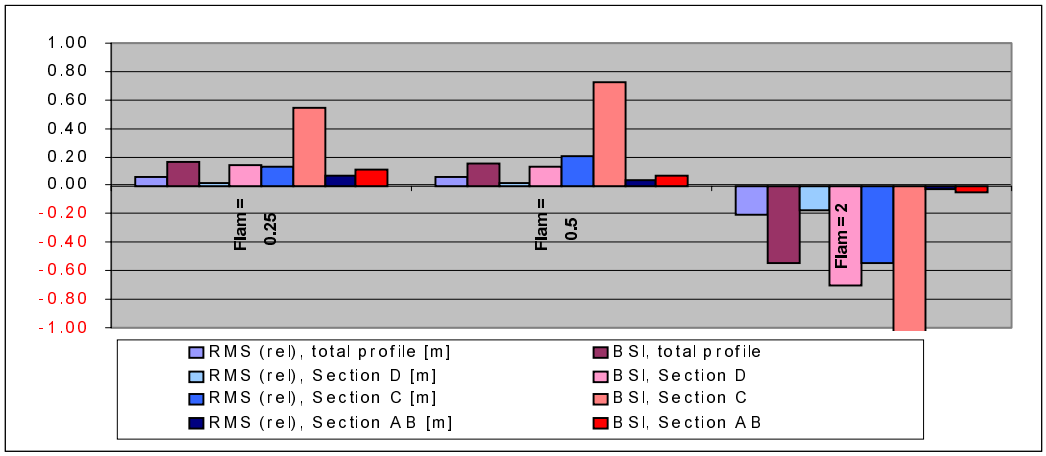

Figure 4.11: BSI-score and relative RMS-error for variations in F_LAM

Factor of fraction of breaking waves that do not contribute to wave asymmetry: FACQB

In the following figures (Figure 4.12 and Figure 4.13) the BSI, the relative RMS-error and the cross-shore profiles are shown for various values of FACQB. The FACQB value of 0.4 gives a better prediction than the default setting, but this value also fails in predicting a reduced height of the second breaker bar. FACQB=0.6 has a small positive score in the statistical results, the cross-shore profiles however show no better prediction than the default one. Since FACQB=0.4 does not result in large improvements, FACQB will be set at its default value.

Variations in FACQB mainly result in changing location of the outer breaker bar. An increasing FACQB leads to a decreasing onshore transport, which explains the seaward movement of both breaker bars for a higher FACQB and vice versa.

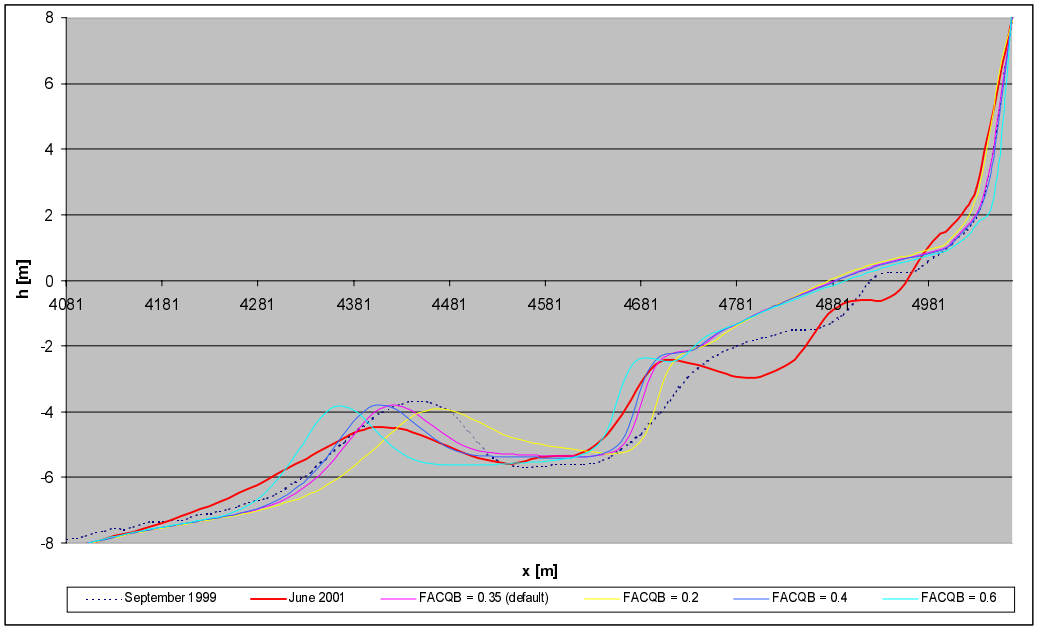

Figure 4.12: cross-shore profiles of variations in FACQB

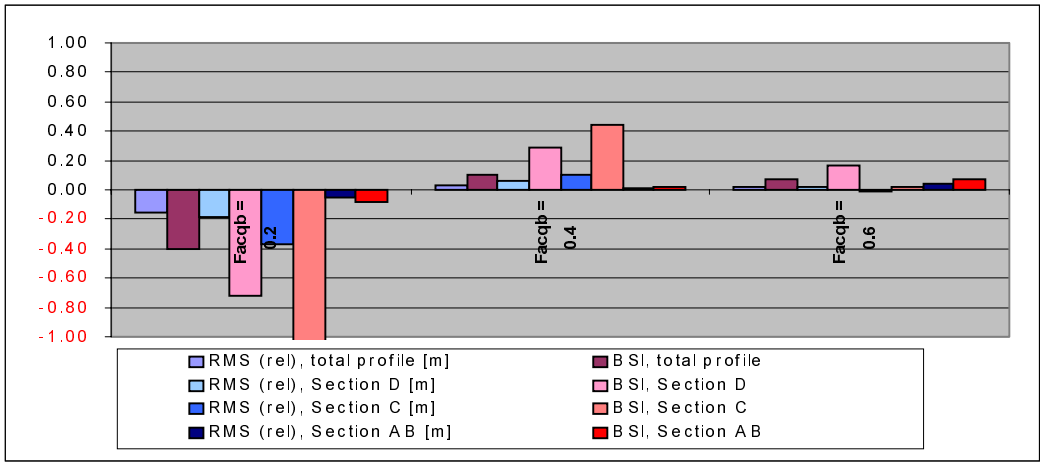

Figure 4.13: BSI-score and relative RMS-error for variations in FACQB

Viscosity coefficient of vertical velocity profile: FCVISC

The figures below (Figure 4.14 and Figure 4.15) show the BSI, the relative RMS-error and the cross-shore profiles for variations in FCVISC. Variations in FCVISC appear not to improve the model results at all. Both figures show that FCVISC has a strong reaction to variations, which makes it a very sensitive parameter. This strong sensitivity might make it worthwhile to develop a local, cross-shore dependent, viscosity model.

Improving the UNIBEST-TC model however is beyond the scope of this study, therefore FCVISC will be set to its default value in this validation study.

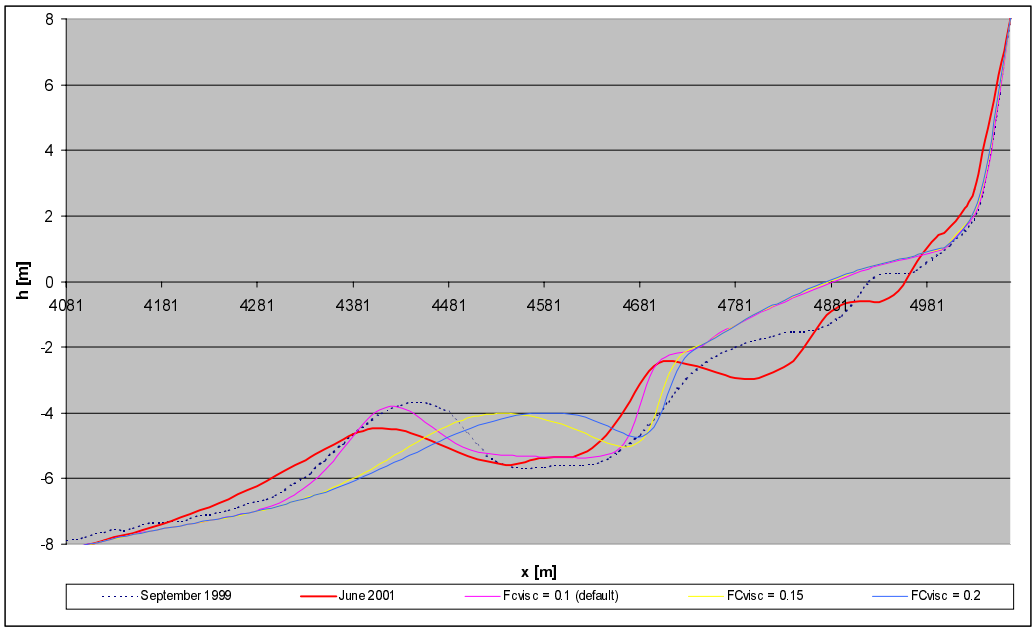

Figure 4.14: cross-shore profiles of variations in FCvisc

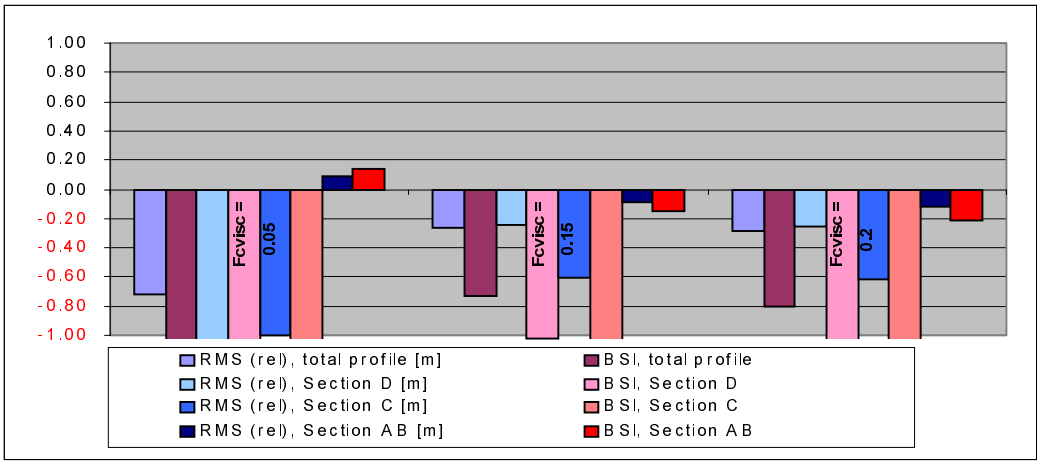

Figure 4.15: BSI-score and relative RMS-error for variations in FCvisc

Sediment grain size parameters: D50, D90, DSS

In Figure 4.16 and Figure 4.17 the BSI score, the relative RMS-error and the cross-shore profile for variations in the sediment characteristics are shown. The appliance of a cross-shore varying grain size does not significantly improve the model results, so no varying grain size will be applied in the validation study.

The other two variations result in a more or less similar prediction of the bottom profile and predict a second breaker bar that is higher than in reality, just as the default settings do.

Strikingly differences in the grain size parameters do not result in large differences in the computed bottom profile.

The grain size parameters of the sand in the shoreface nourishment might be slightly different from those of the sand at the site. This leaves the possibility that one of these variations may result in a better prediction for section 3, than the default settings will. Therefore both variations will be validated on section 3 (with shoreface nourishment).

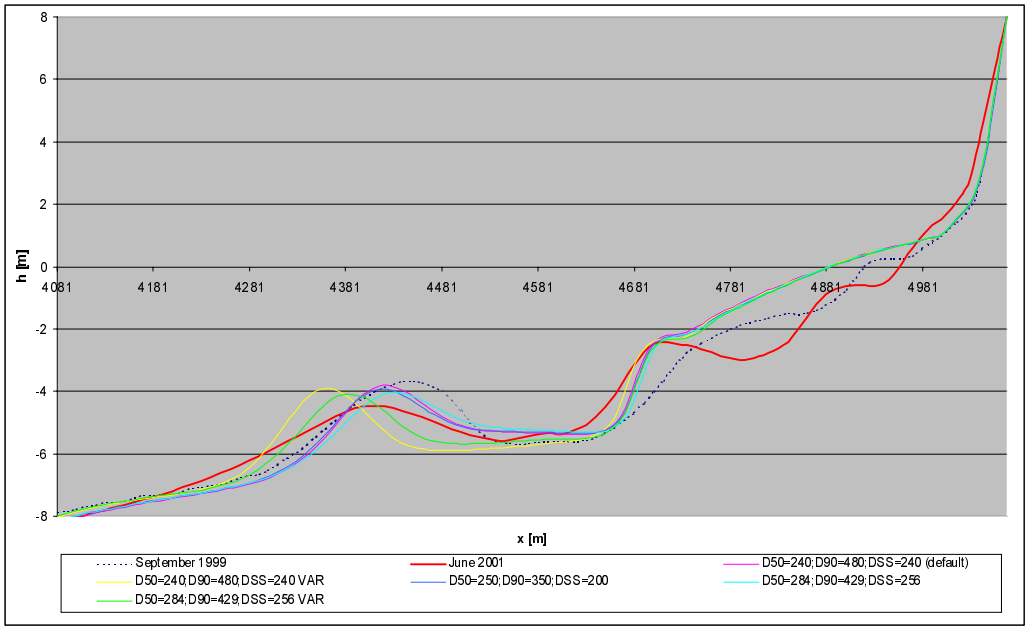

Figure 4.16: cross-shore profiles of variations in D50, D90 and DSS

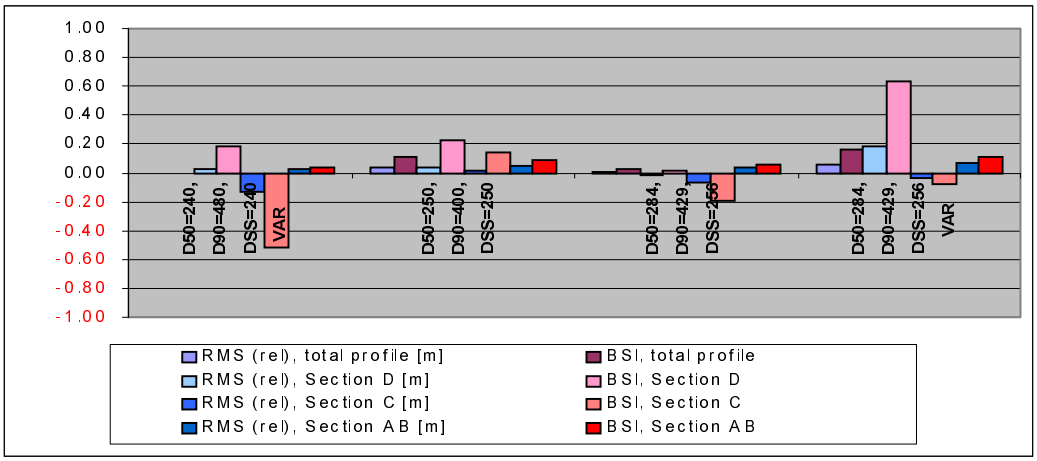

Figure 4.17: BSI-score and relative RMS-error for variations in D50, D90 and DSS

Friction factor for mean current: RKVAL

The figures below (Figure 4.18 and Figure 4.19) show the BSI, the relative RMS-error and the cross-shore profiles for variations in RKVAL. Variations in RKVAL do not improve the model performance. According to the statistical results, the use of RKVAL=0.01 appears to improve the model performance. However, the cross-shore profiles show no improvement at all. Hence, the value of RKVAL is kept at the default value of 0.03.

RKVAL is a friction factor. In Figure 4.18 is clearly visible that increase of this friction factor results in a more shoreward position of the breaker bars and vice versa. Higher values result in larger bed shear stresses, that keep the sediment from moving seaward. RKVAL has no significant influence on the bar heights.

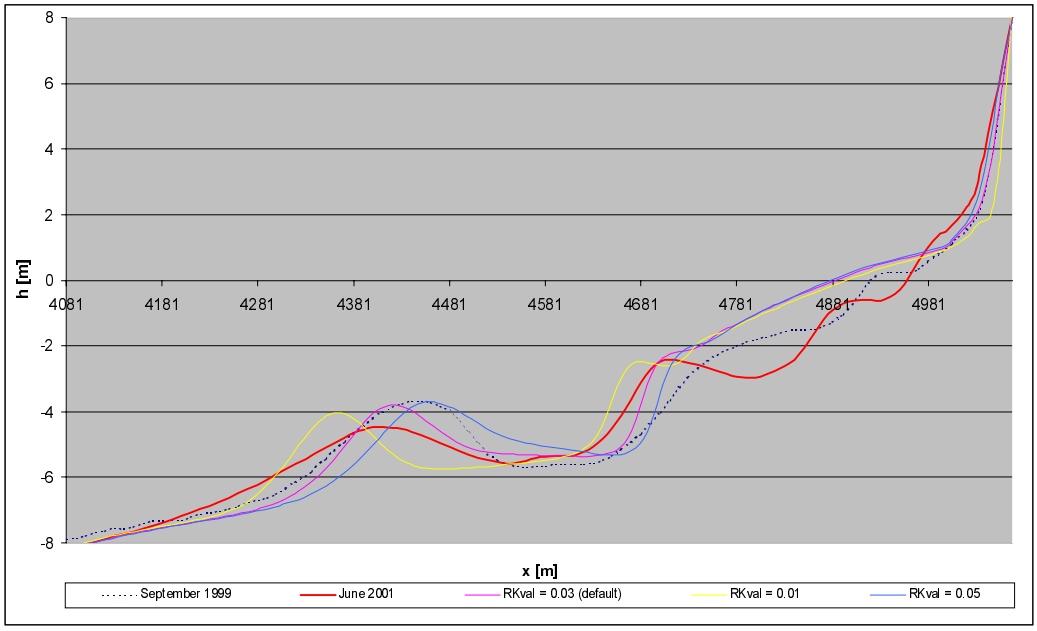

Figure 4.18: cross-shore profiles of variations in RKval

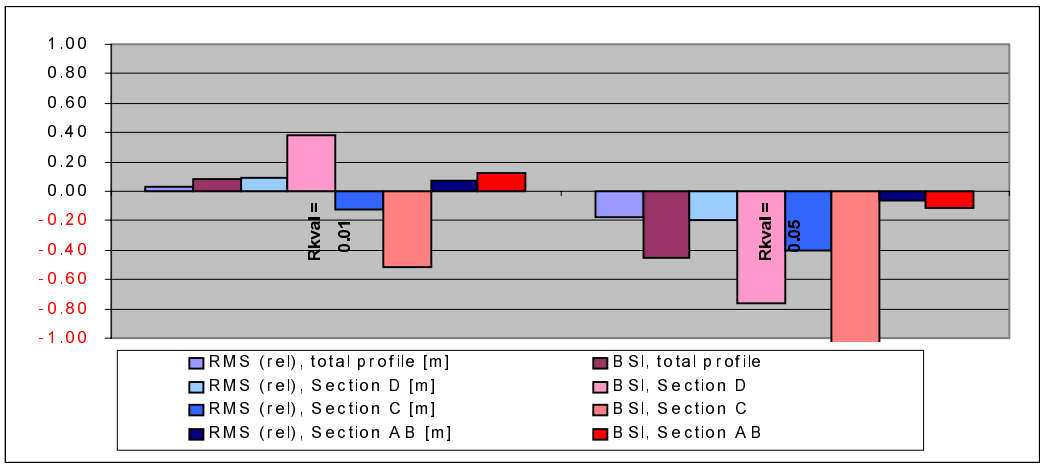

Figure 4.19: BSI-score and relative RMS-error for variations in RKval

Current and wave related roughness: RC and RW

The following figures (Figure 4.20 and Figure 4.21) show the BSI, the relative RMS-error and the cross-shore profiles for variations in RC and RW. It appears that RW should not be smaller than the default value of 0.01, because smaller values result in more onshore transport and thus a too shoreward position of the breaker bars. Slightly larger values of both RW and RC result in a better fit of the predictions to the measured bottom profile. Consequently the combination of RW=0.02 and RC=0.04 will be validated on section 3.

From the statistical results can be deduced that the model is very sensitive for small variations in the current and waves related friction factors RW and RC. This indicates that caution is required when varying friction factors.

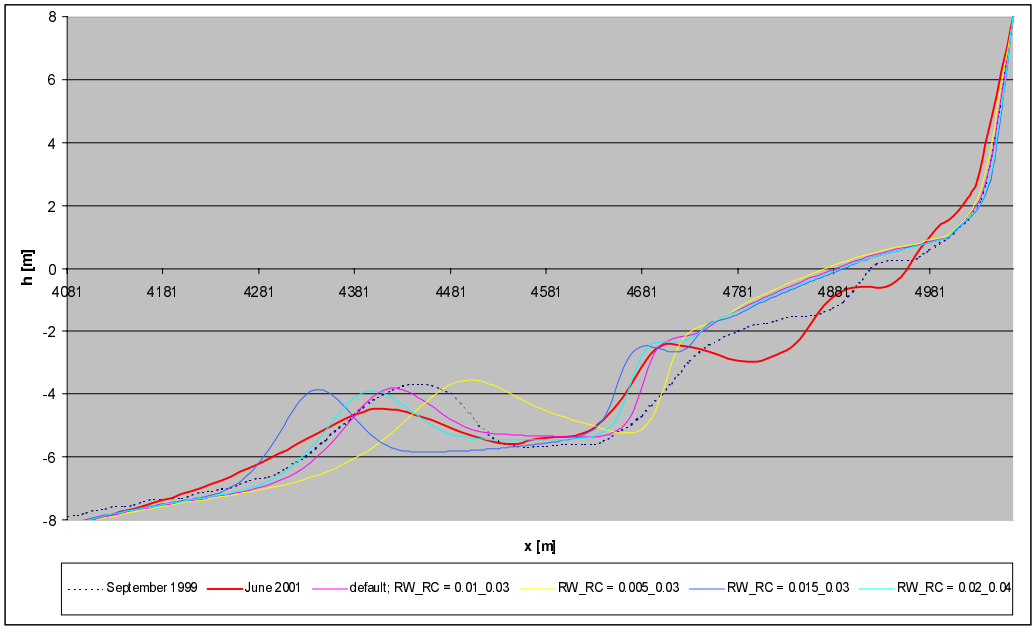

Figure 4.20: cross-shore profiles of variations in RC and RW

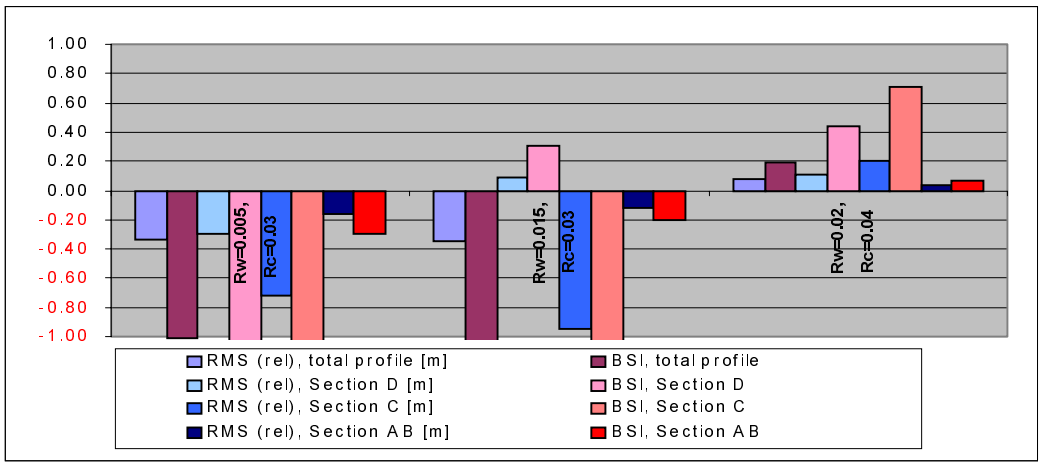

Figure 4.21: BSI-score and relative RMS-error for variations in RC and RW

4.5.3 Synthesis

The calibration study discussed above leads to the following conclusions.

- Varying parameters compared to the default settings mainly results in variations in location and height of the outer breaker bar
- The default values of FCvisc and RKval appear to be the best values for these parameters.
- The model is not sensitive for small variations in the grain size parameters.
- Variation in friction factors (RKval, RW and RC) has large influence on the UNIBEST-TC model
- Variations in FACQB mainly lead to variations in the location of the breaker bars
- Variations in F_LAM mainly lead to differences in the height of the breaker bars
- F_LAM=0.5 results in a significant improvement of the model performance
- The best parameter settings for the undisturbed situation, according to the calibration, are beta is 0.15 and the default setting for all other parameters

The following step of this study is the validation of the model performance for bottom profiles that include a shoreface nourishment (Section 3). The model performance for cross-shore profiles including a shoreface nourishment is not known. Therefore all variations that resulted in a positive BSI score, a positive relative RMS-error and a cross-shore profile similar to reality will be reviewed, in order not to discard variations that might result in good model predictions in this new situation. The validation study will be described in Chapter 5. The parameters that will be validated on Section 3 are:

- GAMMA (variable gamma and gamma = 0.7)
- BETD (variable beta and beta=0.15)
- C_R (C_R=0.5)
- F_LAM (0.5)
- RW_RC (0.02_0.04)

5 Validation of the UNIBEST-TC model

5.1 Introduction

This part of the study contains the validation of the parameter settings of the UNIBEST-TC model, which are extracted from the calibration, for bottom profiles that include a shoreface nourishment. All parameter variations that resulted in a positive BSI score, a positive relative RMS-error during the calibration will be reviewed, since it is uncertain if the best setting in the undisturbed situation will be the best setting for the disturbed situation. Exceptions to the above mentioned criteria are made for gamma = 0.7 and the variable gamma. The model performance with gamma = 0.7 is almost similar to the default model performance, for section D even better than the default performance. The variable gamma appeared to give a good prediction of the bed slope in section AB and therefore interesting for further study. In de next table (Table 5.1) an overview of the parameter variations for the validation study is given.

Table 5.1: overview of varied parameters for validation

Parameter	Dimension	Default	Values
GAMMA	[-]	0	0.7, variable gamma [no breaker delay]
BETD	[-]	0.1	0.15, variable beta [no breaker delay]
C_R	[-]	0.25	0.5
F_LAM	[-]	1	0.25, 0.5
(D50; D90; DSS)	[μm]	(240; 480; 240)	(284; 429; 256), (250; 400; 250)
(RW; RC)	[m]	(0.01; 0.03)	(0.02; 0.04)

GAMMA = Wave breaking parameter to determine maximum local wave height. Default value is '0' according to Battjes&Stive (1985).
BETD = Roller parameter, expressing the steepness of the wave front.
C_R = Correlation coefficient between wave envelope and bound long waves.
F_LAM = Number of wave lengths over which weighted depth is integrated (is part of breaker delay concept).
D50,D90,DSS = D_{50} grain diameter, D_{90} grain diameter, D_{50} grain diameter of suspended sediment.
RW and RC = Wave and Current related roughness for sediment transport computation.

For each value a simulation of the longshore-averaged profile of section 3 (middle part of the nourishment, (see Subsection 4.2, Figure 4.1)) over nearly two years (September 1999 to June 2001) is made.
The model is validated at cross-shore section 3, because this section contains the middle part of the nourishment, which is most representative of the shoreface nourishment The input (except the bottom profile) is similar to the input used in the calibration. The input

bottom profile in the validation study is the longshore averaged bottom profile of section 3 (see Figure 4.1).
The output is evaluated with the Brier Skill Score(base is default prediction) for the cross-shore bottom profile, with the relative RMS-error (see Subsection 4.3) and by comparing the cross-sections predicted by UNIBEST with regard to the position and height of the bars and especially to the behaviour of the outer breaker bar and the nourishment.

5.2 Default run

In the figure below (Figure 5.1) the result of the run with default parameter settings is shown.

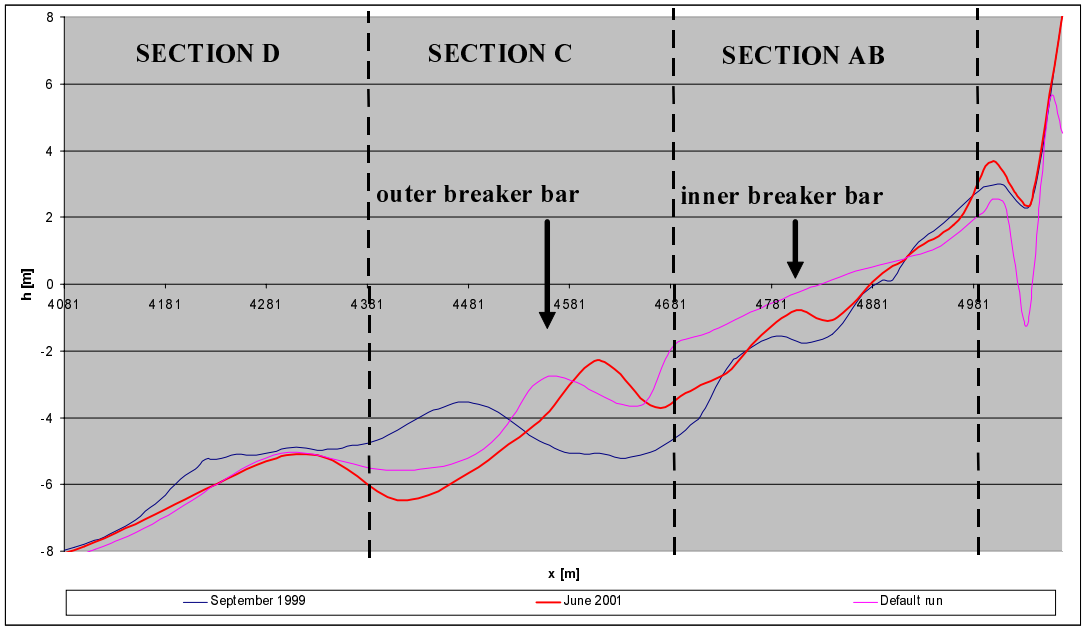

Figure 5.1: default prediction of UNIBEST-TC model for section 3 over two years

Again the default prediction appears to give a fairly satisfying result. Although the prediction is not exactly equal to the real profile in June 2001, it shows the same landward movement of the outer breaker bar. It also gives a good prediction of the shoreface nourishment, which reshapes to a smooth bar and remains at its location. Similar to all runs in the calibration study, the model predicts a too high bed level in section AB. Therefore also in this validation study the attention will be focused on the model performance in section C, in particular the behaviour of the outer breaker bar, and also section D, since this is the section in which the shoreface nourishment is located.

The RMS-error for the default run is 0.72 m for the total profile, 0.19 m for Section D, 0.81 m for Section C and 0.93 m for Section AB. These values also show that the prediction for Section AB is over-estimated. In section C a large error is found as well, though the profiles show a fairly good prediction. The generation of the trough between the nourishment and the outer breaker bar and the shoreward movement of the outer breaker bar are predicted by the UNIBEST-TC model. However, both processes are underestimated.

Shoreward of section AB a deep erosion pit can be observed. This pit is caused by the fact that for the validation study a fixed layer (no sedimentation nor erosion possible at the location of this layer) is applied for the dunes. Without this fixed layer the UNIBEST-TC model shows unstable results around the dune foot, which is probably caused by the bump just in front of the dune foot. The erosion pit in front of the dune foot can be observed in nearly all validation results, but it does not correspond to reality.
At the landward boundary of the cross-shore profile can be observed that in the model prediction, in spite of the fixed layer, the final dune top is lower than the initial dune top. Tests have been done to solve this error. It appeared that this error can be solved by extending the grid more landward (over the dune top). Model runs, using the extended grid, are not significantly different from the present results. The main difference is the generation of a deeper erosion pit at the dune foot.
In most following figures of cross-shore profiles the erosion pit and the low dune top can be found. In each profile this is caused by the reasons mentioned above.

5.3 Validation of the calibrated parameter settings

The main concern of the validation study is to investigate whether the, in the calibration study proposed, variations give better model results for a cross-shore section, including a shoreface nourishment. In this subsection all results of the validation of the different parameter settings (see Table 5.1) are presented.

Wave breaking parameter: GAMMA

In the following figures (Figure 5.2 and Figure 5.3) the BSI, the relative RMS-error and the cross-shore profiles for variations in gamma are shown. The variable gamma is not able to predict the response of the bottom profile to the placement of the nourishment. Remarkable though is the fact that it once again gives a quite good prediction of the slope angle between the beach and the first breaker bar (section AB).

Gamma = 0.7 gives a more satisfying result than the default setting, which is a bit surprising, since the default setting performed better in the undisturbed situation.

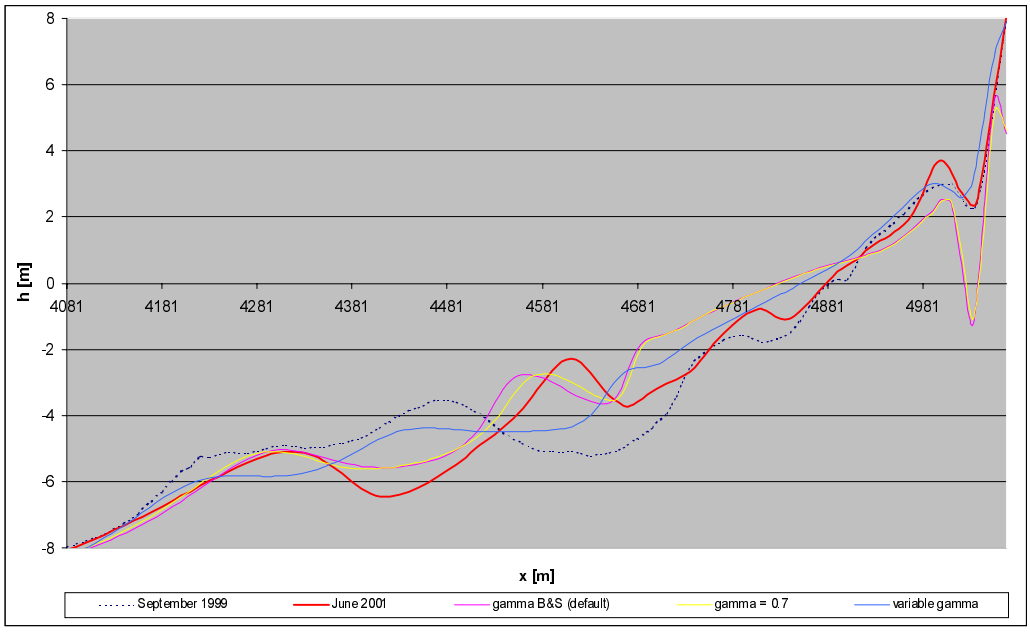

Figure 5.2: cross-shore profile of variations in GAMMA (section 3)

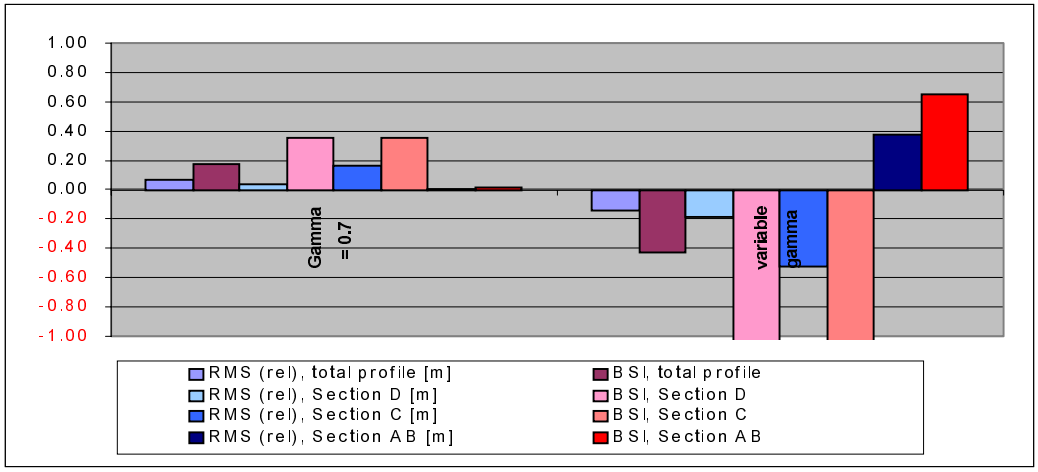

Figure 5.3: BSI-score and relative RMS-error for variations in GAMMA (section 3)

Roller parameter, expressing the steepness of the wave front: BETD

In the following figures (Figure 5.4, Figure 5.5) the BSI, the relative RMS-error and the cross-shore profiles for variations in beta. According to the statistical results a variable beta (without breaker delay) does improve the model performance for section AB. The cross-shore profile confirms this conclusion. In all other sections a variable beta results in disappearance of the breaker bars. A reason for this can be the fact that no breaker delay is applied, which results in more wave breaking on the bars, resulting in disappearance of the bars. Beta = 0.15 is similar to the default setting, but no improvement either. For computations on profiles including a shoreface nourishment the value of beta is best kept at its default value of 0.1.

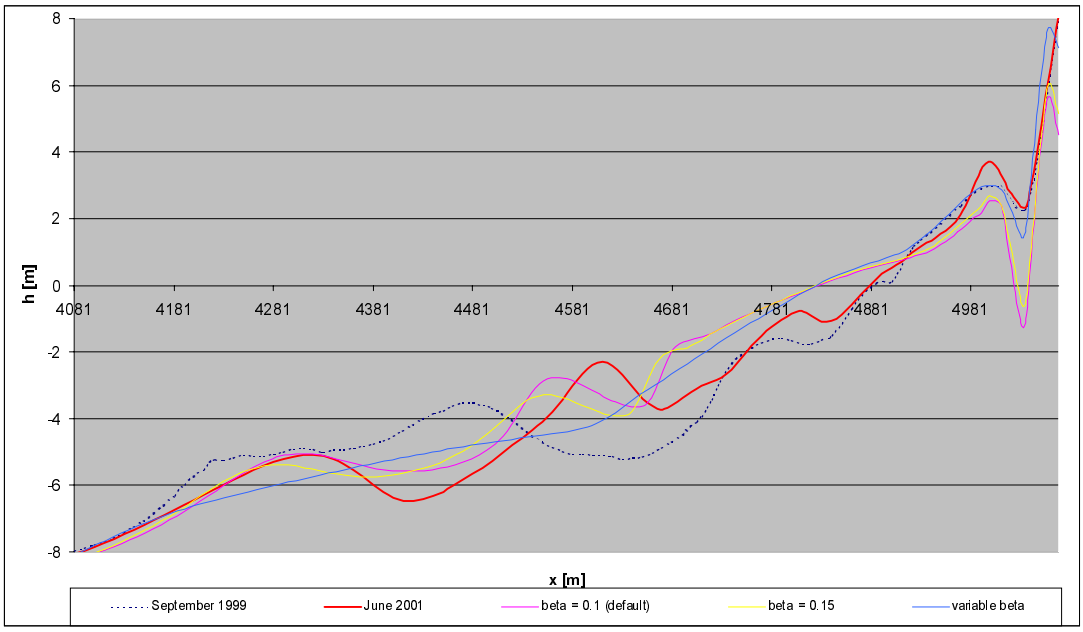

Figure 5.4: cross-shore profile of variations in BETD (section 3)

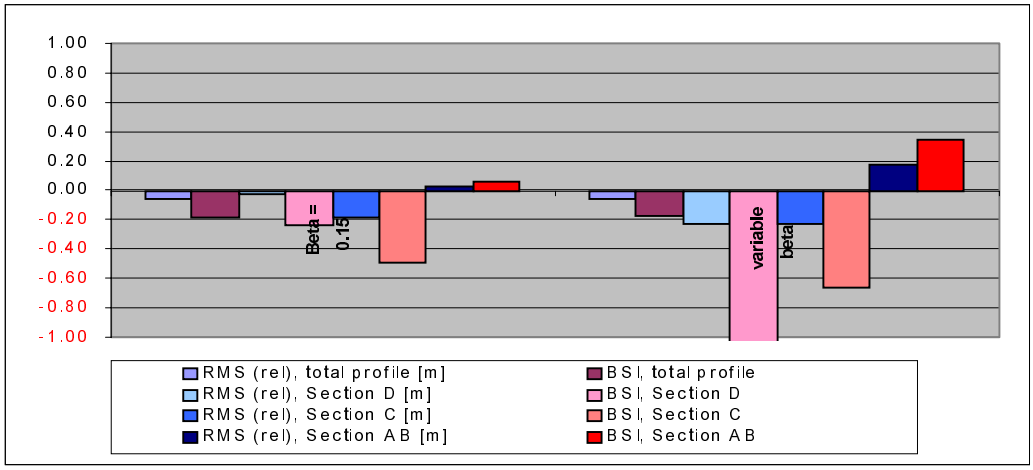

Figure 5.5: BSI-score and relative RMS-error for variations in BETD (section 3)

C_R, RW and RC

The figures below (Figure 5.6 and Figure 5.7) show the BSI, the relative RMS-error and the cross-shore profiles for variations in C_R and RW and RC. Although the variation of C_R results in a positive BSI-score, it does not lead to an improved prediction. In the cross-shore profile can be seen that this parameter setting predicts disappearance of the breaker bars, a phenomenon that does not occur in reality.

The variation in RW and RC does not lead to an improved mode performance. Higher friction factors apparently prevent the outer breaker bar from moving shoreward. In this situation perhaps even a lower friction factor could be appropriate.

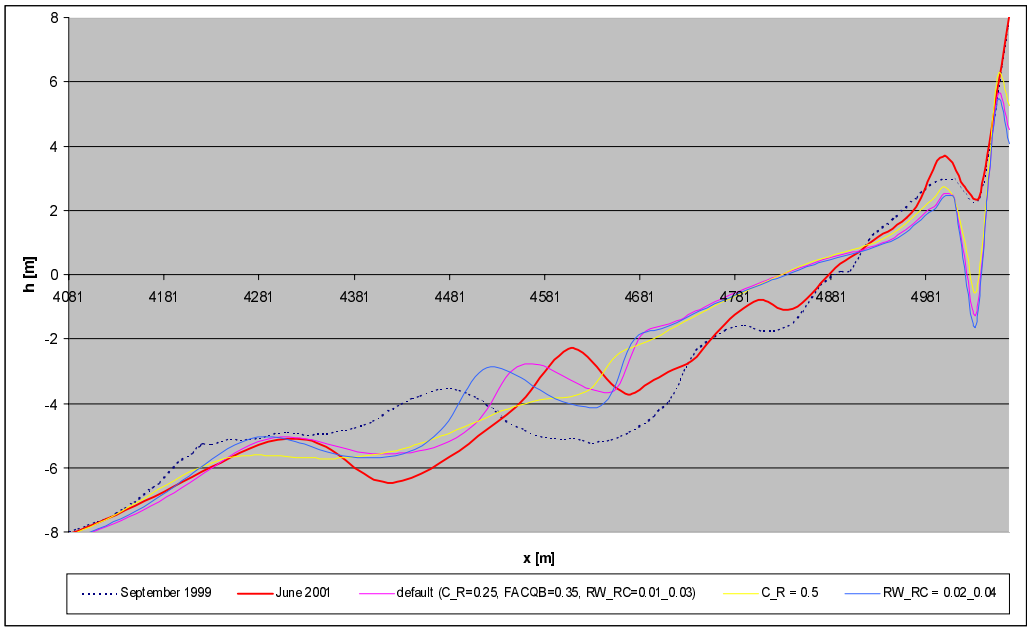

Figure 5.6: cross-shore profile of variations in C_R, and RW and RC (section 3)

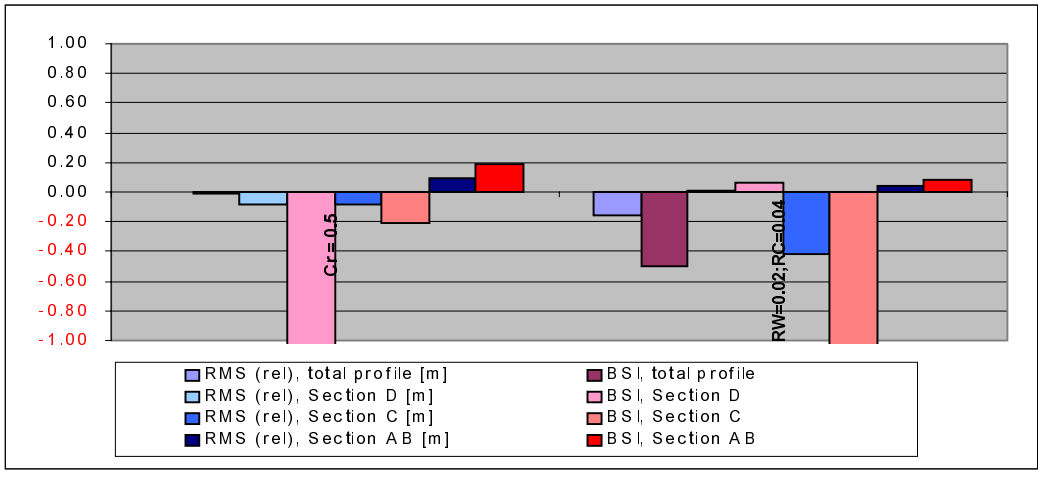

Figure 5.7: BSI-score and relative RMS-error for variations in C_R, RW and RC (section 3)

Breaker Delay concept (number of wave lengths over which weighted depth is integrated): F_LAM

The figures below (Figure 5.8 and Figure 5.9) show the BSI, the relative RMS-error and the cross-shore profiles for variations in F_LAM. The variations in F_LAM mainly lead to decreasing bar heights and do not give improved results. The statistical results show little improvement of the prediction for section AB when applying a smaller F_LAM, but this can not clearly be detected in the cross-profiles.

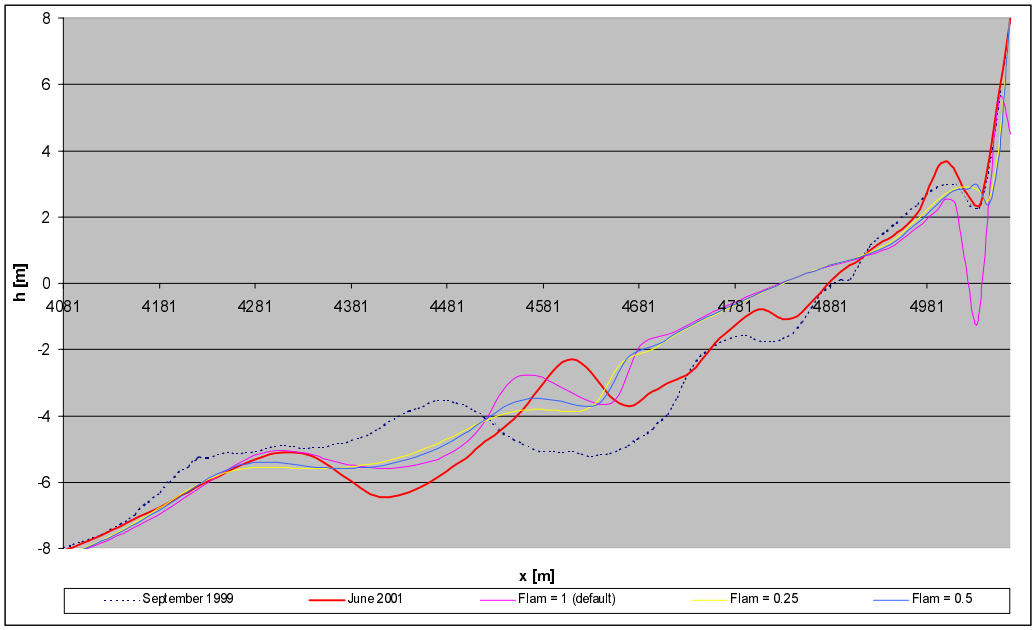

Figure 5.8: cross-shore profile of variations in F_LAM (section 3)

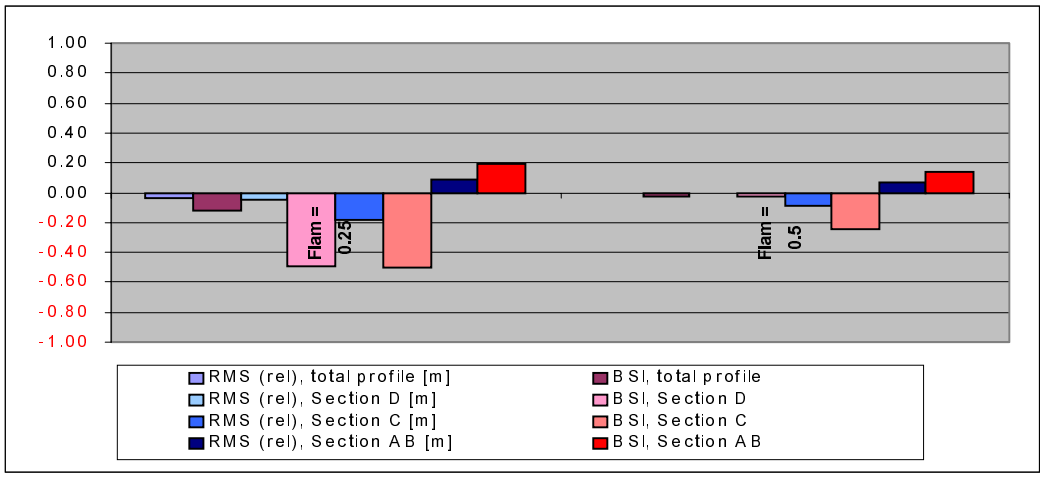

Figure 5.9: BSI-score and relative RMS-error for variations in F_LAM (section 3)

Sediment grain size parameters: D50, D90, DSS

In Figure 5.10 and Figure 5.11 the BSI score, the relative RMS-error and the cross-shore profile for variations in the sediment characteristics are shown. The other variations in the sediment characteristics have a positive BSI score, but do not show a clear improvement in the cross-shore profiles. Therefore it is advised to keep the grain size diameters at their default settings (the surveyed parameters), to avoid changing reality to improve the model results.

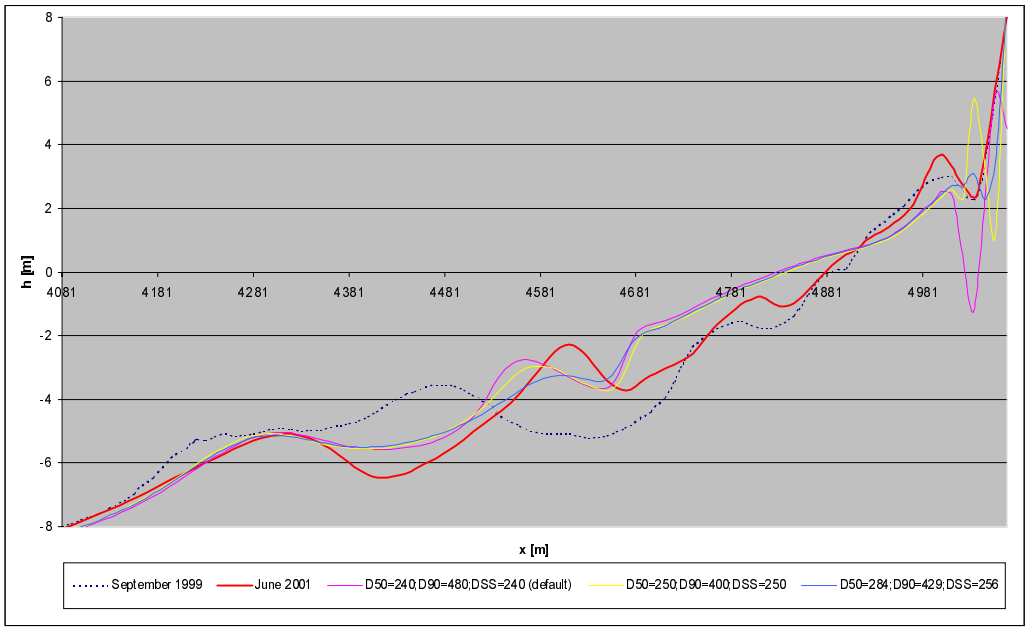

Figure 5.10: cross-shore profile of variations in D50, D90 and DSS (section 3)

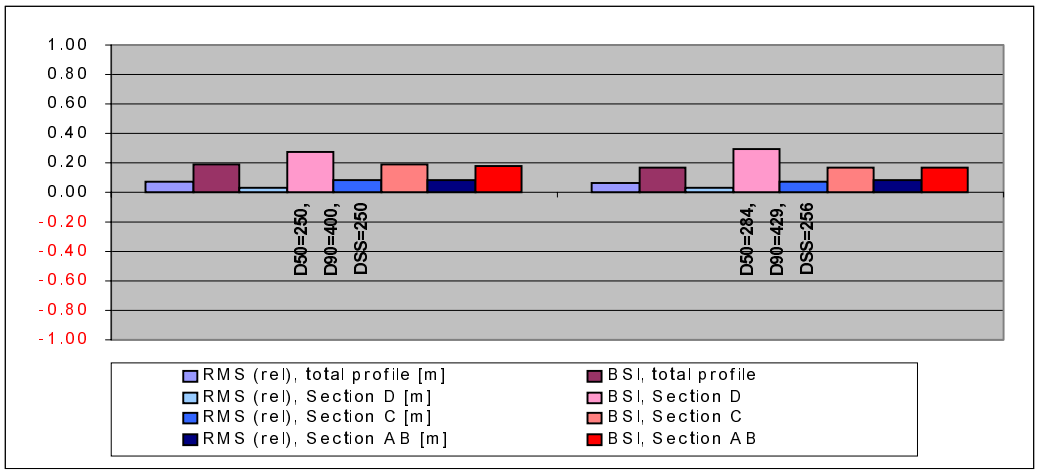

Figure 5.11: BSI-score and relative RMS-error for variations in D50, D90 and DSS (section 3)

5.4 Model performance for section 1, 2 and 4

Besides the validation of all parameter variations on section 3, a model run with default settings is done for section 1, section 2 and section 4 (see Figure 4.1) to see to what extent the default settings are able to generate predictions for these cross-shore profiles. Figures 5.12, 5.13 and 5.14 show the cross-shore profile that result from these model runs.

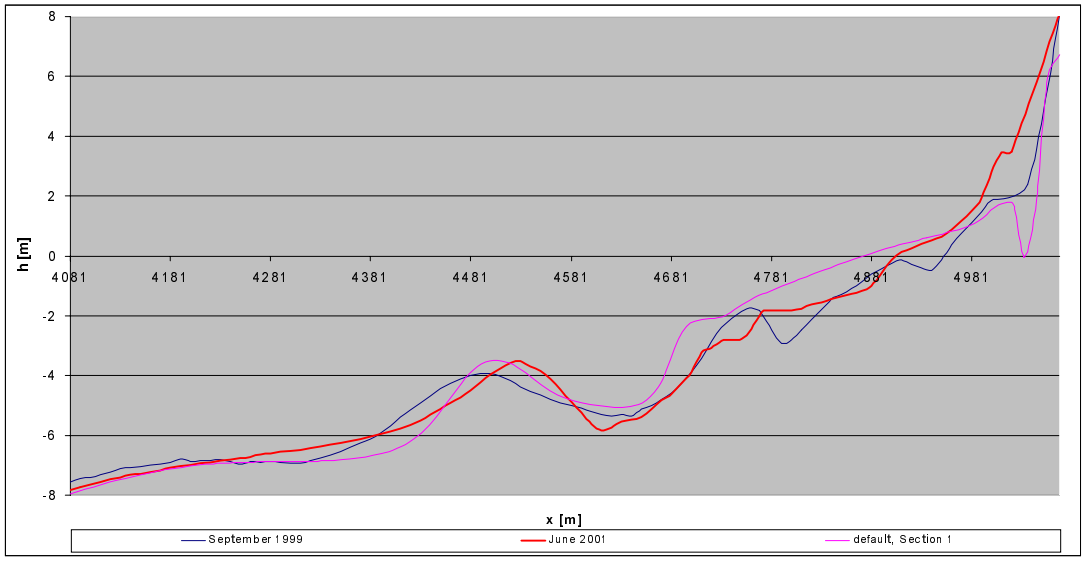

Figure 5.12: cross-shore profile of section 1 with default parameter settings

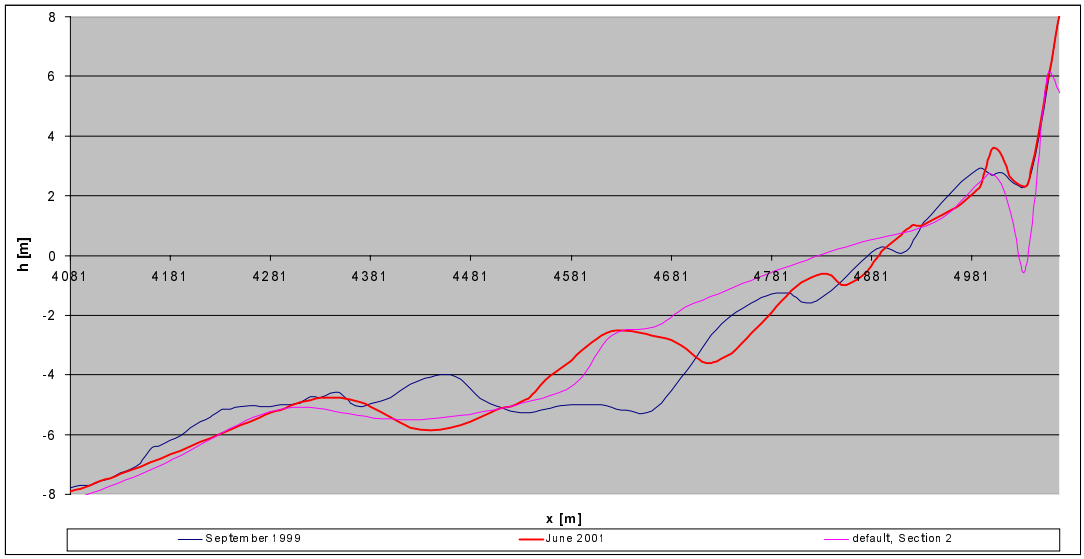

Figure 5.13: cross-shore profile of section 2 with default parameter settings

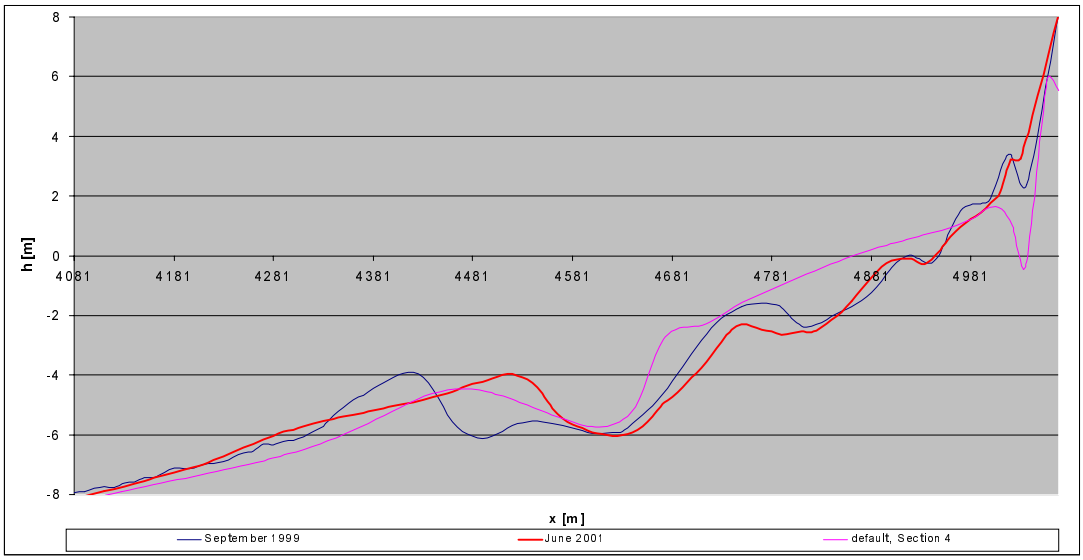

Figure 5.14: cross-shore profile of section 4 with default parameter settings

The figures show that the UNIBEST-TC mode gives a reasonable result for section 1, the most northern section, in which is the shoreface nourishment is not located. For sections 2 and 4 the model gives unsatisfying results. This can be explained by the fact that the northern and the southern end of the nourishment are located in respectively section 2 and section 4. The data analysis (see Part I: Data analysis, Van Duin en Wiersma [2002]) showed that both ends of the nourishment moved more shoreward than the middle part. Therefore, cross-shore averaging of these profiles results in a profile with a relatively wide (in the direction of the X-axis) shoreface nourishment. Besides this, it is supposed that around the ends of the nourishment complicated 3D processes occur, which are not described in the model. These two assumptions can explain the poor model performance for section 2 and section 4.

5.5 Synthesis

The validation study showed that the model is able to compute profile changes for cross-section including a shoreface nourishment. The detachment of the outer breaker bar from the shoreface nourishment as well as the generation of a trough between them is correctly predicted by the UNIBEST-TC model, although both processes are underestimated. Also for cross-shore profiles including a shoreface nourishment, the model predicts a too high bed level in section AB.
With regard to the optimisation of the UNIBEST-TC model the following conclusions can be drawn:

- Application of a variable gamma or a variable beta gives good results for the slope of the nearshore section (section AB). In both cases no breaker delay is applied. This can indicate that the breaker delay function should not be used for predictions of the nearshore section (section AB).
- GAMMA=0.7 results in the most optimal model performance (compared to all other variations investigated in this study)

- Larger values for the grain size parameters lead to a better prediction of the bar location, but to worse bar height predictions.
- For sections south or north of the nourishment and sections, in which the middle part of the nourishment is located, (sections 1, 3 and 5) the performance of the UNIBEST-TC model is satisfying.
- The UNIBEST-TC is not able to give a good prediction for sections, in which one of the ends of the shoreface nourishment is located. This is probably caused by complicated 3D processes around the ends of the nourishment. These 3D processes are not included in the UNIBEST-TC model.

Overall it can be concluded that the default parameter values, that have been calibrated on the undisturbed situation, are the best settings to use for UNIBEST-TC calculations on profile changes for a cross-shore profile including a shoreface nourishment. However the relatively large sensitivity of several parameters makes the model results less reliable.
Without further study it is not clear whether the positive results of GAMMA=0.7 are a coincidence or a real improvement of the model settings.

From now on the default settings will be assumed to be the optimal settings of the UNIBEST-TC model for the Egmond site. Next step of this hindcast study is investigating to what extent the UNIBEST-TC model is able to perform sediment volume predictions and evaluating the sediment transports within the cross-shore sections.

6 Sand distribution in the UNIBEST-TC model

6.1 Introduction

Besides evaluating the cross-shore profile changes, it is desirable to discover where, according to the UNIBEST-TC model, in the cross-shore profile sedimentation or erosion occurs and in what way the sediment in the cross-shore profile is redistributed during the investigated period. An indicator for beach sedimentation or erosion, used by Rijkswaterstaat, is the MCL (Momentary Coast Line) volume (see also Part I: Data analysis, Van Duin and Wiersma [2002]). The MCL volume is the sand volume of the beach zone that has its bed level in the range of 4 meters below to 4 meters above the average low water level. The average low bed water level at Egmond aan Zee is NAP -1 m, therefore the MCL volume is in the present study is the sand volume between NAP -5 m and NAP +3 m.
In the next subsection (Subsection 6.2) the UNIBEST-TC predictions of the MCL volume for section 3 and section 5 are compared to those found in the data analysis (see Part I: Data analysis, Van Duin and Wiersma [2002]).
Subsection 6.3 describes the redistribution of the sediment in cross-shore sections 3 and 5 as computed by the UNIBEST-TC model compared to the results of the data analysis (see Part I: Data analysis, Van Duin and Wiersma [2002]). Finally, the results found in this chapter will be evaluated in Subsection 6.4.

6.2 MCL volume calculations

The figures (Figures 6.1 and 6.2) below show the results of MCL volume calculations by the UNIBEST-TC model compared to the results found in the data analysis (see Part I: Data analysis, Van Duin and Wiersma [2002]). The MCL volume is calculated for the default prediction. The blue line represents the surveyed MCL volume (the line is interpolated between the data points), the pink line represents the MCL volume computed by UNIBEST-TC and the yellow line represents the MCL volume computed by UNIBEST-TC minus the sediment import over the seaward area boundary (d = NAP -8 m) (see Subsection 4.5.1).

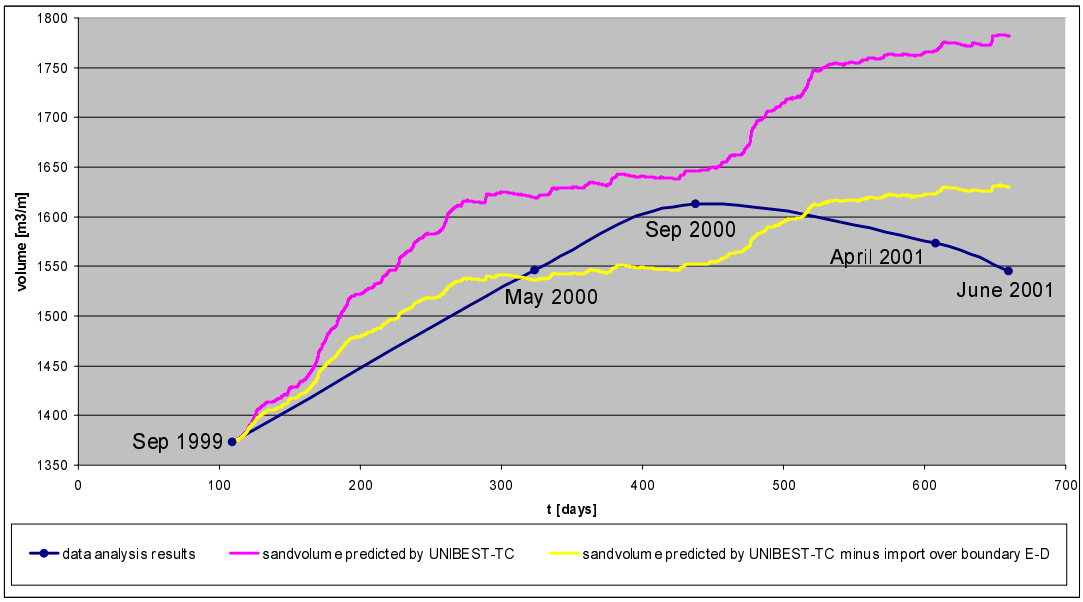

Figure 6.1: MCL volume calculations for section 3 (section with shoreface nourishment)

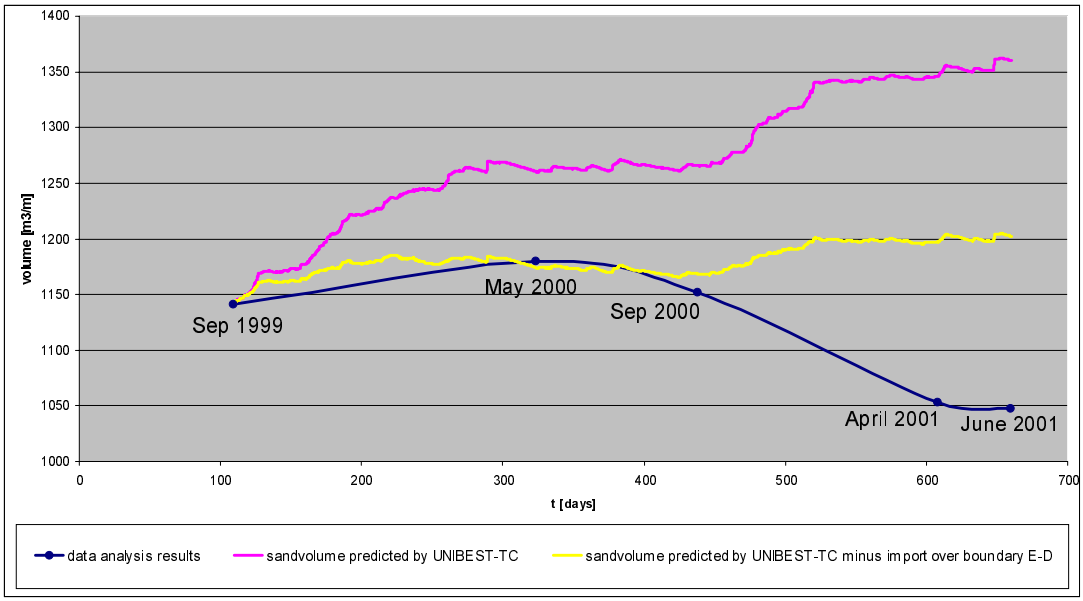

Figure 6.2: MCL volume calculations for section 5 (section without shoreface nourishment)

In the figures can be seen that, for both sections, the UNIBEST-TC model is not able to compute realistic values of the MCL volume. The computed volumes are too large. Subtraction of the sediment import over the seaward boundary reduces the values, but still the computed MCL value is too high. This leads to the conclusion that the model 'error' of importing sediment over the seaward boundary is not the main reason for the over-estimation of the MCL volumes.

Not only the amount of sediment in the MCL zone is over-estimated, but also the development of the MCL volume in time is unsatisfactory predicted by the UNIBEST-TC model. Since the sediment transport over the landward boundary is zero, a possible explanation for these results can be that the model computes too much onshore sediment transport, especially at deep water. In the next subsection this assumption will be investigated.

6.3 Sediment transport

To investigate whether the UNIBEST-TC model imports too much sediment from deep water into the MCL zone, the cross-shore profiles of section 5 and section 3 are divided in the following six parts:

E located between x = 0 m and x = 4081 m (deep water)

D located between x = 4081 m and x = 4381 m (includes shoreface nourishment, similar to section D in previous chapters)

C located between x = 4381 m and x = 4631 m (includes outer breaker bar, similar to section C in previous chapters)

B located between x = 4681 m and x = 4831 m (includes inner breaker bar, shoreward part of section AB in previous chapters)

A located between x = 4881 m and x = 4931 m (shoreward part of section AB in previous chapters)

Beach located between x = 4981 m and x = 5069 m

In the following figure (Figure 6.3) the sediment exchange between the different parts of the cross-shore sections, is presented for section 3 and section 5. Both the results of the UNIBEST-TC model as well as the results of the data analysis are shown. In the data analysis no sand transport could be computed and no information of the beach area and section E was available. Areas that have net sediment export are blue, areas that have net sediment import are yellow.

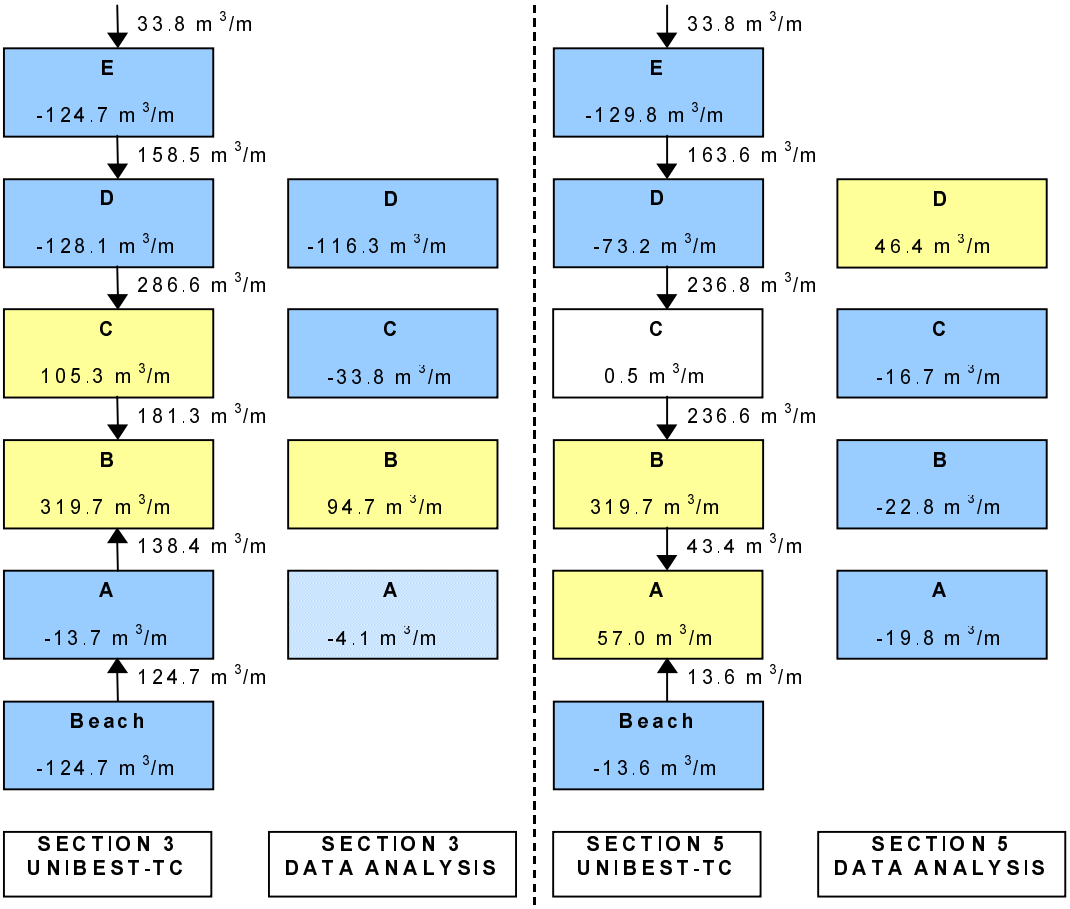

Figure 6.3: sediment exchange between parts of the cross-shore profiles of section 3 and section 5

The transport diagram of the UNIBEST-TC results for section 5 shows large sediment import from deep water (part E), which confirms the assumption (see Subsection 6.2) that the model computes too much onshore sediment transport.
The transport diagram of the UNIBEST-TC results for section 3 also shows large sediment import from deep water, but beside that large sediment export from the beach area to part B and C as well. This beach erosion however is caused by the erosion pit, that occurs as a result of the application of a fixed layer and is not necessary in accordance with reality.

Furthermore the transport diagrams of the UNIBEST-TC results show accretion in part B and C for section 3 and in part A and B in section 5. The presence of the shoreface nourishment seems to result in more seaward accretion (part B and C in stead of A and B in section 5) and erosion of the actual beach area. This accretion pattern in section 3 was also observed in the data analysis, so the UNIBEST-TC might give satisfying predictions at this point.
For section 5, besides erosion in part A, no similarity is found between the sedimentation and erosion patterns presented here and those of the data analysis. In the data analysis was found that part D had much accretion. Part D of section 5 is located just south of the nourishment. The accretion is probably caused by a 3D effect (for example blocking of the longshore current by the shoreface nourishment), that UNIBEST-TC model does not take into account.

6.4 Synthesis

The volume calculations with the UNIBEST-TC model appeared to be an over-estimation of the observed volumes. This is probably caused by the fact that the model imports sediment from deep water into the investigated area. In a 3D situation most of this sediment import would be taken along with the longshore current, the UNIBEST-TC model however does not take this into account.

The model is not able to predict sedimentation and erosion patterns for section 5, for section 3 on the other hand, the predicted patterns are in accordance with the observed patterns. This could indicate that in section 3 the cross-shore processes are dominant, in contrast to those in section 5.

The volume calculations of the model confirm the assumption, made in the data analysis, that behind the shoreface nourishment a lot of sediment is gathered as a result of the lee effect of the nourishment. Waves break at the shoreface nourishment, so behind the nourishment less wave breaking occurs. This results in a relative calm situation behind the nourishment, in which sediment can easily settle.

Whether the shoreface nourishment has a positive effect on the actual beach is, can not be concluded from the results of the UNIBEST-TC model. However, the assumption can be made that the shoreface nourishment has a small negative effect on the actual beach, since the sediment transport diagram of section 3 showed export from part A to part B.

7 Conclusions and recommendations

7.1 Conclusions

Analysis of the data and simulations with the UNIBEST-TC model results in better understanding of the dynamic processes of the Egmond coastal system after the placement of a shoreface nourishment. The profile averaging and data variation have contributed to the interpretation and validation of the model results.

The hindcast study leads to the following conclusions:

- To some extent the UNIBEST-TC model is able to calculate profiles that include a shoreface nourishment. The model predicts the detachment of the outer breaker bar from the nourishment and it indicates the bar movements.
- The UNIBEST-TC model has difficulties in predicting the bed level of the nearshore area. Application of a variable gamma or a variable beta results in a slightly better prediction of the slope of this nearshore area.
- For model calculations on a cross-shore section including a shoreface nourishment in the Egmond area, the default settings of the undisturbed situation can be applied as input settings.
- The UNIBEST-TC model gives unreliable results for predictions of volume changes. The model predicts too high sediment volumes in the surf zone, because the model calculates too much onshore sediment transport at deep water.
- The UNIBEST-TC model confirms the assumption of the shoreface nourishment having a lee effect in cross-shore direction.
- According to the calculations, the shoreface nourishment has a positive effect on the sand volumes in the surf zone. At the volume and width of the 'visible' beach (the part above sea level) however it might have a little negative influence.

7.2 Recommendations

After completion of this hindcast study some questions have been solved. Nevertheless, some questions are still unsolved and new questions are risen during this study. Based on the results of the hindcast study on the UNIBEST-TC model the following recommendations are given:

- More research should be done on the dominant processes that occur after placement of a shoreface nourishment
- The results of the present shoreface nourishment and the dominant processes should be compared to those at other locations, in order to come to a good conclusion whether no shoreface nourishment, this shoreface nourishment or another kind of shoreface nourishment is the best solution for coastal erosion problems.

- A long term study should be started to investigate whether the shoreface nourishment has effect in the long run
- More research should be done on the application of a variable gamma and a variable beta, especially for the nearshore area.
- More research should be done on finding solutions for the extensive sediment import from deep water of the UNIBEST-TC model and on the question whether the MCL calculation results can be edited with a certain key to transform them to reasonable results.
- Since FCvisc is a very sensitive parameter it might be worthwhile to develop a local, cross-shore dependent, model for this parameter.
- More extensive study should be done on currents and transports behind a shoreface nourishment.

References

Battjes, J.A., and J.P.F.M. Janssen, Energy loss and set-up due to breaking in random waves, Proceedings 16th International Conference on Coastal Engineering, pp. 569-587, American Society of Civil Engineers, New York, 1978.

Battjes, J.A., and M.J.F. Stive, Calibration and verification of a dissipation model for random breaking waves, J.Geophys. Res., vol. 90(C5): 9159-9167, 1985.

Boers, M., Voorspelling vooroeversuppletie met UNIBEST-TC, RIKZ, 1999.

Bosboom, J., S.G.J. Aarninkhof, A.J.H.M. Reniers, J.A. Roelvink and D.J.R. Walstra, Unibest-TC 2.0, overview of model formulations, WL | Delft Hydraulics, 1997.

Caljouw, M., and K. Kleinhout, 2000. Morphodynamics of the Egmond field site: May 1998 - September 1999. WL | Delft Hydraulics report z2822.25, November 2000.

Dijk, M., Vergelijking UNIBEST-TC en DUROSTA: twee tijdsafhankelijke dwarstransport modellen, Delft University of Technology, Department of Civil Engineering, January 2002.

Duin, M.J.P. van, and N.R. Wiersma, Evaluation of the Egmond shoreface nourishment, Part I: data analysis. WL | Delft Hydraulics report Z3054 / Z3148, June 2002

Duin, M.J.P. van, Evaluation of the Egmond shoreface nourishment, Part III: validation morphological modelling Delft3D-MOR. WL | Delft Hydraulics report Z3054 / Z 3148, June 2002

Gootjes, G., Dunes as source of sediment for Delft3D-MOR, Msc. thesis Delft University of Technology, Delft, The Netherlands, 2000.

Kleinhout, K., 2000. Hydrodynamics and morphodynamics in the Egmond field site: data analysis and UNIBEST-TC modelling. Delft University of Technology, Department of Civil Engineering, September 2000.

Nairn, R.B., J.A. Roelvink and H.N. Southgate, Transition zone width and implications for modelling surfzone hydronamics, Proceedings 22nd International Conference on Coastal Engineering, pp. 68-82, Delft, The Netherlands, 1990.

Rienecker, M.M., and J.D. Fenton, A Fourier approximation method for steady water waves, J. Fluid Mechanics, vol. 104, pp. 119-137, 1981.

Rijn, L.C., Principles of sediment transport in rivers, estuaries and coastal seas, Amsterdam: Aqua Publications, 1993.

Roelvink, J.A., and A.J.H.M. Reniers, Upgrading of a quasi-3D hydronamic model. Abstracts-in-depth, MAST G8-M overall workshop, Gregynog, 1994.

Roelvink, J.A., and M.J.F. Stive, Bar-generating cross-shore flow mechanisms on a beach, J. Geophys. Res., vol. 94, pp. 4785-4800, 1989.

Ruessink, B.G., D.J.R. Walstra and H.N. Southgate, Calibration and verification of a parametric wave model on barred beaches, submitted in Coastal Engineering, WL | Delft Hydraulics, May 2002.

Sand, S.E., Long wave problems in laboratory models, J. Waterw. Port Coastal Ocean Div., American Society of Civil Engineers, vol. 108, pp. 492-503, 1982.

Veuger, A.J., Gradient in longshore transport of sediment in UNIBEST-TC, Msc. thesis Delft University of Technology, Delft, The Netherlands, June 2001.

Vriend, H.J. de, and M.J.F. Stive, Quasi-3D modelling of nearshore currents, Coastal Engineering, vol. 11, pp. 565-601, 1987.

Walstra, D.J.R., Userguide for Unibest-TC, WL | Delft Hydraulics, October 2000.

Walstra, D.J.R., M. van Koningsveld, S.G.J. Aarninkhof and B.G. Ruessink, Methodological approach to model development for Unibest-TC, Part B: Development and testing, WL | Delft Hydraulics, October 2001.

Walstra, D.J.R., G.P. Mocke, F. Smit, Roller contributions as inferred from inverse modelling techniques, Proceedings of the 25th International Conference on Coastal Engineering, pp. 1205-1218, American Society of Civil Engineers, 1996.

WL | Delft Hydraulics, Unibest-TC, version 2.02, a generic tool to investigate the morphodynamic behaviour of cross-shore profiles, user manual, April 1999.

A Sensitivity analysis

Before calibrating the UNIBEST-TC model, it is desirable to get a general idea of the model response to specific parameter variations. To get a quick view on the model behaviour, a sensitivity analysis is carried out by varying several parameters in model runs over a short period (September 1999 to May 2000). The extensive results of this sensitivity analysis, including cross-shore profile figures and statistical results, are presented in this Appendix.

In the table below (Table A.1) an overview is given of the investigated parameters and the used parameter variations in the sensitivity analysis. All other parameters are kept at the default values (see Subsection 3.3). For each value a simulation of the longshore-averaged profile of section 5 (south of the nourishment, see Figure 4.1) over the first winter period (September 1999 to May 2000) is made. Section 5 is chosen because this section the least influenced by the shoreface nourishment, since the net sand transport along the coast at Egmond is in northern direction.
The output is evaluated with the Brier Skill Score, the Relative RMS-error (see Chapter 4) for the cross-shore bottom profile and by comparing the cross-sections predicted by UNIBEST-TC with regard to the position and height of the bars.

Table A.1: overview of varied parameters for sensitivity analysis

Parameter	Dimension	Default	Values
GAMMA	[-]	Battjes&Stive ('0')	0.6, 0.7, 0.8, 0.9, variable gamma, variable gamma [no breaker delay], Battjes&Stive ('0') [no breaker delay]
BETD	[-]	0.1	0.05, 0.15, 0.2, 1, variable beta
FWEE	[-]	0.01	0.001, 0.02, 0.04, 0.05, 0.06, 0.1, 0.2
C_R	[-]	0.25	0, 0.5, 1
F_LAM	[-]	1	0.25, 0.5, 2
FACQB	[-]	0.35	0, 0.2, 0.4, 0.6, 0.8, 1
FCVISC	[-]	0.1	0.01, 0.025, 0.05, 0.15, 0.2
(D50; D90; DSS)	[μm]	(240; 480; 240)	(284; 429; 256), (200; 325; 200), (200; 325; 150), (240; 480; 240) with cross-shore varyin grain size, (250; 400; 250), (300; 480; 300), (284; 429; 256), (284; 429; 256) with cross-shore varying grain size
RKVAL	[-]	0.03	0.001, 0.005, 0.01, 0.05, 0.1
(RW; RC)	[m]	(0.01; 0.03)	(0.001; 0.003), (0.002; 0.01), (0.005; 0.01); (0.01; 0.02); (0.015; 0.03); (0.02; 0.04); (0.005; 0.03)

GAMMA = Wave breaking parameter to determine maximum local wave height. Default value is '0' according to Battjes&Stive (1985).
BETD = Roller parameter, expressing the steepness of the wave front.
C_R = Correlation coefficient between wave envelope and bound long waves.
F_LAM = Number of wave lengths over which weighted depth is integrated (is part of breaker delay concept).
FACQB = Factor for the fraction of breaking waves which does not contribute to the wave velocity moment.
FCVISC = Viscosity coefficient for mean current computation.
D50,D90,DSS = D_{50} grain diameter, D_{90} grain diameter, D_{50} grain diameter of suspended sediment.
RKVAL = Friction factor for mean current computation.
RW and RC = Wave and Current related roughness for sediment transport computation.

Wave breaking parameter: GAMMA

In the figures below (Figure A.1 and A.2) the BSI, the relative RMS-error and the cross-shore profiles are shown for variations in gamma. The default prediction is the base prediction. The figures show that the model is not very sensitive for variations in gamma. Since the model responds quite subtle to variations and gamma is a fairly uncertain parameter, gamma is an interesting parameter to vary in order to find the optimal parameter settings.

A new appliance in UNIBEST-TC is a variable gamma, which applies an in space variable gamma. In this stage of the analysis it seems to improve the model performance in the area of bank location and near shore slope.

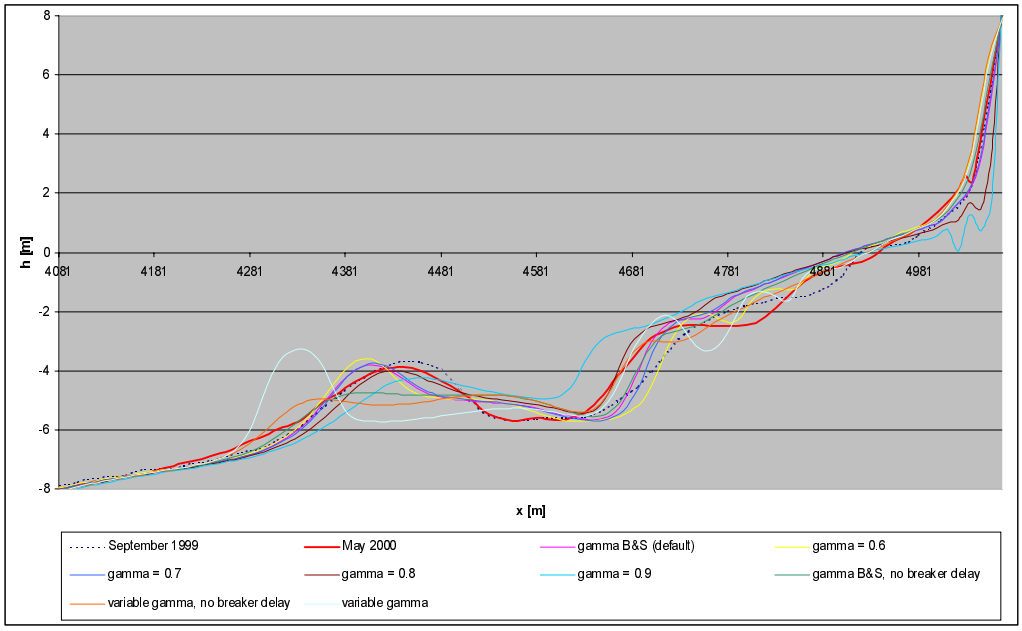

Figure A.1: cross-shore profiles of variations in GAMMA

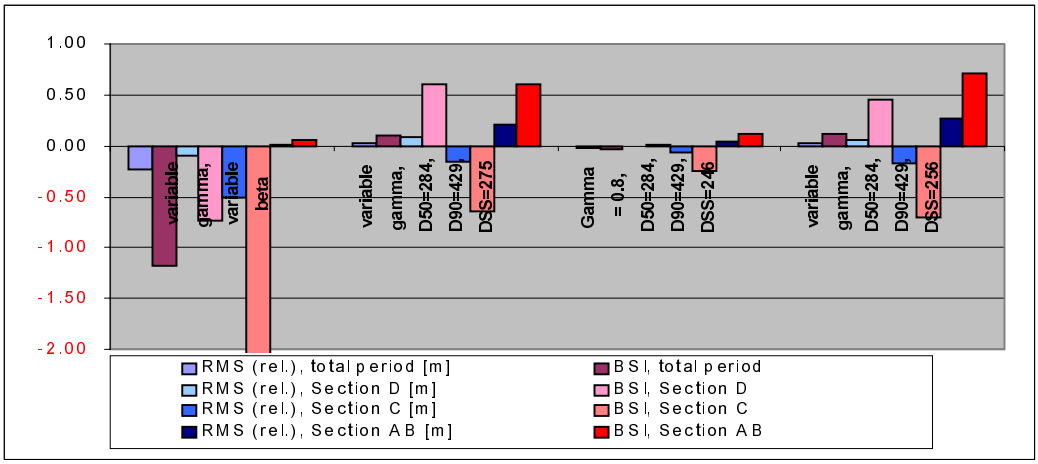

Figure A.2: BSI-score and relative RMS-error for variations in GAMMA

Roller parameter, expressing the steepness of the wave front: BETD

In the following figures (Figure A.3 and Figure A.4) the BSI, the relative RMS-error and the cross-shore profiles are shown for various values for beta. Beta appears to be little sensitive for variations of value. This sensitivity mainly shows in the height predictions of the second breaker bank, the bank locations are for every value of beta are all but the same.

Fairly new is the appliance of a variable beta, in which beta varies in time and space. Though the run with a variable beta has a small positive BSI score, it seems not to create an improved prediction. Nevertheless, it will be tested again in the calibration study.

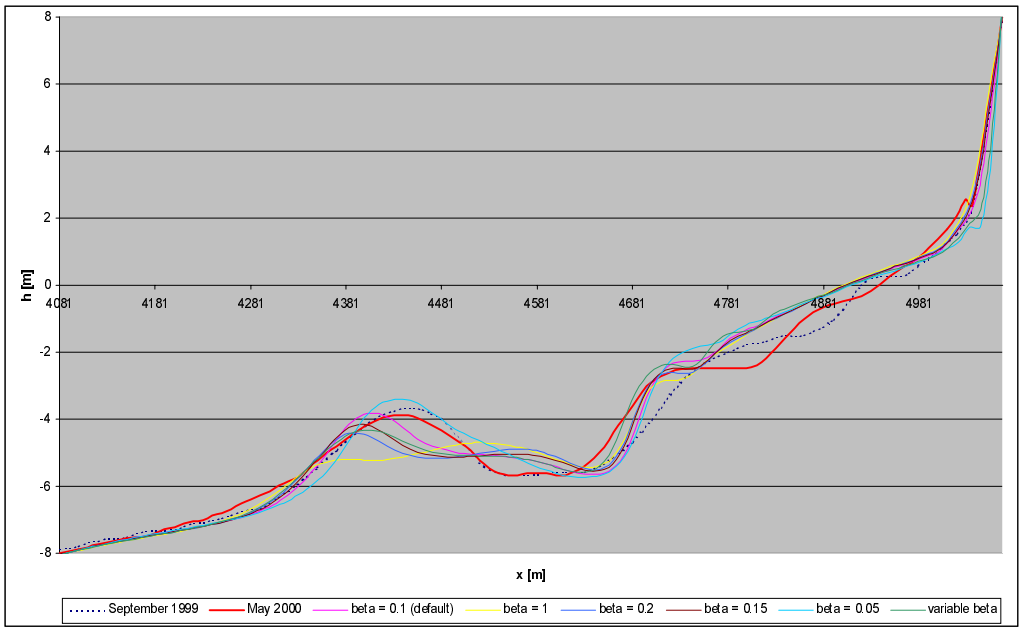

Figure A.3: cross-shore profiles of variations in BETA

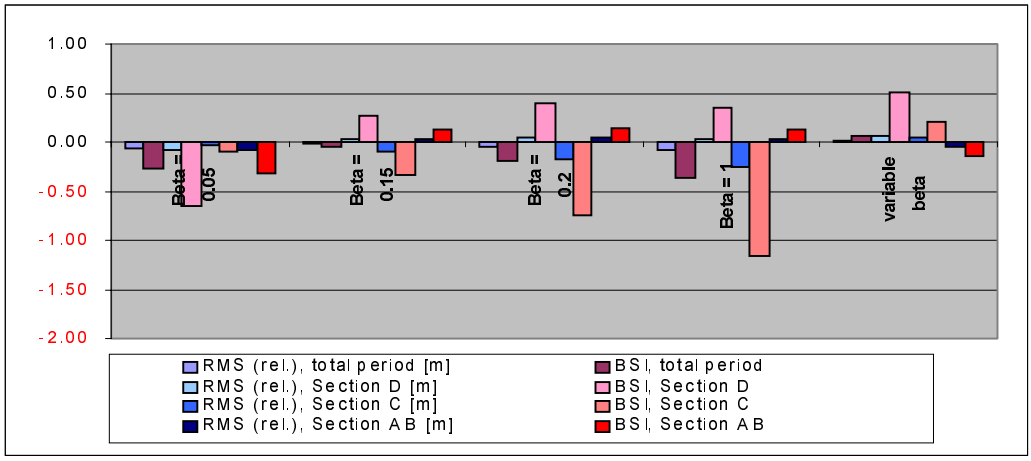

Figure A.4: BSI-score and relative RMS-error for variations in BETA

Friction factor for wave dissipation due to bottom friction: FWEE

In Figure A.5 and Figure A.6 the results of runs with different values for FWEE are compared. The figures show that the model turns out to be very sensitive for variations in FWEE and that none of the variations leads to an improvement of the model predictions compared to the default settings. Because of these results and according to precious studies on the Egmond coast [Boers, 1999; Walstra et al., 1999], the value for FWEE will be set at its default value of 0.01 during the calibration and validation of the UNIBEST-TC model.

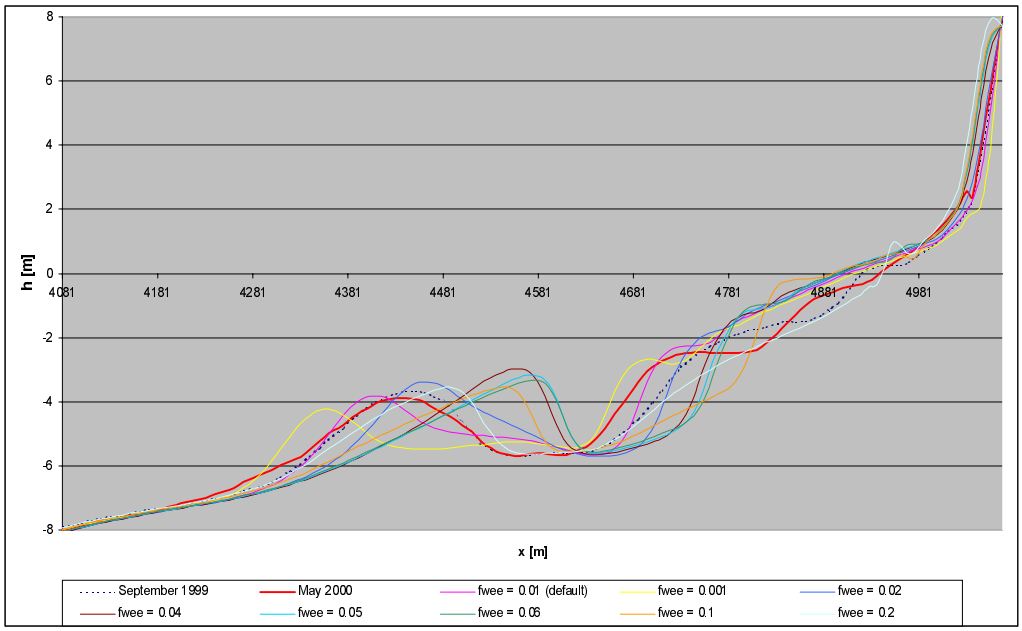

Figure A.5: cross-shore profiles of variations in FWEE

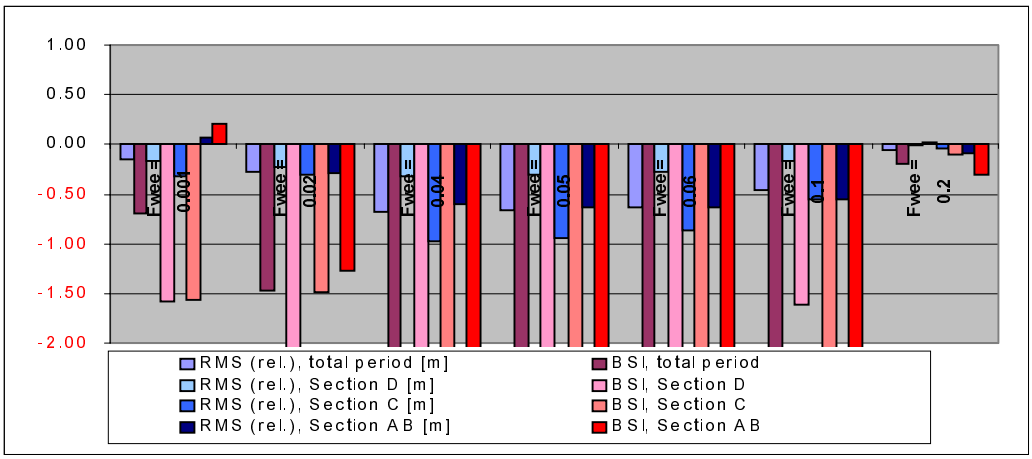

Figure A.6: BSI-score and relative RMS-error for variations in FWEE

Correlation coefficient between wave envelope and bound long waves: C_R

The figures below (Figure A.7 and Figure A.8) show the BSI, the relative RMS-error and the cross-shore profiles for variations in C_R. The model appears to be quite sensitive for variations in this parameter. The predictions for the height of the outer breaker bank are most sensitive for changes in the value of C_R. The run with C_R = 0.5 has a small positive BSI score, but however gives a poor prediction for the outer breaker bank. This once again shows the statistical results should be used with care and never without the cross-shore profiles next to them.

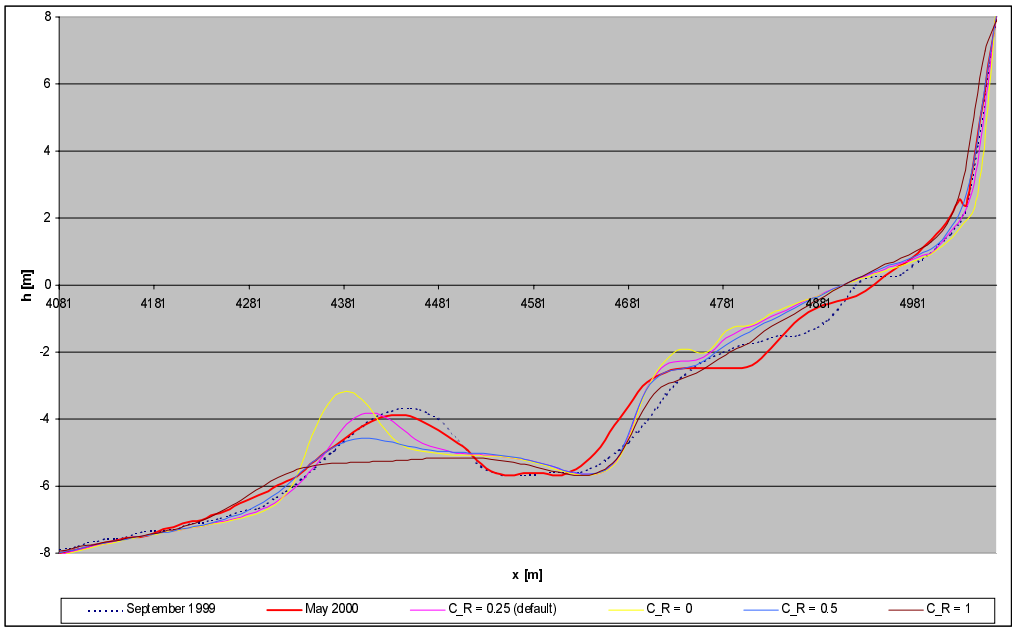

Figure A.7: cross-shore profiles of variations in C_R

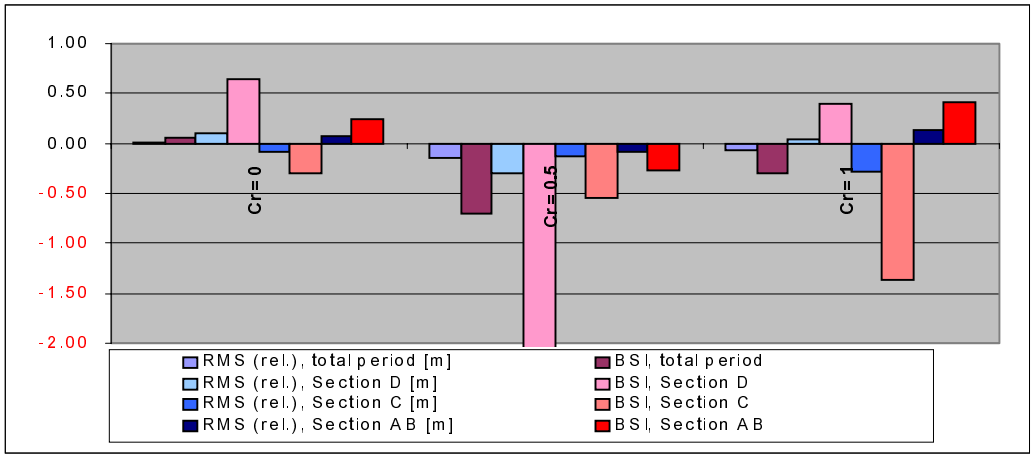

Figure A.8: BSI-score and relative RMS-error for variations in C_R

Breaker Delay concept (number of wave lengths over which weighted depth is integrated): F_LAM

In the following figures (Figure A.9 and Figure A.10) the BSI, the relative RMS-error and the cross-shore profiles are shown for various values for F_LAM. It can be seen that the model does not respond very sensitive to variations in F_LAM. Rather large variations cause only small changes in the predicted bottom profile. The changes that occur are a linear response to the variations and mainly in the height of the second breaker bank. A smaller value for F_LAM causes a lower prediction for the outer bank height and vice-versa.

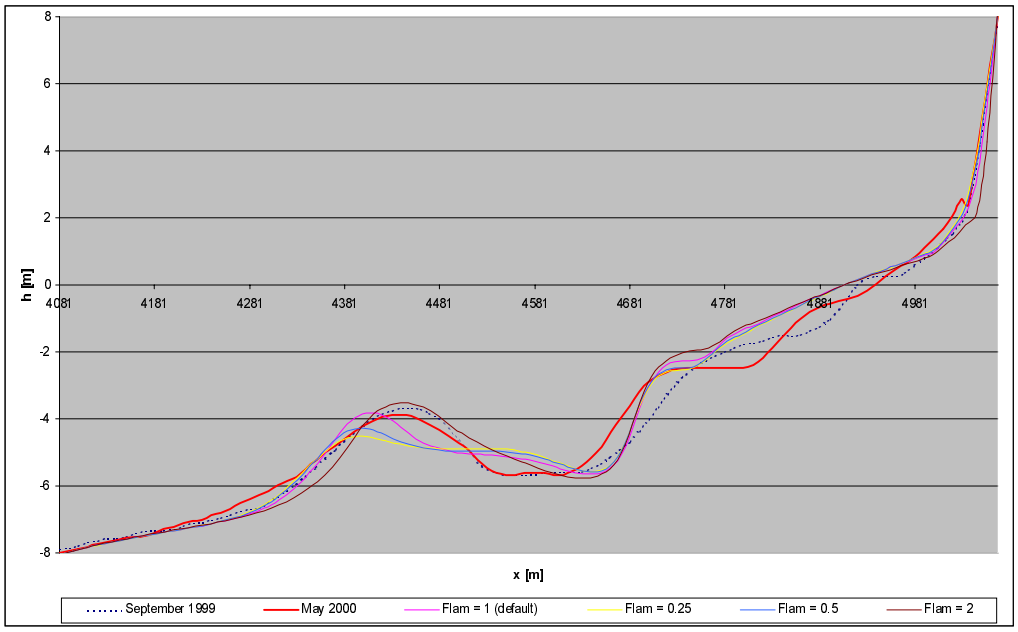

Figure A.9: cross-shore profiles of variations in F_LAM

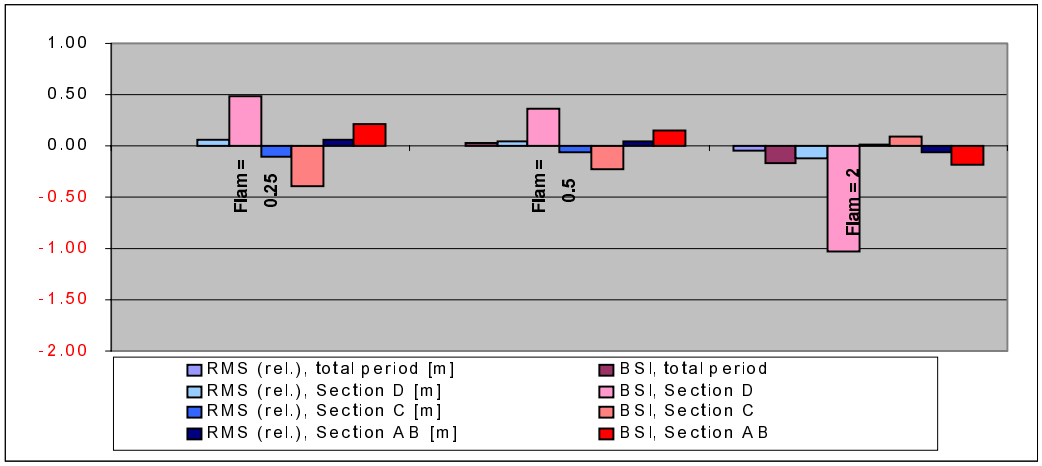

Figure A.10: BSI-score and relative RMS-error for variations in F_LAM

Factor of fraction of breaking waves that do not contribute to wave asymmetry: FACQB

Figure A.11 shows the cross-shore profiles for various values of FACQB, Figure A.12 shows the BSI and the relative RMS-error for various values of FACQB. In these figures can be seen that the model is sensitive for variations in FACQB. The smaller FACQB is chosen, the further seaward the location of both breaker banks is predicted and the other way around. Bank height appears to be nearly independent of the value of FACQB.

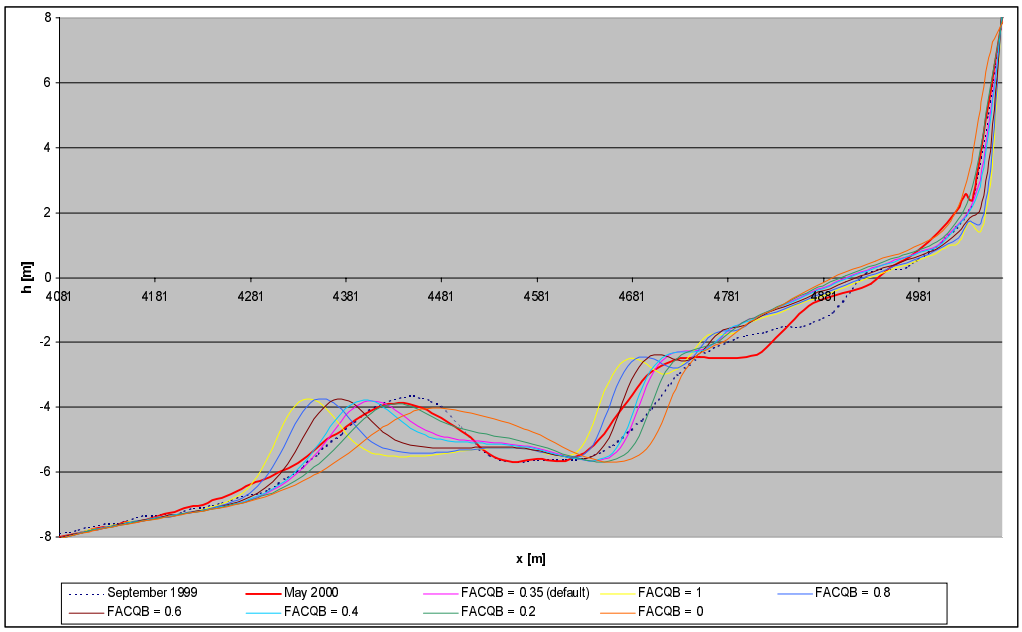

Figure A.11: cross-shore profiles of variations in FACQB

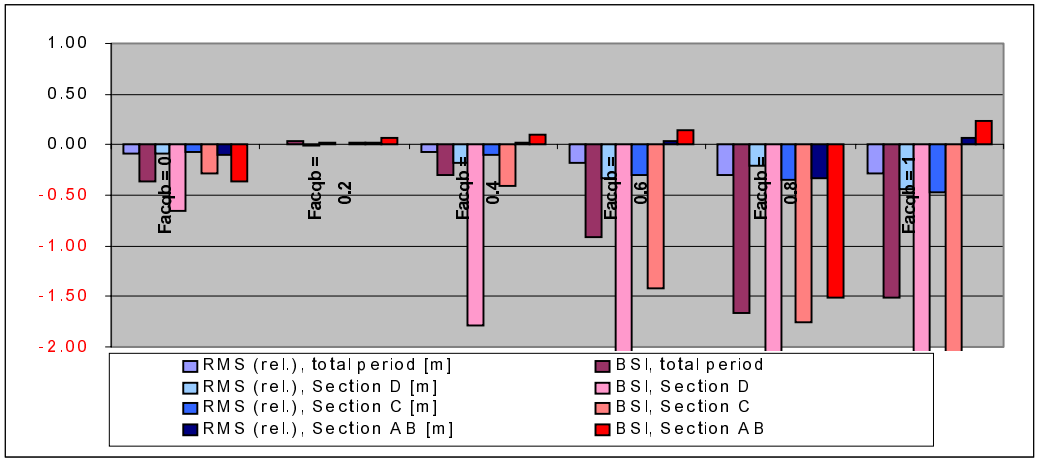

Figure A.12: BSI-score and relative RMS-error for variations in FACQB

Viscosity coefficient of vertical velocity profile: FCVISC

Cross-shore profiles for variations in FCVISC are shown in Figure A.13, the BSI and the relative RMS-error for various values of FCVISC are shown in Figure A.14. The model appears to be very sensitive for variations in FCVISC. Compared to the default settings, smaller values of FCVISC result in a more seaward position of both breaker banks. The bank height is less influenced by variations in FCVISC.

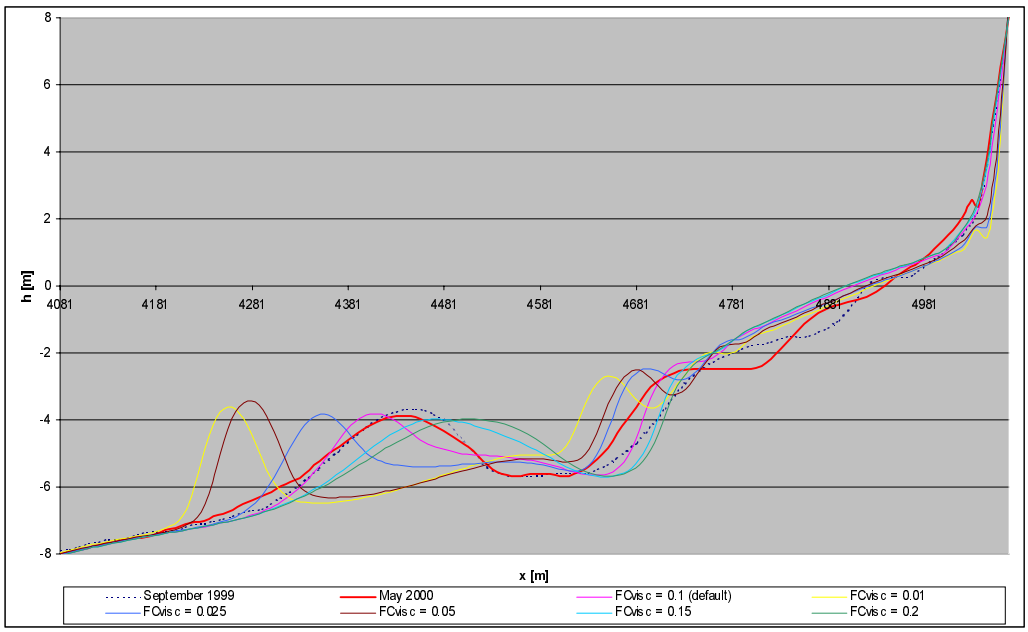

Figure A.13: cross-shore profiles of variations in FCvisc

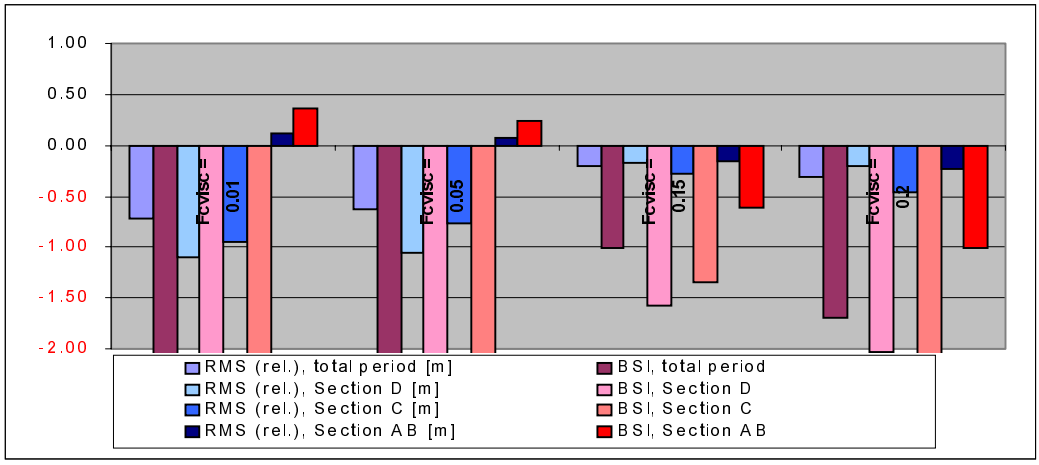

Figure A.14: BSI-score and relative RMS-error for variations in FCvisc

Sediment grain size parameters: D50, D90, DSS

In Figure A.15 and Figure A.16 the BSI score, the relative RMS-error and the cross-shore profile for variations in the sediment characteristics are shown. The model appears to be very sensitive for small variations in the sediment characteristics. Since these small variations have so much influence on the model results and the default sediment characteristics are extracted from field measurements, the variations in these values will not deviate much from the default settings, to avoid obtaining satisfying model results based on unreal sediment characteristics.

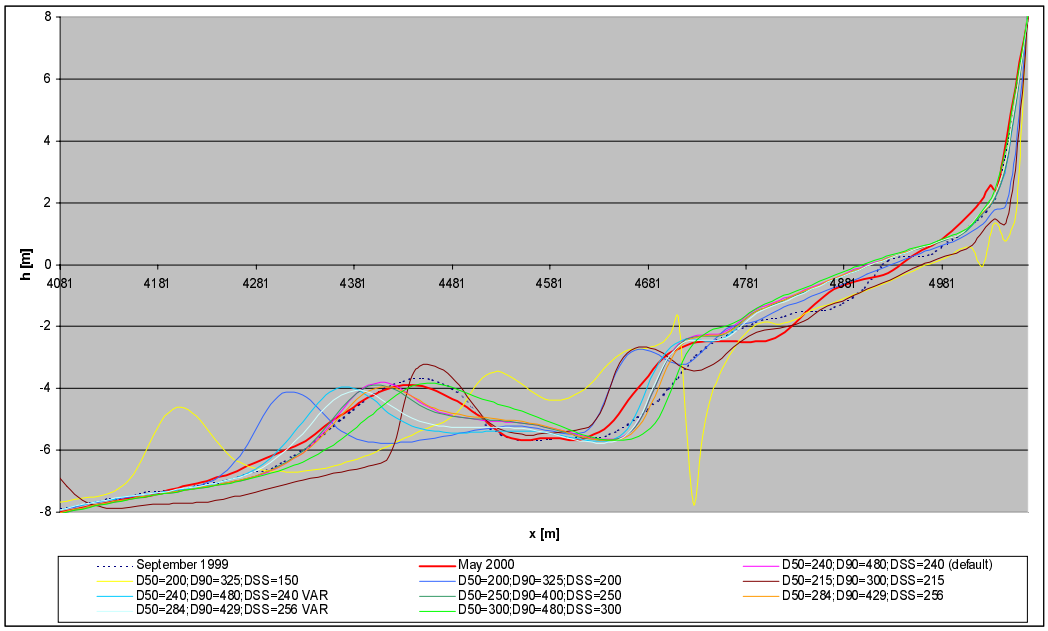

Figure A.15: cross-shore profiles of variations in grain size parameters

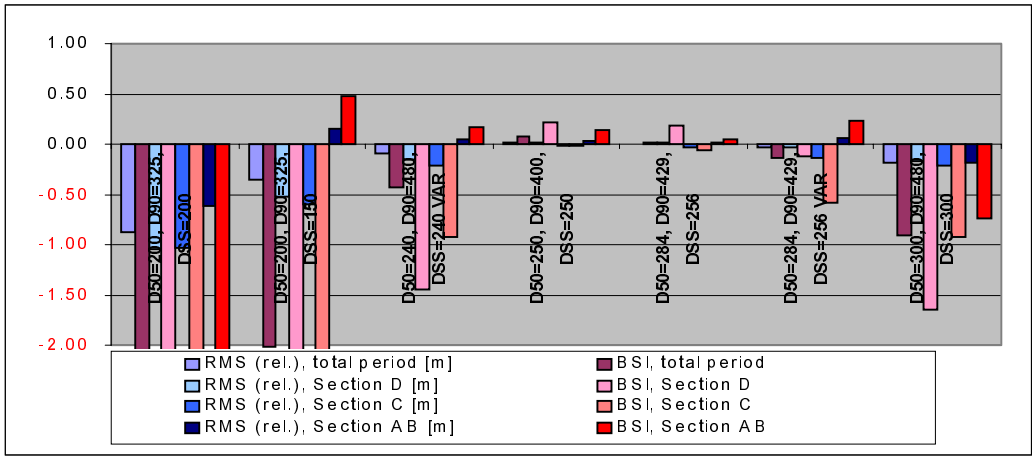

Figure A.16: BSI-score and relative RMS-error for variations in grain size parameters

Friction factor for mean current: RKVAL

In the following figures (Figure A.17 and Figure A.18) the BSI, the relative RMS-error and the cross-shore profiles are shown for various values for RKVAL. In these figures can be seen that the model responds quite sensitive to variations in RKVAL, mainly by adjusting the position of the breaker banks. The lower RKVAL, the more seaward the position of the breaker banks is predicted.

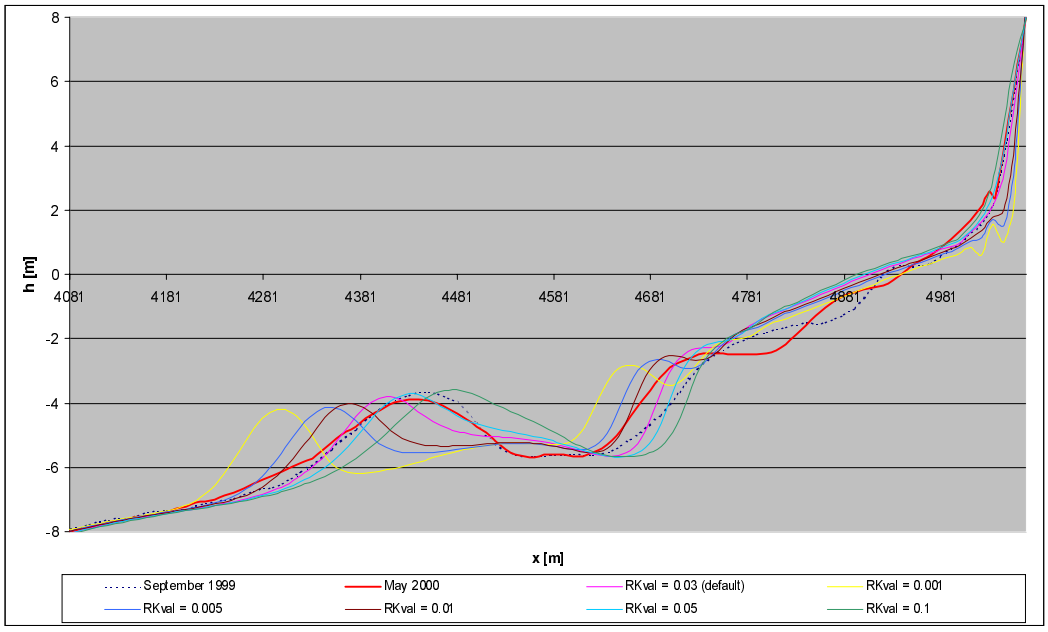

Figure A.17: cross-shore profiles of variations in RKval

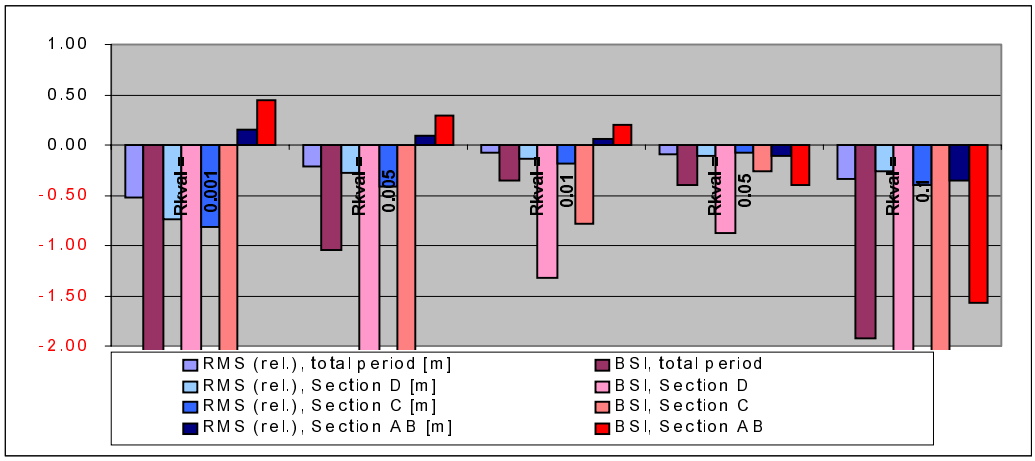

Figure A.18: BSI-score and relative RMS-error for variations in RKval

Current and wave related roughness: RC and RW

The figures below (Figure A.19 and Figure A.20) show the BSI, the relative RMS-error and the cross-shore profiles for variations in RC and RW. Variations in these roughness factors appear to have a lot of influence on the model results, not only on the position of the breaker banks but also on the bottom height in the near-shore area. RC and RW have a significant effect on the resulting transports. The way in which these parameters influence the transports is not known beforehand as these parameters not only determine the effective shear stress, but also, among others, the effective grain size diameter. These parameters can be used to tune the transports and thus the bottom profile [see Walstra, October 1999].

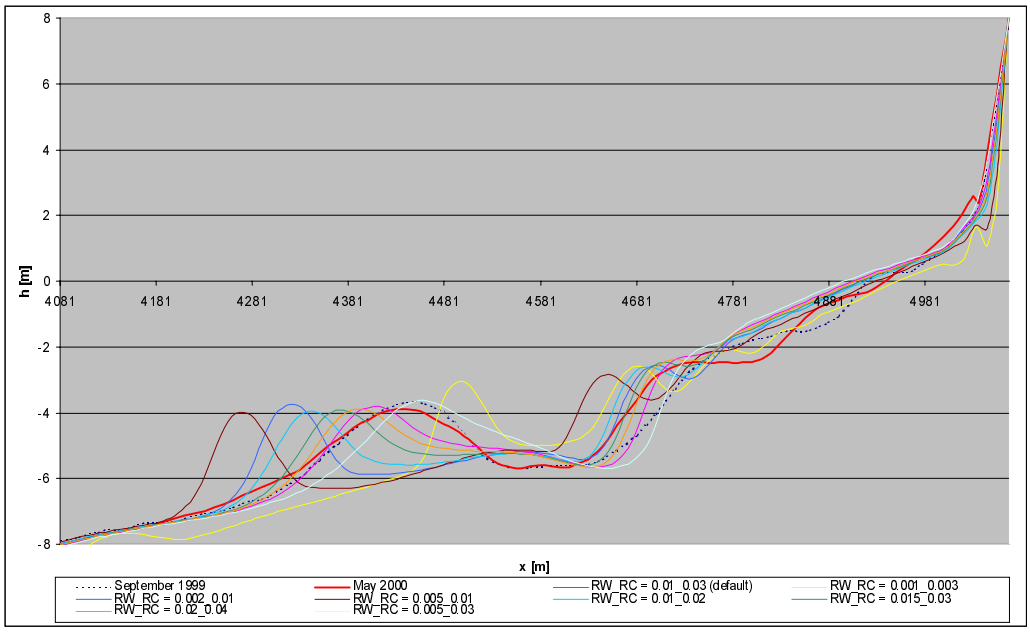

Figure A.19: cross-shore profiles of variations in RW and RC

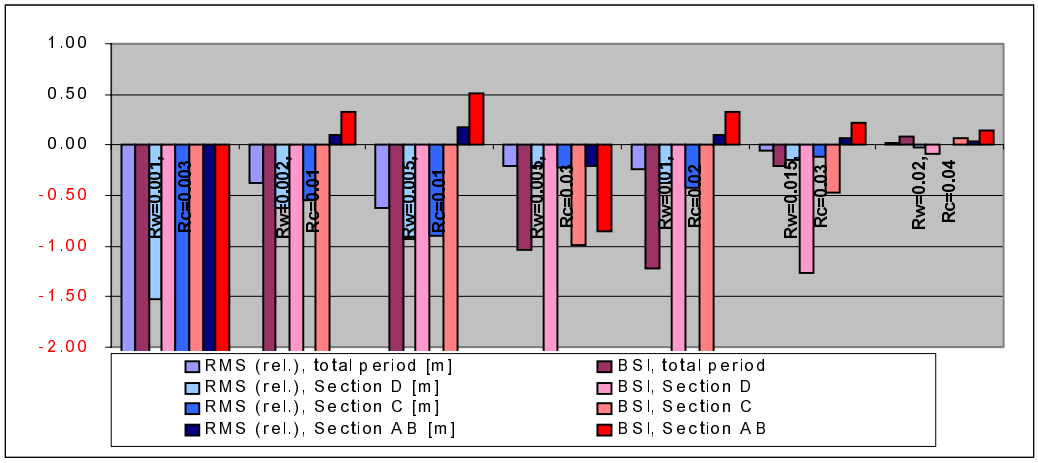

Figure A.20: BSI-score and relative RMS-error for variations in RW and RC

Varying GAMMA and a second parameter

Figure A.21 and Figure A.22 show the BSI, the relative RMS-error and the cross-shore profiles for variations in GAMMA simultaneously with variations in a second parameter. Analysing the results, it can be concluded that, although the statistical parameters show positive results, varying two parameters simultaneously causes a lot of irregularities. A phenomenon that is not very odd because the two variations might influence each-others positive or negative effect. On the basis of these results, the calibration of the model will be done by varying the parameters one by one to keep a good vision on the effect of the concerned parameter.

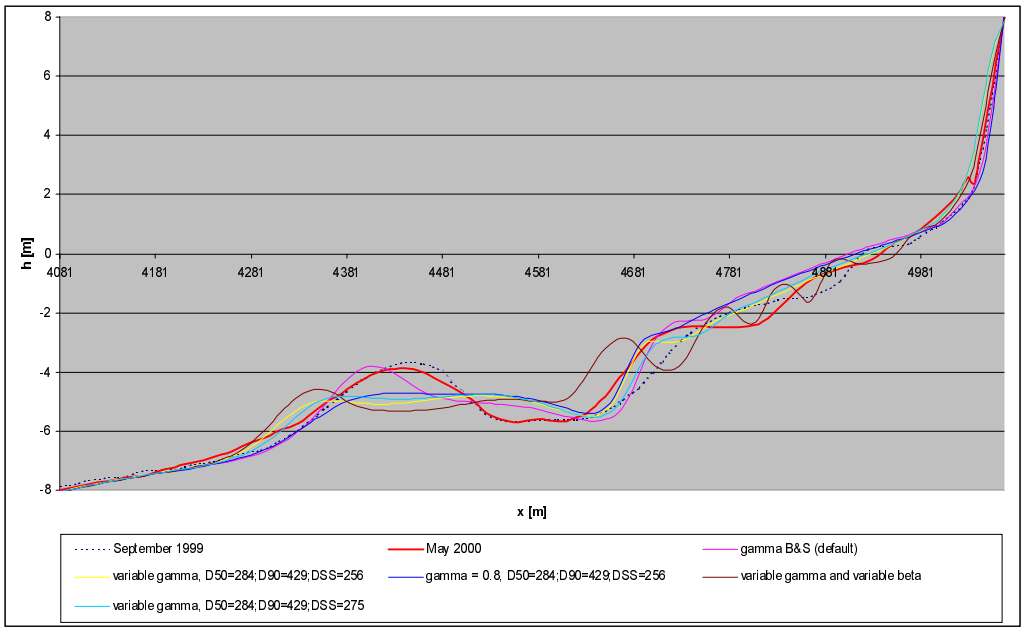

Figure A.21: cross-shore profiles of variations in GAMMA and a second parameter

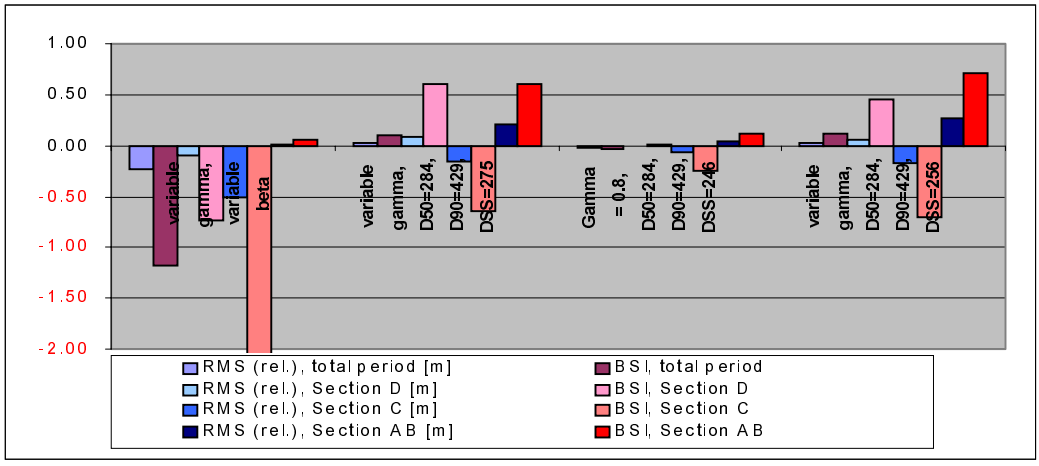

Figure A.22: BSI-score and relative RMS-error for variations in GAMMA and a second parameter